

Regulation von spannungsgesteuerten Kaliumkanälen durch Häm

Dissertation

zur Erlangung des akademischen Grades doctor rerum naturalium

(Dr. rer. nat.)

**vorgelegt dem Rat der Biologisch-Pharmazeutischen Fakultät
der Friedrich-Schiller-Universität Jena**

von **Nirakar Sahoo, M.Sc.**

geboren am 01.07.1978 in Kendrapara, Orissa, Indien

1. Gutachter: **Prof. Dr. Stefan H. Heinemann**

Friedrich Schiller-Universität, Jena

2. Gutachter: **Prof. Dr. Ralf Oelmüller**

Friedrich Schiller-Universität, Jena

3. Gutachter: **Prof. Dr. Heinrich Terlau**

University of Kiel, Kiel

Zusammenfassung

Häm ist seit langem als stabile prosthetische Gruppe in Proteinen bekannt, denen dadurch Reaktionen mit Sauerstoff oder anderen Gasen möglich werden. Klassische Beispiele sind die Cytochrome, Hämoglobin, Myoglobin oder die lösliche Guanylatzyklase. Darüber hinaus gibt es aber auch neue Befunde, die zeigen, dass Häm als sehr potenter nicht-genomischer Regulator von Ionenkanälen wirken kann. Der spannungs- und kalziumabhängige Kaliumkanal Slo1 (BK) war das erste Beispiel für eine Regulation durch direkte Bindung von Häm. Bindung an das klassische Häm-Bindemotiv „CxxCH“ im C-Terminus des Kanalproteins führt zu einer Reduktion des Kaliumstromes von Slo1. Nach dieser Entdeckung stellte sich die Frage, ob auch andere Kanalproteine auf ähnliche Weise durch Häm reguliert werden können. Aufgabe dieser Arbeit war es daher, mit Hilfe von *patch-clamp*-Studien an heterolog exprimierten Kaliumkanälen nach bisher unbekannten Wechselwirkungen von Häm mit Kanalproteinen zu suchen. In der vorliegenden Arbeit konnten zwei neue Klassen Häm-sensitiver Kaliumkanäle nachgewiesen werden: A-Typ-Kanäle und Kanäle der EAG-Familie.

A-Typ Kaliumkanäle wie Kv1.4 zeigen eine typische schnelle Inaktivierung nach initialer Porenöffnung. Mit diesem Verhalten sind sie besonders in der frühen Phase der Repolarisation von Aktionspotentialen in Neuronen und in Herzmuskelzellen von besonderer Bedeutung. Applikation von Hämin auf der zytosolischen Membranseite führte zum Verlust der schnellen Inaktivierung bei Kv1.4 Kanälen mit einer EC₅₀-Konzentration von 24 nM. Dieser Effekt trat nicht ein, wenn ein Cystein (C13S) und ein Histidin (H16A) im aminoterminalen Inaktivierungsball des Kanals mutiert waren. Eine direkte Interaktion von Häm mit der Balldomäne konnte mit Hilfe synthetischer Ball-Peptide gezeigt werden, wobei Austausch von C13 oder H16 die Häm-Bindung verhinderte. A-Typ-Kanäle können auch durch Interaktion nichtinaktivierender α -Untereinheiten wie Kv1.1 oder Kv1.5 mit Kv β -Untereinheiten entstehen. Dabei stellen die Kv β -Untereinheiten die Inaktivierungsbälle zum Verschluss der Kanalpore. Ein Sequenzvergleich der Balldomänen in Kv β -Untereinheiten mit Kv1.4 zeigte, dass in einigen Kv β -Balldomänen das potentielle Häm-Bindemotiv CxxH vorkommt. Inaktivierung durch Kv β 1.1 Untereinheiten, in denen das Motiv vorkommt, war sensitiv gegenüber Hämin. Dagegen waren Kv β 1.1 Untereinheiten, in denen dieses Motiv fehlt, unempfindlich gegen Hämin-Applikation.

Der durch Depolarisation aktivierbare Kaliumkanal hEAG1 hat ein breites Expressionsspektrum in neuronalen Geweben, einschließlich Hippocampus und Cortex, wo er zur Modulation neuronaler Erregbarkeit beiträgt. Zur Untersuchung der Oxidationsempfindlichkeit von hEAG1 applizierten wir thiolreaktive Agenzien wie DTNB auf der zytolischen Seite exzidiierter Membranflecken. Der Kanal zeigte dabei eine biphasische und zustandsabhängige Reaktion. Das Schaltverhalten des Kanals änderte sich mit einer schnellen Kinetik, während eine langsamere Reaktion den Kanal vollständig inhibierte. Ein systematischer Austausch aller Cysteine ergab, dass beide Effekte eliminiert werden, wenn gleichzeitig die Cysteine C145, C214, C532 und C562 gegen Alanin getauscht werden. Die schnelle Oxidationsreaktion mit Einfluss auf das spannungsabhängige Schalten konnte auf die aminoterminalen Reste C145 und C214 zurückgeführt werden, während die C-terminalen Aminosäuren C532 und C562 für den langsameren Verlust der Kanalaktivität verantwortlich sind. Die Lokalisation dieser oxidationsempfindlichen Reste legt nahe, dass Cystein-Oxidation in hEAG1 die Interaktion zwischen aminoterminalen und carboxyterminalen Kanaldomänen beeinträchtigt.

Die Untersuchung von hEAG1 auf mögliche Wechselwirkungen mit Häm zeigte, dass dieser Kanal noch empfindlicher reagiert als Kv1.4. Applikation von Hämin auf der zytosolischen Seite des Kanals in exzidierten Membranflecken führte zu verändertem Schaltverhalten und einem sehr schnellen Rückgang des Kaliumstromes. Dabei lag die Sensitivität mit einem IC_{50} Wert von ≈ 2 nM etwa 10 bzw. 40-fach höher als bei Kv1.4- oder Slo1-Kanälen. Biochemische Bindungsstudien mit hEAG1-Fragmenten und Hämin-Agarose deuteten darauf hin, dass es zu einer direkten Bindung von Hämin an den Kanal kommt, ein eindeutiges Bindemotiv konnte aber noch nicht identifiziert werden. Im Gegensatz zu Kv1.4 zeigte sich, dass Mutation von oxidationsempfindlichen Cysteinen in hEAG1 nicht zu einem Verlust der Häm-Empfindlichkeit führt. Systematische Mutagenese von Histidinen in hEAG1, Untersuchung von Kanalchimären und spektroskopische Untersuchungen an Peptiden deuten aber darauf hin, dass Histidinreste eine zentrale Rolle bei der Hämregulation von hEAG1 spielen.

Die mögliche physiologische Bedeutung der Hämregulation bei A-Typ- und EAG-Kanälen wird in nachfolgenden Studien zu untersuchen sein. Man kann davon ausgehen, dass die intrazelluläre Konzentration von freiem Häm im mikromolaren Bereich liegen kann, da beispielsweise für Hämoxygenasen HO1 und HO2 K_m -Werte von 1 μ M, bzw. 0,4 μ M beschrieben wurden. Vergleicht man diese Affinitäten mit der Sensitivität von hEAG1 und Kv1.4 gegen Häm im

niederen nanomolaren Bereich, so ist es sehr wahrscheinlich, dass es *in vivo* zur Inhibition dieser Kanäle durch Häm kommen kann. Die starke Verlangsamung der Inaktivierung von A-Typ-Kanälen könnte die Ausschüttung von Neurotransmitter hemmen und damit neuroprotektiv wirken. Andererseits würde die Hemmung von hEAG1-Kanälen wahrscheinlich zu Übererregbarkeit von Neuronen führen und könnte damit neurologische Krankheitsbilder wie Epilepsie oder Schmerz auslösen. Diese eindrucksvolle Komplexität der möglichen Reaktionen macht Häm zu einem vielseitigen Modulator neuronaler Erregbarkeit, der damit eine Vielzahl physiologischer Funktionen beeinflussen könnte.

Regulation of voltage gated potassium channels by heme

THESIS

for acquiring a
Doctor rerum naturalium
academic degree

**Presented to the Faculty of Biology and Pharmacy
Friedrich Schiller University of Jena**

by **Nirakar Sahoo, M.Sc.**

born on 01.07.1978 in Kendrapara, Orissa, India

Summary

Traditionally, heme was viewed as a stable prosthetic group, often conferring gas sensitivity as exemplified in cytochromes, hemoglobin, myoglobin, and soluble guanylyl cyclase. Emerging evidence suggests a new paradigm of the heme function: intracellular free heme may be a potent non-genomic modulator of ion channels. The large-conductance Ca^{2+} - and voltage-gated (Slo1 BK) K^+ channels inaugurated the role of heme as a direct regulator of ion channel function. It binds with high affinity to a classical “CxxCH” heme-binding motif in the C-terminus of the channel, leading to Slo1 BK current reduction. At this stage of our understanding, two questions arose. First, does heme modulate other ion channels? Second, what is the mechanism of heme-mediated modulation of ion channels? To address these questions, we screened several voltage-gated potassium channels heterologously expressed in *Xenopus* oocyte and mammalian cells, for heme effects using the inside-out patch-clamp technique. In this study we identified two additional classes of potassium channels to be modulated by heme: A-type and EAG potassium channels.

A-type potassium channels such as Kv1.4 are rapidly inactivating channels with importance in the initial notch of repolarization in cardiac cells and the fast-spiking behavior of some neurons. Hemin applied to the cytoplasmic side potently removed N-type inactivation of Kv1.4 channels with $\text{EC}_{50} \sim 24 \text{ nM}$. This effect was abolished by concurrent mutation of the cysteine (C13S) and histidine (H16A) residues in the ball domain of the Kv1.4 channel protein. The inactivation ball domain-hemin interaction was probed with a synthetic ball-domain. We found that this peptide interacts with hemin while a mutant peptide lacking C13 and H16 did not interact with hemin, suggesting a direct interaction of heme and the channel protein. A-type channels can also be formed by association of non-inactivating α -subunit, such as Kv1.1 and Kv1.5, with Kv β -subunits that provide inactivation ball domains and thereby induce fast inactivation. A sequence alignment of the ball domain of Kv β -subunits with Kv1.4 channels revealed that a potential heme binding site (CxxH) is present in some, but not all Kv β -subunits. We found that inactivation conferred by Kv β 1.1 subunits containing a CxxH motif was sensitive to hemin, while Kv β 1.3 subunits, lacking this motif, were unaffected by cytosolic hemin.

hEAG1 channels are depolarization-activated K^+ channels expressed abundantly in neuronal tissues, including the cerebral cortex and the hippocampus, and contributing to modulation of action potential firing pattern. SH-reagents such as DTNB applied from cytosolic side

inhibited hEAG1 current in a biphasic and gating dependent manner: a fast fraction modifies the gating property of the channel and a slow fraction gradually blocked the hEAG1 channel. Our systematic cysteine mutagenesis result revealed that concurrent mutation of C145, C214, C532 and C562A removes this oxidative sensitivity. The fast component was contributed by two cysteine residues (C145 and C214) in the N-terminus and voltage dependent, while the slow component was contributed by two cysteine residues (C532 and C562) in the C-linker region of the C-terminus, suggesting that cysteine oxidation might interfere the crosstalk between the N- and C-terminus of the hEAG1 channel.

Subsequently, we analyzed the impact of heme/hemin on hEAG1 channels. Hemin applied to the cytoplasmic side acutely and dramatically decreased hEAG1 current in cell-free membrane patches with a high affinity ($IC_{50} \sim 2$ nM), indicating that the hemin effect on hEAG1 is 10-40 fold more potent than on Kv1.4 and Slo1 channels. Our result also suggests that hemin alters the gating properties of hEAG1 channels. Furthermore, we provided evidence that hemin directly interacts with the hEAG1 channel, as revealed by hemin-agarose pull-down assay. Based on our initial hypothesis whether redox-sensitive cysteines take part in hemin sensitivity in hEAG1 channels, we found that oxidation insensitive channels still retained hemin sensitivity. Our systematic histidine mutagenesis, chimeric and spectroscopic study revealed that histidines might play a role in hemin sensitivity of hEAG1 channels.

The physiological significance of heme regulation of the A-type and hEAG1 potassium channels need to be elucidated in the future. It has been reported that intracellular free heme level can reach up as high as ~ 1 μ M, in line with K_m values for heme of heme oxygenase HO1 and HO2 are 1 μ M and 0.4 μ M. The comparison of these values to the low nanomolar hemin sensitivity of hEAG1 and Kv1.4 channels suggests that heme could be sufficient to regulate native hEAG1 and A-type K^+ channels *in vivo*. Pronounced slowing of A-type K^+ channel inactivation by hemin may inhibit the release of neurotransmitter, reducing excitotoxicity and probably induce neuroprotection. On the contrary, inhibition of hEAG1 channel may lead to hyperexcitability of neurons, inducing neurological disorders such as epilepsy or pain. This complexity is daunting but may render heme a versatile and multifaceted modulator with importance in a multitude of physiological functions.

Dedicated to my parents

Contents

| | |
|---|----|
| 1. Introduction..... | 1 |
| 1.1 Heme and heme degradation products (HHDPs) and their physiological functions | 1 |
| 1.1.1 Heme synthesis..... | 2 |
| 1.1.2 Physiological functions of heme..... | 2 |
| 1.1.3 Heme degradation..... | 4 |
| 1.1.3.1 Carbon monoxide..... | 4 |
| 1.1.3.2 Iron..... | 5 |
| 1.1.3.3 Biliverdin and bilirubin..... | 5 |
| 1.1.3.4 BOXes | 6 |
| 1.2 Ion channels..... | 6 |
| 1.2.1 Kv channels..... | 6 |
| 1.2.2 A-type potassium channels..... | 8 |
| 1.2.2.1 Kv1.4 potassium channel..... | 9 |
| 1.2.3 The EAG family..... | 10 |
| 1.2.3.1 EAG1 potassium channel..... | 10 |
| 1.3 Interaction of ion channels with heme and heme degradation products..... | 13 |
| 1.4 Objectives..... | 14 |
| 2. Materials and methods..... | 15 |
| 2.1 Materials..... | 15 |
| 2.1.1 Bacterial strains and cell lines..... | 15 |
| 2.1.2 Plasmids and vectors..... | 15 |
| 2.1.3 Other materials..... | 17 |
| 2.1.4 Buffers and solutions..... | 18 |
| 2.2 Methods..... | 20 |
| 2.2.1 Plasmid construction and mutagenesis..... | 20 |
| 2.2.2 Cell culture and transfection..... | 20 |
| 2.2.3 Hemin agarose pull-down assay..... | 21 |
| 2.2.4 SDS-PAGE and Western blot analysis..... | 21 |
| 2.2.5 Spectroscopic characterizations of hemin-peptide interaction..... | 22 |
| 2.2.6 Channel expression and electrophysiological measurements in <i>Xenopus</i> oocytes..... | 22 |
| 2.2.7 Channel expression and electrophysiological measurements in mammalian cells..... | 24 |
| 2.2.8 Data acquisition and analysis..... | 24 |
| 2.2.8.1 Analysis of Kv1.4 and Kv1.1/Kv β 1.1 current measurements..... | 24 |
| 2.2.8.2 Analysis of hEAG1 current measurements..... | 25 |
| 3. Results..... | 28 |
| 3.1 Intracellular hemin impairs inactivation of A-type potassium channels..... | 28 |

| | | |
|---------|---|----|
| 3.1.1 | Effects of intracellular hemin on Kv1.4 channel inactivation..... | 28 |
| 3.1.2 | Extracellular hemin does not modulate Kv1.4 inactivation..... | 31 |
| 3.1.3 | Effects of heme and heme-related chemicals on Kv1.4 inactivation..... | 32 |
| 3.1.4 | Hemin does not affect C-type inactivation of Kv1.4 channels..... | 33 |
| 3.1.5 | Elucidation of the molecular loci required for the heme action on Kv1.4 channels..... | 34 |
| 3.1.6 | Hemin interacts with the Kv1.4 inactivation peptide..... | 35 |
| 3.1.7 | Spectroscopic characterization of hemin-Kv1.4-IP interaction..... | 37 |
| 3.1.8 | Effect of hemin on rapid N-type inactivation induced by Kv β subunits.. | 38 |
| 3.2 | Oxidative modification of EAG1 potassium channels..... | 42 |
| 3.2.1 | Cytosolic cysteines are responsible for hEAG1 channel function..... | 42 |
| 3.2.2 | Time course of DTNB effect on hEAG1 potassium channels..... | 44 |
| 3.2.3 | DTNB alters the gating of hEAG1 potassium channels..... | 46 |
| 3.2.4 | Effects of DTNB on single-channel activity..... | 47 |
| 3.2.5 | Critical cysteines responsible for thiol-dependent modulation of hEAG1 channels..... | 48 |
| 3.2.5.1 | Concurrent mutation of C145, C214, C532 and C562A removes the oxidative sensitivity | 50 |
| 3.2.5.2 | Evaluation of critical cysteines via a knock-in approach..... | 51 |
| 3.3 | Heme is a potent inhibitor of EAG potassium channels..... | 54 |
| 3.3.1 | Effect of hemin on delayed rectifier potassium channels..... | 54 |
| 3.3.2 | Hemin reduces K ⁺ currents through hEAG1 potassium channels..... | 55 |
| 3.3.3 | Hemin inhibits hEAG1 channels in a voltage-dependent manner..... | 57 |
| 3.3.4 | Effects of heme and heme-related chemicals on hEAG1 channels..... | 58 |
| 3.3.5 | Pull-down assay for hemin binding to hEAG1 channels..... | 59 |
| 3.3.6 | Annotation of the molecular loci required for the hemin channel interaction..... | 60 |
| 3.3.6.1 | Histidine 364 in the S5 region and histidine 543 and 552 in the C-linker region may represent heme binding sites in hEAG1 channels..... | 64 |
| 3.3.6.2 | Chimeric approach to identify molecular loci required for the hemin-channel interaction..... | 66 |
| 4. | Discussion..... | 68 |
| 4.1 | Heme is a potent non-genomic modulator of ion channels..... | 68 |
| 4.2 | Free heme concentration inside the cell..... | 69 |
| 4.3 | Physiological and pathophysiological role of free heme..... | 71 |
| 4.4 | Mechanism of heme modulation of A-type potassium channels..... | 73 |
| 4.4.1 | The effect of hemin on N-type inactivation is specific..... | 73 |
| 4.4.2 | Identification of hemin target sites that regulate N-type inactivation..... | 74 |
| 4.4.3 | Different hemin sensitivities of Kv β 1.1 and Kv β 1.3..... | 75 |
| 4.4.4 | A model for hemin action on A-type channels..... | 76 |
| 4.5 | Possible physiological role of heme modulation of A-type potassium channels..... | 78 |
| 4.6 | Mechanism of heme modulation of EAG1 potassium channels..... | 80 |

| | | |
|---------|--|-----|
| 4.6.1 | Identification of hemin target sites that regulate hEAG1 channel function | 81 |
| 4.6.1.1 | Evaluation of critical cysteine residues responsible for hEAG1 channel function..... | 81 |
| 4.6.1.2 | Hemin interacts with the histidine residues of hEAG1 channels..... | 83 |
| 4.6.1.3 | A chimeric approach narrowed down the hemin binding site on hEAG1 channels..... | 84 |
| 4.7 | Possible physiological role of heme modulation of hEAG1 potassium channels. | 87 |
| 5. | Outlook..... | 89 |
| 6. | References..... | 90 |
| 7. | Appendix..... | 104 |

1. Introduction

1.1 Heme and heme degradation products (HHDPs) and their physiological functions

Heme is the most ubiquitous cofactor found in nature and the most functionally diverse. Heme plays an essential role in various biological reactions, such as oxygen transport, respiration, drug detoxification and signal transduction (Ponka, 1999). It interacts with various inactive apo-proteins giving rise to functional heme–proteins. The ability of hemoproteins to catalyze extremely diverse reactions arises largely from the protein environment in which the heme molecule resides and specifically the nature of the heme–ligands (Dawson, 1988). Structurally, heme is a metallo-compound composed of iron atom complexes with the tetrapyrrole ring protoporphyrin through its 4 nitrogen atoms (Kaplan, 1977). The iron center of heme exists in 2 states: in the ferrous state, the complex is called ferroprotoporphyrin or heme, and the molecule is electrically neutral and the ferric state, the complex is called ferriprotoporphyrin or hemin, and the molecule carries a unit positive charge and is consequently associated with an anion (Fig. 1).

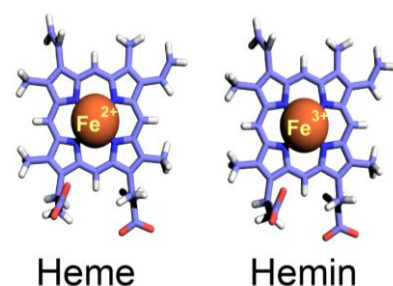


Fig. 1: Schematic representation of heme and hemin.

Three types of heme are known in eukaryotes: protoheme and heme *a*, *b* and *c* (Tyler, 1992). Protoheme is a pool of “free heme” that is not associated or is only loosely associated with proteins (i.e. tryptophan pyrrolase) (Badawy, 1978) and is the precursor for the other types of heme. Heme *b* and *c* are essentially similar to protoheme, with minor modifications (Tyler, 1992). Hemoglobin, cytochrome P450, Catalase, and mitochondrial complexes II and III consist of heme *b*, while heme *c* is present in cytochrome *c* and cytochrome *c1* of complex III. Heme *a*, is synthesized from protoheme by two modifications: farnesylation and addition of a formyl group to position 8 of the protoheme (Mogi et al., 1994; Weinstein et al., 1986). Subunit I of complex IV of cytochrome *c* oxidase consist of two groups of heme *a* and *a3* (Tyler, 1992).

1.1.1 Heme synthesis

Heme synthesis is a multistep process that mainly occurs in liver and erythroid tissues where most of the heme is incorporated into cytochrome P450 and hemoglobin. It is accepted that 75-80% of heme is synthesized in bone marrow cells, and the liver is responsible for 15-20% of heme production (Berk et al., 1976, 1979). Heme biosynthesis involves eight enzymatic steps in the conversion of glycine and succinyl-coenzyme A (CoA) to heme (Fig. 2). The first and last three enzymes in the pathway are located in the mitochondria, whereas the other four are in the cytosol (Woodard and Dailey, 2000). Heme synthesis begins with condensation of glycine and succinyl-CoA in mitochondria, a reaction catalyzed by the first enzyme in the pathway, 5-aminolevulinate synthase (ALAS). In the final step, ferrous iron is inserted into protoporphyrin IX to form heme, a reaction catalyzed by the eighth enzyme in the pathway, ferrochelatase (also known as heme synthetase or protoheme ferrolyase) (Kaplan, 1977; Woodard and Dailey, 2000). Heme synthesized in mitochondria is then transported into the cytosol to bind to apo-proteins and to form hemoproteins (Taketani, 2005).

Regulation of heme synthesis differs in the liver and erythroid tissues. Regulation is needed to maintain relatively low levels of intracellular heme. In the liver, “free” heme regulates the synthesis of 5-aminolevulinate synthase (ALAS1). Heme represses the synthesis of ALAS1 mRNA and interferes with the transport of the enzyme from the cytosol into mitochondria (May et al., 1995). The differentiating erythroid cells must produce massive amounts of heme during a short period to satisfy the needs of hemoglobinization. In erythroid precursor cells the erythroid-specific ALAS2 is expressed at higher levels than the hepatic enzyme, and all pathway enzymes are induced via erythroid-specific regulatory elements located in the 5' end of the mRNA (Kaya et al., 1994).

1.1.2 Physiological functions of heme

Biological systems depend on heme-proteins to serve several essential functions for their survival. Heme is required for a variety of heme proteins, such as hemoglobin, myoglobin, respiratory cytochromes, the cytochrome P450 enzymes (CYPs), oxidases, and catalases. All these proteins are vital to processes such as oxygen transport, xenobiotic detoxification, oxidative metabolism, and thyroid hormone synthesis (Tsiftoglou et al., 2006).

Heme has been shown to be a key modulator of several processes at the transcriptional level. The first evidence that heme regulates transcription came from the iso-1-cytochrome *c* gene (CYC1) of the electron transport chain in yeast. Transcription of CYC1 was reduced 200-fold

in cells grown in heme deficient conditions (Guarente and Mason, 1983). In mammals, respiration is transcriptionally controlled by the amount of available heme. The transcriptional regulation of globin chain by heme is mediated through Bach1, the first mammalian transcription factor shown to bind heme. Bach1 binds DNA and represses transcription when it is not bound to heme. Therefore Bach1- mediated repression only occurs in low heme conditions (Tahara et al., 2004; Sinclair, 2008). Heme has also been shown to repress transcription of tartrate-resistant phosphatase (TRAP), an iron-containing protein that may function in iron homeostasis (Reddy et al., 1996).

Another family of hemoproteins is the heme-based sensor family. These proteins are key regulators of adaptive responses to changing levels of oxygen, carbon monoxide, and nitric oxide. More than 100 heme-based sensors have been investigated in bacteria and mammalian cells.

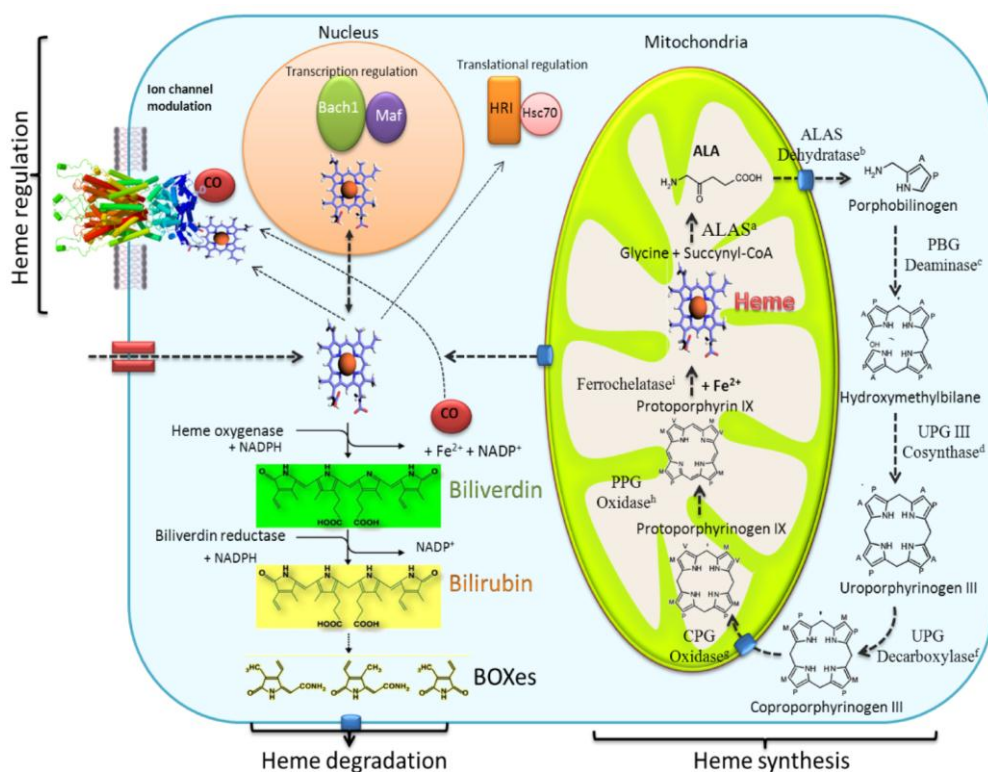


Fig. 2: Schematic diagram depicting heme homeostasis: synthesis, degradation and regulation.

The heme-based sensors are categorized into 6 different types of heme-binding modules: the heme-binding PAS domain, globin-coupled sensor (GCS), CooA, heme-NO-binding (HNOB) domain, heme-binding GAF domain, and heme-associated ligand-binding domains (LBD) of the nuclear-receptor class groups (Gilles-Gonzalez and Gonzalez, 2005).

Heme also plays a regulatory role in many physiological processes including cell growth, cell cycle progression, cellular differentiation, gene regulation, and microRNA processing. Heme promotes cellular differentiation in PC12 pro-neuronal cells and K562 erythroid cells (Mense and Zhang, 2006). In HeLa cancer cells, heme directly controls the cell cycle and promotes cell growth, by acting on two key cell cycle regulators, cyclin-dependent kinases (CDKs) and p53 (Ye and Zhang, 2004).

1.1.3 Heme degradation

Heme is essential for life, but excess heme is toxic to the cell. In order to maintain intracellular heme at low levels, multiple mechanisms exist; one of the regulatory mechanisms is catabolism of heme which produces biliverdin, CO, bilirubin and boxes (Fig. 2). Heme oxygenase is the first and the rate-limiting enzyme of the microsomal heme degradation pathway that yields biliverdin, carbon monoxide (CO), and iron (Maines, 1988). There are three forms of heme oxygenase (HO): the 33 kDa inducible heme oxygenase 1 (HO1) is a heat-shock protein that is induced by heme, iron, heat shock, free radicals, and other stimuli in a variety of cells, including vascular smooth muscle cells, macrophages, brain microglia, and participates in cellular defense mechanisms and its induction in mammalian cells is an indicator of oxidative stress (Maines, 2000). Heme oxygenase 2 (HO2), a 36 kDa protein, constitutively expressed in a variety of cells such as neurons and vascular endothelial cells, confers neuroprotection in the developing brain (Maines, 2000). Heme oxygenase 3 (HO3), a third isoform is not catalytically active, but is thought to take part in oxygen sensing (McCoubrey et al., 1997).

1.1.3.1 Carbon monoxide

The carbon monoxide (CO) released directly from heme during HO activity may function as a soluble second messenger molecule in a fashion similar to the free radical gas NO• (Verma et al., 1993). CO is the diatomic oxide of carbon and a colorless and odorless gas. CO is considered as a “silent killer”. An increase in ambient CO level leads to human intoxication. Elevated CO concentration in the bloodstream facilitates binding of CO to normal adult hemoglobin (HbA), forming COHb, which reduces the oxygen storage function of HbA and causes hypoxia. The brain and heart are the organs most vulnerable to CO-induced acute hypoxia, due to their high demand for oxygen (Stewart, 1975; Wu and Wang, 2005). In recent years, several studies have reported that CO is also generated endogenously produced, and that under specific pathophysiological conditions CO production is greatly increased. The

predominant biological source of CO (> 86%) is from the catabolism of heme by the enzyme heme oxygenase (HO) with minor amounts formed by lipid peroxidation, photo-oxidation, and xenobiotic metabolism (Wu and Wang, 2005). The production rate of CO is 16 $\mu\text{mol/h}$ in the human body (Coburn, 1970) and the daily production of CO is substantial, reaching more than 12 ml (500 μmol) (Coburn et al., 1965).

There are wide ranges of physiological effects of CO documented in the literature. CO can act as an anti-inflammatory. It attenuates endotoxic shock (Otterbein et al., 2000) and also reduces allergic inflammation by blocking eosinophil flux and IL-5 production (Chapman et al., 2001). CO protects against ischemia (Amersi et al., 2002) and pancreatic β cells from apoptosis (Gunther et al., 2002). CO also protects against hyperoxia, pre-exposure of a rat to CO gas protected its lung from oxidative injury (Stupfel and Bouley, 1970). CO modulates spermatogenesis under conditions of stress (Ozawa et al., 2002) and also regulates blood pressure under stress conditions (Motterlini et al., 1998).

1.1.3.2 Iron

Little is known about the immediate consequences of HO-mediated iron release, nor the immediate molecular acceptor of this “free iron”. It has been reported that iron released from heme is mobilized into bone marrow for reincorporation into newly synthesized heme in mitochondria and the residual iron is stored in transferrin extracellularly or, ferritin intracellularly. Free form of iron can interact with H_2O_2 and produce hydroxyl free radicals which may oxidize bilirubin, biliverdin or heme (Nagababu and Rifkind, 2004).

1.1.3.3 Biliverdin and bilirubin

Biliverdin and bilirubin released by breakdown of heme possess in vitro antioxidant properties (Stocker et al., 1987). The hydrophobic bilirubin is produced by the reduction of water soluble biliverdin by the cytoplasmic NADPH biliverdin reductase enzyme (Tenhunen et al., 1970). The immediate consequences of intracellular bilirubin formation are poorly understood. Bilirubin is generally regarded as a toxic compound when accumulated at abnormally high concentrations in biological tissues and is responsible for the clinical symptoms of kernicterus (Heirwegh and Brown, 1982). The bilirubin formed in the various tissues effluxes into blood serum where it forms a complex with albumin. It is taken up by hepatocytes by facilitated diffusion, stored in hepatocytes bound to glutathione-S-transferases and which then undergoes phase-II glucuronidation by uridine diphosphate: glucuronosyl

transferase, forming water soluble mono and di-glucuronides, which are eliminated by the bile and feces (Wang et al., 2006).

1.1.3.4 BOXes

A recent finding of Clark and co-workers (Kranc et al., 2000; Clark and Pyne-Geithman, 2005) has found the existence of bilirubin oxidation end products abbreviated as BOXes (see also Fig. 2). There are two isomers of the BOXes formed from the two ends of the bilirubin molecule (differing by the position of the methyl and vinyl groups), as BOX A and BOX B (Kranc et al., 2000), however, no significant differences in the biologic activity of BOX A and BOX B were observed. BOXes are found in the brain after experimental intracerebral hemorrhage (Clark et al., 2008) as well as clinically post-subarachnoid hemorrhage (SAH) and are known to play a role in SAH-induced vasospasm and are vasoactive *in vivo*, constricting rat cerebral vessels (Pyne-Geithman et al., 2005).

1.2 Ion channels

Ion channels play an important role in a wide range of physiological functions such as generation of electrical activity in nerves and muscle, control of cardiac excitability, intracellular signaling, hormone secretion, cell proliferation, cell volume regulation, and many other biological processes. These pore-forming proteins allow the flow of ions across the plasma membrane and are classified according to their ion selectivity for example sodium, potassium, calcium, chloride channels. Among the entire ion channels, potassium channels represent a largest group of ion channels. The K^+ channel structures fall into three major groups: comprising either two passes (2TM), four passes (4TM), or six passes (6TM) through the membrane. The 2TM channels form a large group (at least 12 members) of inward rectifying K^+ channels (Kirs), the 4TM channels form a group of at least 11 so-called 'leak' channels, (Goldstein et al., 2001) and the very large group of 6TM channels are subdivided into the families of voltage-gated delayed-rectifier (Kv) channels, Ca^{2+} -activated K^+ channels, hyperpolarization- and cyclic-nucleotide gated channels (Gutman et al., 2005).

1.2.1 Kv channels

Kv channels constitute about half of the known K^+ channels in the human genome (Gutman et al., 2005).

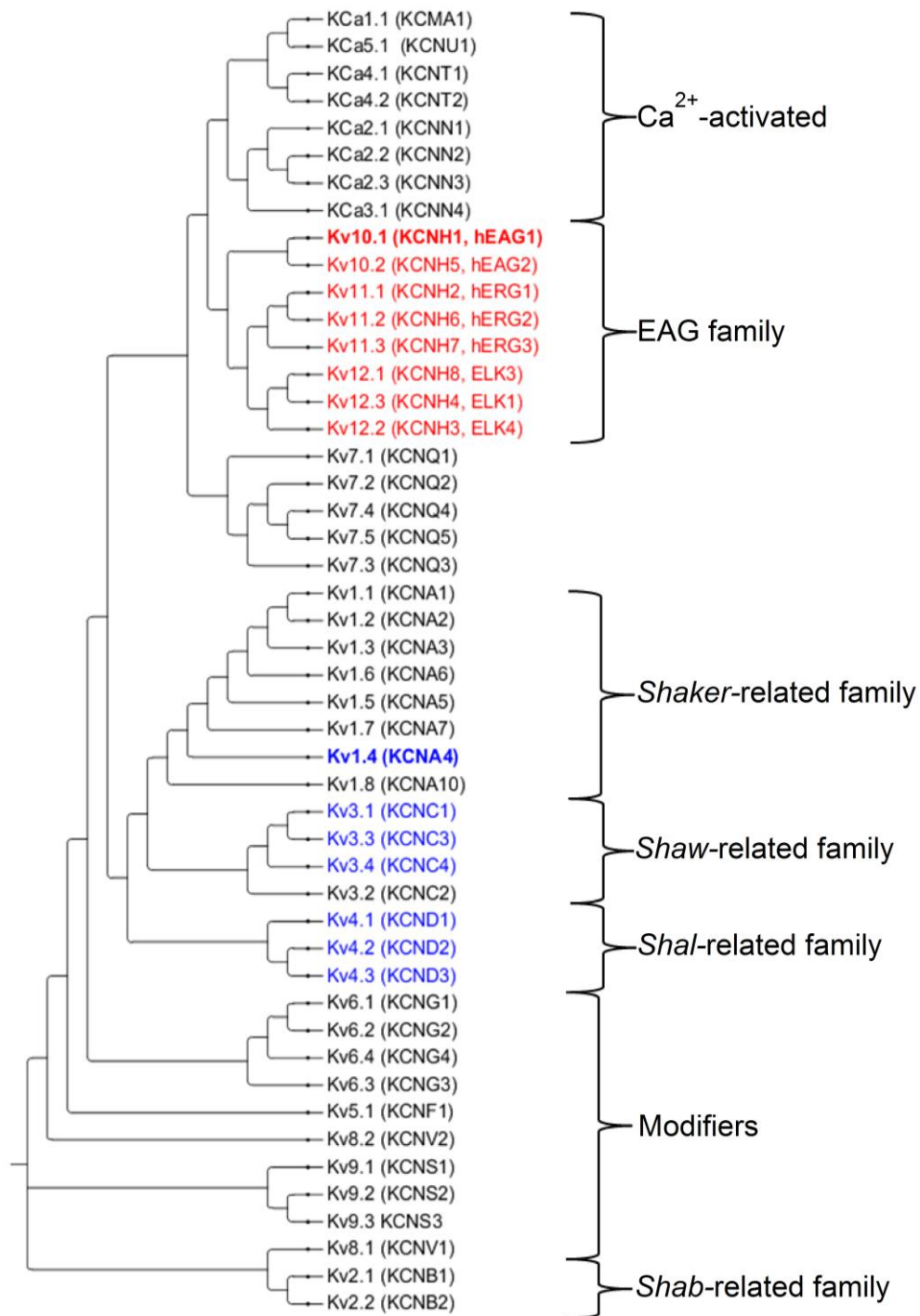


Fig. 3: Phylogenetic tree for the Kv1–9 and Ca²⁺-activated channel families. The phylogenetic tree was constructed using Vector NTI (Invitrogen) and processed with treegraph2 (treegraph.bioinfweb.info). The International Union of Pharmacology (IUPHAR), HUGO Gene Nomenclature Committee (HGNC) and commonly used names are shown together. EAG family and A-type potassium channels are marked red and blue, respectively.

All the Kv channel subunits have a 6TM topology with a “P-loop” region between the fifth and sixth transmembrane segments that forms the K⁺ selectivity filter and positively-charged residues in the fourth transmembrane segment constitute the voltage sensor. Four subunits

assemble to a functional channel (Doyle et al., 1998). Kv channels are categorized into four groups: (a) the Shaker/Shab/Shaw/Shal-related families: Kv1.x (KCNAx), Kv2.x (KCNBx), Kv3.x (KCNCx) and Kv4.x (KCNDx), (b) the KCNQ sub-family: Kv7.x, (c) Kv modifying sub-family: Kv5.x (KCNFx), Kv6.x (KCNGx), Kv8.x (KCNVx) and Kv9.x (KCNStx), and (d) the EAG sub-family: Kv10.x, Kv11.x and Kv12.x (KCNHx) (Gutman et al., 2005) (Fig. 3).

1.2.2 A-type potassium channels

By using time dependence as a basis for classification, Kv currents can be classified into two categories: slow “delayed rectifier” currents and rapid “A-type” currents. The delayed rectifier type possesses delayed onset of activation followed by little or slow inactivation, while, A-type possesses rapid rates of inactivation. Strong steady-state, voltage-dependent inactivation is a feature typical of A-type currents. The inactivation of A-type potassium channels can be divided into fast and slow processes (Hoshi et al., 1990, 1991). The fast inactivation is initiated by the N-terminus, and was early named “N-type inactivation”, while the slow inactivation originally was suggested to be related to the C-terminus, and was consequently named “C-type inactivation” (Hoshi et al., 1990, 1991). The N-type inactivation is due to a “ball-and-chain” mechanism, the plugging of the internal mouth of the channel with its N-terminus (Hoshi et al., 1990; Zagotta et al., 1990; Hoshi et al., 1991) (Fig. 4B). N-type inactivation is abolished by deletion or enzymatic removal of the N-terminus, and can be restored by intracellular application of peptides derived from the N-terminus of one of many N-type inactivating channels (Antz et al., 1999; Zagotta et al., 1990). A single inactivation domain is sufficient to confer N-type inactivation (MacKinnon et al., 1993; Lee et al., 1996). Inhibition by 4-aminopyridine (4-AP) and insensitivity to extracellular tetraethyl ammonium (TEA) ions are considered to be pharmacological hallmarks of A-type currents (Thompson et al., 1977). The A-type potassium channels were divided into 3 major types: (a) Kv α 1.x - Shaker-related: Kv1.4 (KCNA4), (b) Kv α 3.x - Shaw-related: Kv3.3 (KCNC3), Kv3.4 (KCNC4) and (c) Kv α 4.x - Shal-related: Kv4.1 (KCND1), Kv4.2 (KCND2), Kv4.3 (KCND3) (Fig. 3). Although only a limited number of Kv α -subunit channels demonstrate N-type inactivation on their own, auxiliary cytoplasmic β -subunits with a similar N-terminal “ball” domain may also interact with Kv1 family α -subunits to create an N-type inactivating A-type channel (Rettig et al., 1994; Heinemann et al., 1996) (Fig. 4A).

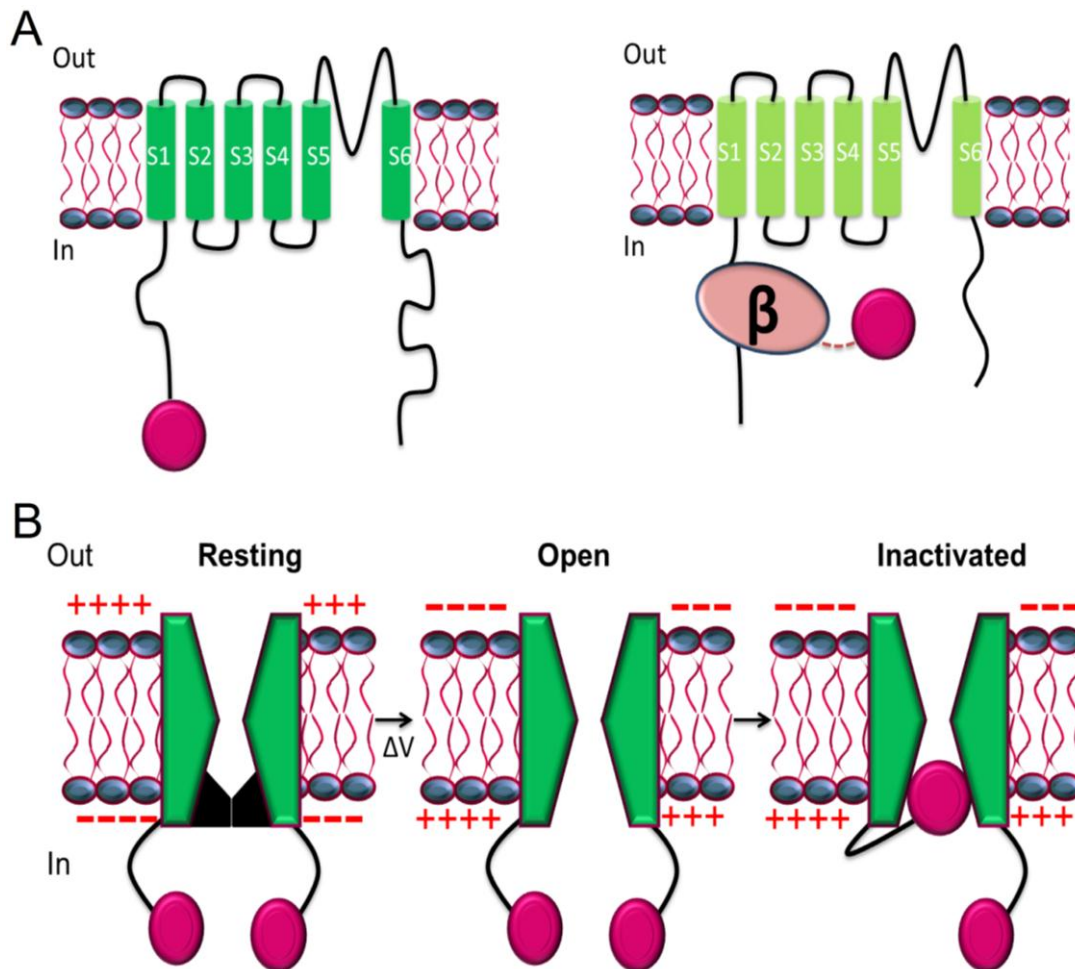


Fig. 4: Architectures of A-type potassium channels. (A) Representation of an α -subunit of Kv1.4 channels (left) and delayed rectifier channels co-assembled with an accessory β -subunit (right). The N-terminus of Kv1.4 and β -subunits bear a ball domain that is responsible for fast N-type inactivation. (B) A simplified diagram illustrates the N-type ball-chain inactivation: A-type channels are usually silent at resting membrane potentials. On depolarization, the channels first open by transition of the activation gate(s) and then enter a long-living non-conducting state, the inactivated state. The latter result from inactivation particle (ball) that binds to its receptor, once exposed by channel activation, and thereby physically occludes the ion pore.

1.2.2.1 Kv1.4 potassium channel

The Kv1.4 gene was the first mammalian gene identified that encoded rapidly inactivating or transient K^+ channels. Kv1.4 exhibits rapid “ball-and-chain”-type inactivation gating, along with slow C-type inactivation gating (Stühmer et al., 1989; Tseng-Crank et al., 1990). Kv1.4 channels are present in nerve terminals, axons and in many areas of the brain, including cells that secrete glutamate and other excitatory neurotransmitters (Sheng et al., 1992). It has been reported that Kv1.4 channels present in axons and nerve terminals plays a vital role in the regulation of presynaptic spike duration, Ca^{2+} entry, and neurotransmitter release (Lipton and Rosenberg, 1994).

In the hippocampus, Kv1.4 immunoreactivity is detected at greatest density in two regions: (a) the middle molecular layer (MML), where perforant path axons synapse with dentate granule cells, and (b) the *stratum lucidum* (SL) of CA3, where the mossy fibers travel in tight fasciculi and form en passant synapses onto CA3 pyramidal cells (Cooper et al., 1998). In a recent study Prüss et al. (2010) found temporal age-dependent expression of Kv1.4 with Kv1.1, Kv1.2, and Kv3.4 channels during postnatal hippocampal development. This age-dependent expression is thought to link neuronal activity with hippocampal network maturation. Kv1.4 channels are also expressed in small diameter (A δ and C fiber) dorsal root ganglion (DRG) neurons and a great reduction in Kv1.4 expression was found after nerve injury (Rasband et al., 2001). Furthermore, Kv1.4 is coexpressed with TRPV1, TRPV2 and cannabinoid receptors 1 (CB1) in nociceptive DRG neurons, and probably plays a role in pain signaling (Binzen et al., 2006). In addition, Kv1.4 channels may underlie the transient outward K⁺ current (I_{to}) in cardiac muscle and contribute to the initial repolarization phase of cardiac action potentials (Tseng-Crank et al., 1990).

1.2.3 The EAG family

The term EAG stands for Ether à go-go as the gene as originally identified in *Drosophila melanogaster* mutants that exhibit leg-shaking behavior under ether anesthesia (Kaplan and Trout, 1969). This shaking movement was similar to a dance performed in the late 60s at the popular night-club in West Hollywood, the Whisky à Go-Go. The identity as an ion channel gene was not appreciated until later studies that found an enhancement of neurotransmission defects in *eag*/Shaker double mutants (Ganetzky and Wu, 1983). Molecular studies and sequence comparison resulted in the classification of EAG into a distinct potassium channel group: the EAG family. The EAG family consisting of 3 sub-families (a) EAG (b) EAG-related gene (ERG) and (c) EAG-like K⁺ channel (ELK) (Fig. 3). The first cloned mammalian EAG channels were the mouse EAG1 and the human ERG1 (HERG) channel (Warmke and Ganetzky, 1994). The EAG family comprises of 8 channels: two EAG (EAG1: Ludwig et al., 1994; EAG2: Saganich et al., 1999), three ERG (ERG1: Sanguinetti et al., 1995; ERG2, ERG3: Shi et al., 1997) and three ELK channels (Engeland et al., 1998; Shi et al., 1998) (Fig. 3).

1.2.3.1 EAG1 potassium channel

EAG1 is the founding member of the EAG family, which contain a Per-Arnt-Sim (PAS) domain in the N-terminus (Morais Cabral et al., 1998), a signature GFG motif that forms the

K⁺ ion selectivity filter, and a cyclic nucleotide binding domain (cNBD) within the C-terminus. In addition the EAG channel harbors 3 calmodulin-binding motifs in the N and C-terminus (Fig. 5).

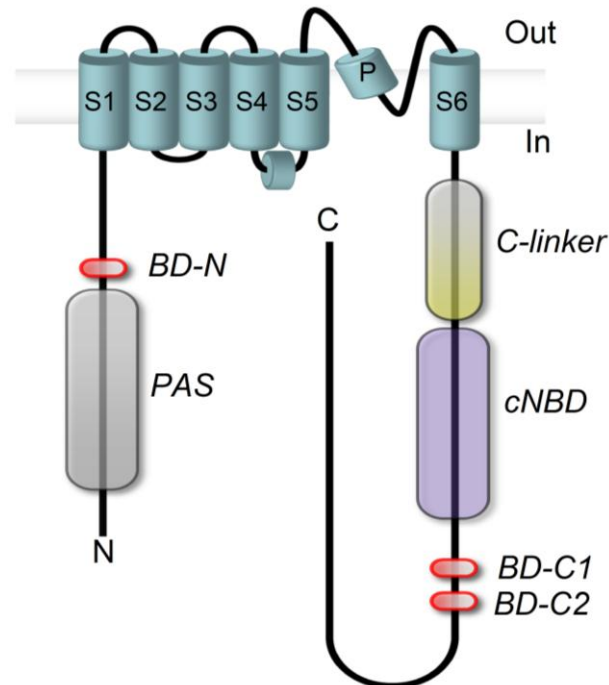


Fig. 5. An overview of the EAG channel. Schematic representation of a single hEAG1 α -subunit: S1-S6 represents transmembrane helices. The N- and C-termini are believed to be located intracellularly. Characteristic domains are: *PAS*: Per-Arnt-Sim domain, *cNBD*: cyclic nucleotide binding domain, *BD-N*, *BD-C1* and *BD-C2*: Calmodulin binding sites, *C-linker*: The linker between the last transmembrane segment (S6 gate) and cNBD domain.

Mammalian EAG1 channels activate slowly and do not inactivate during a sustained depolarization. Moreover, voltage dependent activation of EAG channels is strongly dependent on the holding potential and the time course of the activation is slowed down by negative prepulses, an effect similar to the Cole-Moore shift (Ludwig et al., 1994). In addition, activation slows down further in the presence of extracellular Mg²⁺ in the millimolar range (Terlau et al., 1996). This Cole-Moore shift of EAG1 currents is so distinctive that its occurrence is a strong indication for the presence of native EAG1 channels (Meyer and Heinemann, 1998). Pharmacologically, EAG1 channels are sensitive to Ba²⁺ and quinidine (Ludwig et al., 1994) and exhibit very low sensitivity to classical channel blockers like tetraethyl ammonium (TEA) or 4-amino-pyridine or the HERG blocker E4031 (Saganich et al., 1999; Engeland et al., 1998).

A role for EAG1 in neuronal function was first suggested by an ether-induced leg shaking phenotype associated with EAG, as well as Sh and Hk, mutants (Kaplan and Trout, 1969; Warmke et al., 1991). This initial observation, along with later ones showing physiological and behavioral defects in EAG mutants (Warmke et al., 1991), demonstrates that the EAG channel is an important player in neuronal function. In mammals, EAG is widely expressed in the nervous system, including the CA1 and CA3 regions of the hippocampus, neocortex, olfactory bulb, retinal ganglion, photoreceptors, cochlear spiral ligament, and skeletal muscle (Frings et al., 1998; Lecain et al., 1999; Ludwig et al., 1994; Occhiodoro et al., 1998). In-situ hybridization studies have detected EAG1 transcripts predominantly in the hippocampus, cerebral cortex, olfactory bulb and granular layer of the cerebellum of adult rats (Ludwig et al., 2000; Saganich et al., 2001). A study by Gomez-Varela et al. has visualized the endogenous EAG1 channels entering and leaving synapses by lateral diffusion in the plasma membrane of rat hippocampal neurons by using a specific extracellular antibody and single-particle-tracking techniques with quantum dots nanocrystals. This provided first evidence of the real-time visualization of an endogenous EAG1 channels in neurons (Gomez-Varela et al., 2010).

EAG1 channels may be involved in auditory transduction in the cochlea. Rat EAG1 mRNA has been detected in the organ of Corti and in the fibrocytes of the spiral ligament (Lecain et al., 1999). However, no genetic deafness or hearing impairments have yet been linked to the human EAG1 gene. EAG1 also may play a role in phototransduction. In-situ hybridization of bovine retinal tissue localizes two alternatively spliced EAG1 channel transcripts (bEAG1 and bEAG2) to photoreceptors and retinal ganglion cells (Frings et al., 1998). They probably contribute to an outward K^+ current, named IKx, which stabilizes the dark resting potential and accelerates the voltage response to small photocurrents (Beech and Barnes, 1989). EAG1 channels were described for differentiating human myoblasts. Undifferentiated myoblasts have a resting membrane potential of about -10 mV, which upon transient expression of a non-inactivating K^+ current IK (ni), carried by human EAG1 channels, causes hyperpolarization of the membrane of about -30 mV, resulting in induction of myoblasts differentiation (Occhiodoro et al., 1998; Bauer and Schwarz, 2001).

Apart from their physiological function, EAG1 channels were abnormally up-regulated in many cancer cells while absent from the corresponding healthy tissues. These include breast carcinoma lines (MCF7, EFM-19 and BT-474), cervical carcinoma (HeLa) and neuroblastomas (Pardo et al., 1999; Meyer and Heinemann, 1998), melanomas (Meyer et al.,

1999), soft tissue sarcoma (Mello de Queiroz et al., 2006), gliomas (Patt et al., 2004), gastric cancer, colorectal cancer and esophageal squamous cell carcinomas (Ding et al., 2007, 2008). In addition, when EAG1 channels are transfected to CHO cells they result in tumor growth in xenograft mouse model, increased cell proliferation rate, and oncogenic properties such as loss of contact inhibition and substrate independence (Pardo et al., 1999). The specific blockade of hEAG1 by monoclonal antibodies inhibited tumor cell growth both *in vitro* and *in vivo* (Gomez-Varela et al., 2007). This provides a proof of concept that EAG1 is a promising target for novel cancer drugs, as well as a potential marker for early tumor detection and diagnosis (Pardo et al., 2005).

1.3 Interaction of ion channels with heme and heme degradation products

The past few years have witnessed intense research into the biological significance of heme as an essential ion channel modulator. The first report came in 2003 when T. Hoshis laboratory found that heme can bind and inhibit voltage-gated large conductance calcium-activated (Slo1) potassium channels (Tang et al., 2003). These channels are expressed in almost every tissue in our body and are essential for the regulation of several key physiological processes including neuronal excitability, vascular tone regulation, and neurotransmitter release (Hou et al., 2009). The interaction of heme with the channel was mediated by a classical cytochrome *c* heme-binding motif “CxxCH” present in the linker segment between the regulator of K⁺ conductance (RCK) domains (Tang et al., 2003). Mutation in the potential heme-binding site (C615S or H616R or C615S:H616R) rendered the channel insensitive to heme (Tang et al., 2003; Jaggar et al., 2005). The inhibitory effect was quite potent; the IC₅₀ value was ~70 nM in the absence of cytoplasmic Ca²⁺. The concentration dependence suggested that the Slo1 channel is more sensitive to heme than the transcription factors HAP1 and Bach1 (Zhang and Hach, 1999; Ogawa et al., 2001).

The heme degradation product carbon monoxide also modulates Slo1 channel function. CO causes relaxation of vascular smooth muscle tone by interacting with Slo1 channels (Wang and Wu, 1997). A recent study by Hou et al. revealed the mechanism of CO modulation of Slo1 channels. CO gas and the CO donor (CORM2) consistently and repeatedly increased open probability of Slo1 channels in HEK 293 cells. The stimulatory action of CO on the Slo1 BK channel requires an aspartic acid and two histidine residues located in the cytoplasmic RCK1 domain (Hou et al., 2008).

Another study also revealed that the bilirubin oxidation end products (BOXes) altered functional properties of the Slo1 channel. Application of BOXes to the cytoplasmic side of a membrane patch containing Slo1 channels progressively decreased the current. The channel sensitivity to BOXes requires two specific lysine residues located downstream of the S6 transmembrane segment in the primary sequence (Hou et al., 2010).

1.4 Objectives

The discovery of heme modulation of Slo1 potassium channels opened a new age of heme signaling and also opened potentially highly significant areas of investigation. At this stage of our understanding, two questions arose. First, does heme modulate other ion channels? Second, what is the mechanism of heme-mediated modulation of ion channels?

To address these questions, we screened several voltage-gated potassium channels for heme effect using the patch-clamp technique (inside-out). We found that two voltage gated potassium channels are modulated by heme: Kv1.4 and hEAG1 potassium channels. Kv1.4 is a rapidly inactivating A-type potassium channel, present in the hippocampus, DRG neurons and heart. Our study indicates that heme/hemin selectively interfere the fast inactivation of Kv1.4 channels. The following points were addressed in this study: (a) characterization of the heme/hemin effects on the Kv1.4 channel, (b) Elucidation of the molecular loci required for the heme-channel interaction, and (c) Investigation of whether heme/hemin confers sensitivity to other A-type potassium channels.

It has been reported that reversible binding of heme to the heme-regulated initiation factor eIF-2 alpha kinase (HRI) involved in genomic actions of heme, is dependent on its cysteine residues, potentially causing their oxidation (Yang et al., 1992). Studies on Kv1.4 channels suggest that a cysteine residue inside the ball domain is known to be responsible for redox regulation of fast N-type inactivation (Ruppersberg et al., 1991; Stephens et al., 1996; Rettig et al., 1994). This observation prompted us to study the role of cysteine residues in hEAG1 for their redox modulation by sulfhydryl-modifying (SH) reagents. The α -subunits of hEAG1 channels harbor 19 cysteine residues that are distributed throughout the major cytosolic domains such as PAS domain, C-linker and CNG- binding domain. Our study indicates that 4 critical cysteines in the N and C-terminus are responsible for hEAG1 function. Subsequently, we characterized the effects heme/hemin on the hEAG1 channels and elucidated the gating transitions regulated by hemin. In addition, we analyzed the molecular loci required for the hemin-hEAG1 channel interaction.

2. Materials and Methods

2.1 Materials

2.1.1 Bacterial strains and cell lines

E.coli strains

XL1 Blue- for cloning recombinant DNA (Stratagene)

C29251 *dam*⁻/*dcm*⁻ - for cloning methylated DNA (New England Biolabs)

Cell lines

HEK293- human, transformed, embryonic kidney fibroblasts (German Collection of Microorganisms and Cell Culture, DSMZ, Braunschweig, Germany)

2.1.2 Plasmids and vectors

Available vectors

pcDNA3- for transient CMV promoter-driven expression in mammalian cells (Invitrogen)

pGEM-HE- for transient T7 promoter-driven expression in *Xenopus* oocytes

p21-1- for transient SP6 promoter-driven expression in *Xenopus* oocytes

Table 1: List of plasmids and constructs used from the laboratory (CMB)

| Gene | Expression plasmid | Restriction enzyme for linearization and promoter for mRNA synthesis | Source |
|-------------|--------------------|--|----------------------|
| rKv1.1 | rKv1.1-pGEM-HE | <i>NheI</i> -T7 | Lab |
| hKv1.5 | hKv1.5-HE | <i>EcoRI</i> -T7 | Lab |
| rKv1.4 | rKv1.4-p21-1 | <i>Sall</i> -SP6 | Lab |
| rKv1.4 C13S | rKv1.4 C13S-p21-1 | <i>Sall</i> -SP6 | Lab |
| hKvβ1.1 | pβ1 | <i>Sall</i> -SP6 | Lab |
| hKvβ1.3 | hKvB1.3- pSP64T | <i>EcoRI</i> -T7 | Gift from Dr. Decher |
| mKv1.3 | mKv1.3-p21-1 | <i>EcoRI</i> -T7 | Lab |
| hCD8 | pCD8 | CMV | Gift from Dr. Seed |

Table 2: List of DNA constructs or mutants generated during this work. All hEAG1 mutants were cloned in plasmid pGEM-HE, linearized with *NheI* and promoter T7 was used for RNA synthesis. Kv1.4 mutants were cloned in plasmid p21-1, linearized with *SalI* and promoter SP6 was used for RNA synthesis.

| Mutants | Mutants | Mutants | Mutants |
|---|---|--|---|
| hEAG1 C50A | hEAG1 C67A | hEAG1 C128A | hEAG1 C145A |
| hEAG1 C214A | hEAG1 C303A | hEAG1 C357A | hEAG1C357V |
| hEAG1 C368A | hEAG1 C368V | hEAG1 C532A | hEAG1 C532S |
| hEAG1 C541A | hEAG1 C562A | hEAG1 C575A | hEAG1 C592A |
| hEAG1 C631A | hEAG1 C640A | hAG1 C794A | hEAG1 C804A |
| hEAG1 C817A | hEAG1 C853A | hEAG1 C145A-C214A | hEAG1 C532A-C562A |
| hEAG1 C145-562A (C145A-C214A-C532A- C562A) | hEAG1 Cysless-T (C303A-C357V-C368V) | Cysless-N (C50A-C67A- C128A-C145A-C214A) | Cysless-C (C532A- C541A-C562A-C575A- C592A-C631A-C640A- C794A-C804A- C817A- C853A) |
| hEAG1 Cysless-NC (C50A-C67A-C128A- C145A-C214A-C532A- C541A-C562A-C575A- C592A-C631A-C640A- C794A-C804A-C817A- C853A) | hEAG1 A214C-NC (C50A-C67A-C128A- C145A-C532A-C541A- C562A-C575A-C592A- C631A-C640A-C794A- C804A-C817A-C853A) | hEAG1 A145C-NC (C50A-C67A-C128A- C214A-C532A-C541A- C562A-C575A-C592A- C631A-C640A-C794A- C804A-C817A-C853A) | hEAG1 A128C-NC (C50A-C67A-C145A- C214A-C532A-C541A- C562A-C575A-C592A- C631A-C640A-C794A- C804A-C817A-C853A) |
| hEAG1 A532C-NC (C50A-C67A-C128A- C145A-C214A-C532A- C541A-C575A-C592A- C631A-C640A-C794A- C804A-C817A-C853A) | hEAG1 A562C-NC (C50A-C67A-C128A- C145A-C214A-C541A- C562A-C575A-C592A- C631A-C640A-C794A- C804A-C817A-C853A) | hEAG1 Cysless (C50A- C67A-C128A-C145A- C214A- C303A-C357V- C368V C532A-C541A- C562A-C575A-C592A- C631A-C640A-C794A- C804A-C817A-C853A) | hEAG1 H486R-H662R (H486R-H574R-H583R- H643R-H662R) |
| hEAG1 H56R | hEAG1 H179R | hEAG1 H181R | hEAG1 H208R |
| hEAG1 H214R | hEAG1 H270R | hEAG1 H343R | hEAG1 H364A |
| hEAG1 H364Q | hEAG1 H364W | hEAG1 H364E | hEAG1 H364V |
| hEAG1 H486R | hEAG1H543R | hEAG1 H552R | hEAG1 H574R |
| hEAG1 H583R | hEAG1 H643R | hEAG1 H662R | hEAG1 H708R |
| hEAG1 H753R | hEAG1 H784R | hEAG1 H885R | hEAG1 H904R |
| hEAG1 H270R-H343R | hEAG1 H708-904R (H708R-H748R-H753R- H784R-H885R-H904R) | hEAG1 Hisless-N (H56R-H179R-H181R- H208R-H212R) | (15-15-E)-HE (chimera between Kv1.5 & hEAG1) (1414-2889 residue of hEAG1 is cloned into Kv1.5 <i>AflIII</i> - <i>NheI</i>) |

| | | | |
|---|---|---|--|
| (1-E-E)-HE (chimera between hEAG1 & Kv1.1) (1-558 residue of Kv1.1 is cloned into hEAG1 <i>BamHI-PsiI</i>) | (E-1-E)-HE (chimera between hEAG1 & Kv1.1) (551-1237 residue of Kv1.1 is cloned into hEAG1 <i>PsiI-SexAI</i>) | (E-E-1)-HE (chimera between hEAG1 & Kv1.1) (1244-1484 residue of Kv1.1 is cloned into hEAG1 <i>SexAI-HindIII</i>) | (21-E-E)-HE (chimera between hEAG1 & Kv2.1) (1-602 residue of Kv2.1 is cloned into hEAG1 <i>BamHI-PsiI</i>) |
| (E-21-E)-HE (chimera between hEAG1 & Kv2.1) (582-1333 residue of Kv2.1 is cloned into hEAG1 <i>PsiI-SexAI</i>) | (E-E-21)-HE (chimera between hEAG1 & Kv2.1) (1263-2562 residue of Kv2.1 is cloned into hEAG1 <i>SexAI-HindIII</i>) | (E-E-HCN2)-HE (chimera between hEAG1 & HCN2) (1403-2667 residue of HCN2 is cloned into hEAG1 <i>SexAI-HindIII</i>) | rKv1.4 H16A |
| rKv1.4 C13S-H16A | | | |

2.1.3 Other materials

Antibodies

Polyclonal rabbit anti-EAG antibody (Antagene, Inc, Sunnyvale, CA, USA)

Polyclonal rabbit IgG, whole antibody, peroxidase-conjugated (from donkey) (Amersham Pharmacia Biotech)

Hemin and hemin related-chemicals

Hemin (Fe(III) protoporphyrin IX chloride), Zn(II) protoporphyrin IX, Co(II) protoporphyrin IX, Protoporphyrin-IX, Microperoxidase (MP-11), Hemin–Agarose Type I, saline suspension were purchased from Sigma-Aldrich-Fluka, Germany

Peptides

Synthetic peptides corresponding to the 22 amino acids of the N-terminal ball-domain of the Kv1.4 channels (Kv1.4-IP) (MVSAESSGCNSHMPYGYAAQAR) and Kv1.4-IP-mt, where cysteine and histidine residues were replaced by serine and alanine (MVSAESSGSNSAMPYGYAAQAR), were synthesized by PANATecs GmbH (Germany). Peptides corresponding to the 5 amino acids of S5 region of AKT1 channels (CHAAC) and 22 amino acids of the C-linker region of hEAG1 channels (DICVHLNRKVFKEHPAFRLASD) and hEAG1 mutant, where 2 histidines were replaced by alanine (DICVALNRKVFKEAPAFRLASD), were synthesized by the Dr. Diana Imhof group, University of Jena (Germany). The purified peptide was kept at -20°C , working solutions were freshly prepared in 100 mM HEPES (pH 7.0).

Other reagents and chemicals

Expand High fidelity PCR Kit, Protease inhibitor tablets (Roche), DNA Clean & Concentrator Kit, Zymo Clean Gel extraction Kit (Zymo Research), Qiaex Midi Plasmid purification Kit, Superfect Transfection Reagent (Qiagen), Restriction enzymes (New England Biolabs), T4 DNA ligase & Ligase Buffer (Fermentas), Lysozyme, DTT, DTNP (2,2'-dithio-bis [5-nitropyridine]), DTNB (5, 5'-dithiobis[2-nitrobenzoic acid]) (Sigma), TritonX100 (Fluka BioChemika), Immobilon-P Transfer Membrane (Millipore Corporation, Bedford, MA), ECL+plus Western blotting detection system (Amersham Pharmacia Biotech), BioMax MR-1 Film (Kodak Company, Rochester), Dulbecco's Modified Eagle Medium, Trypsin-EDTA, Fetal calf serum (FCS) (Life Technologies, Inc.), Nutrient Mix F-12 (HAM) (Biochrom), mMessage mMachine kit (Ambion), MTSET ([2-(trimethylammonium)ethyl] methane thiosulfonate bromide), MTSES (2-sulfonatoethyl methanethiosulfonate sodium salt) (Toronto Research Chemicals)

2.1.4 Buffers and solutions

Molecular biology

TY medium for growth of *E.coli*

| | |
|--|------|
| Bacto-Trypton | 10 g |
| Yeast extract | 5 g |
| NaCl | 5 g |
| H ₂ O add 1l, autoclave | |
| for agar plates: 15 g agar for 1l medium | |

4x SDS-PAGE loading buffer

| | |
|-------------------|-------|
| TrisHCl pH 6.8 | 70 mM |
| β-mercaptoethanol | 5% |
| Glycerol | 40% |
| SDS | 3% |
| bromophenyl blue | 0.05% |

Coomassie-stain

| | |
|---------------------------|-------|
| Coomassie R250 (for gels) | 2 g/l |
| Acetic acid | 10% |

Phosphate-buffered saline (PBS)

| | |
|--|--------|
| Na ₂ HPO ₄ ·7 H ₂ O | 4.3 mM |
| KH ₂ PO ₄ | 1.4 mM |
| NaCl | 137 mM |
| KCl | 2.7 mM |
| pH 7.4 | |

Cell lysis buffer

| | |
|-------------------|--------|
| Tris-HCl pH 7.5 | 20 mM |
| NaCl | 100 mM |
| MgCl ₂ | 5 mM |
| NP40 | 0.5% |

Semi-dry transfer buffer

| | |
|----------|--------|
| TrisBase | 25 mM |
| Glycine | 192 mM |

Methanol 50%

SDS 10%

Methanol 20%

pH 9-10

50X-TAE buffer

Tris base 2 M

Acetic acid 1 M

EDTA 100 mM

10X-Agarose gel loading buffer

Urea 3 M

Sucrose 30%

EDTA 25 mM

Bromophenol blue 0.1%

Electrophysiology

Inside-out patch-clamp

External solution

Na-aspartate 103.6 mM

or, K-aspartate 103.6 mM

(Symmetrical potassium solution)

KCl 11.4 mM

CaCl₂ 1.8 mM

HEPES 10 mM

(pH 7.2 with NaOH)

Whole-cell patch-clamp

External solution

NaCl 135 mM

KCl 5 mM

CaCl₂ 2 mM

HEPES 10 mM

(pH 7.4 with NaOH)

Two-electrode voltage clamp

External solution

NaCl 115 mM.

KCl 2.5 mM

Internal solution

K-aspartate 100 mM

KCl 15 mM

EGTA 10 mM

HEPES 10 mM

(pH 7.2 or 8.0 with KOH)

Internal solution

KCl 130 mM

MgCl₂ 2.56 mM

EGTA 10 mM

HEPES 10 mM

(pH 7.4 with KOH)

Internal solution

KCl 2 mM

| | |
|--------------------|--------|
| CaCl ₂ | 1.8 mM |
| HEPES | 10 mM |
| (pH 7.2 with NaOH) | |

2.2 Methods

2.2.1 Plasmid construction and mutagenesis

Point mutations of hEAG1 and Kv1.4 channels were generated by using overlap extension PCR method as described previously (Ho et al., 1989). In case of hEAG1 mutants, there were 4 sets of restriction enzymes used for cloning into the wild-type hEAG1-HE plasmid. The first set of enzymes was *Bam*HI-*Bsa*AI which covered (C50A, C67A, C128A, C145A, C214A, H56R, H179R, H181R, H208R and H212R) mutants, the second set of enzymes was *Bsa*AI-*Acc*I which covered (C303A, C357V, C368V, H270R, H343R and H364R) mutants, the third set of enzymes was *Blp*I-*Bsp*EI which covered (C532A, C541A, C562A, C575A, C592A, C631A, C640A, H543R, H552R, H574R, H583R and H643R) mutants and the fourth set of enzymes were *Bsp*EI-*Bsu*36I which covered (C794A, C804A, C817A, C853A, H708R, H748R, H753R, H784R, H885R and H904R) mutants. Point mutations H16A, C13S/H16A of Kv1.4 channels were introduced in to rKv1.4-p21-1 plasmid using *Hind*III-*Bsa*AI restriction enzymes.

To create the E-E-21 chimera (chimera between hEAG1 and Kv2.1), a PCR fragment encoding the C-terminus of Kv2.1 (residues 1263–2562) was replaced to a DNA fragment covering the C-terminal region of hEAG1 (residues 1497–2889) by overlap extension PCR and the end product was subcloned into hEAG1- pGEM-HE using *Sex*AI-*Hind*III. Wild-type and mutated channel clones were transferred into pGEM-HE and pcDNA3 for expression in *Xenopus* oocytes or HEK293 cells. All constructs were verified by DNA sequencing (MWG-Biotech AG, Ebersberg, Germany; GATC-biotech, Konstanz, Germany). PCR primers were purchased from MWG-Biotech AG (Ebersberg, Germany).

2.2.2 Cell culture and transfection

HEK293 cells were cultured in 250 ml culture-flasks in Dulbecco's modified Eagle's medium-HAM'S F-12 supplemented with 10% FCS. Cell lines were maintained at 37°C in a humidified atmosphere with 5% CO₂. Subconfluent HEK293 cells were transfected by the SuperFect method (Qiagen, Hilden, Germany). The day before transfection cells were trypsinized and plated on coverslips. On the day of transfection, 1 µg of cDNA of interest and pCD8 (0.2 µg/dish) was diluted in 100 µl of FCS-free medium and combined with 100 µl of

FCS-free medium containing 3 μ l of SuperFect reagent. Complexes were incubated at room temperature for 30 min and then added to the dish. Transfected cells were incubated at 37°C in air with 5% CO₂ added and 98% relative humidity and used within 3 days. Transfection-positive cells were identified by binding immunobeads (CD8-Dynabeads, Dynal, Oslo, Norway) coated with a mAb (ITI-5C2) specific for the CD8 antigen and were selected for patch-clamp experiments.

2.2.3 Hemin agarose pull-down assay

hEAG1 wild-type channel DNA in pcDNA3 vector were transfected in HEK293 cell lines and maintained at 37°C in a humidified atmosphere of 5% CO₂. hEAG1 bindings to Hemin-Agarose— Hemin-agarose binding was performed essentially as described by Lee (1992). A confluent tissue culture flask (25 cm²) containing cells described above was rinsed three times with PBS (ice cold) and lysed with 500 μ l of lysis buffer containing PBS and 0.5% NP 40. Cell debris and nuclei were removed by centrifugation at 20,000 x g for 30 min and 500 μ l of postnuclear supernatant was recovered. To the postnuclear supernatant, a protease inhibitor mixture (Complete, Roche Applied Science) was added according to the manufacturer's instructions. The final volume was adjusted to 1000 μ l. Hemin-agarose beads (Sigma) were washed three times with PBS prior to use. Washed beads (20 μ l) were added to 300 μ l of cell lysate and incubated at 4 °C overnight. After incubation, the beads were washed three times with the same lysis buffer used for the binding step. The beads were resuspended in 30 μ l of SDS-PAGE sample buffer and boiled at 100 °C for 5 min, and centrifuged and the supernatant was subjected to SDS-PAGE on a 7% gel. Immunoblotting analyses were performed by using rabbit anti-hEAG1 antibody.

2.2.4 SDS-PAGE and Western blot analysis

Proteins to be subjected for Western blot analysis were separated using a 7% (wt/vol) polyacrylamide gel. Two gels: a 'stacking gel' with a low level of cross-linkage and low pH, allowing proteins to enter the gel and collect without smearing, and a 'resolving gel' with a higher pH, in which the proteins are separated according to molecular weights, were poured between two glass plates.

Following SDS-PAGE, protein transfer onto a polyvinylidene difluoride membrane (PVDF) was performed by a semi-dry method. The filter paper was soaked in semi-dry transfer-buffer and the PVDF-membrane was pre wet in methanol for 10 seconds before it was also submerged in transfer-buffer for 15 minutes to allow for equilibration the membrane. The

sandwich of filter paper, membrane, gel and filter paper was then connected to the cathode and the proteins were transferred at a set current of 2 mA/cm² for 1 hour. Afterwards, the membrane was removed from the blotting chamber and blocked with 5% (wt/vol) skim milk powder in TN buffer (PBS and 0.1% tween 20 [pH 7.4]) at 25°C for 1 h. The membrane was then incubated with the primary antibody (Rabbit anti-hEAG1, 1/250) at 4°C overnight. The membrane was washed three times in TN buffer and then incubated at 25°C for 1 h with the second antibody (horseradish peroxidase-conjugated donkey anti-rabbit immunoglobulin G [IgG] diluted 1/10,000 in TN buffer). After the incubation, the membrane was washed again thoroughly for a minimum three times to remove unbound antibody. For detection of the hEAG1/antibody complex an ECL+plus detection reagent (Amersham Pharmacia Biotech) was applied to the membrane according to the manufacturers protocol. The membrane was thereafter exposed to the film for 5-10 sec.

2.2.5 Spectroscopic characterizations of hemin-peptide interaction

UV-Visible (UV-Vis) spectroscopy

UV-vis spectra were recorded on a Perkin–Elmer Lambda 2 spectrophotometer using quartz cells of 0.2- and 1.0-cm path lengths. Peptide concentrations were between 20-40 µM. Hemin incorporation was achieved by directly mixing hemin and peptide in 100 mM HEPES (pH 7.0) and incubation of the sample mixture for 25–30 min before recording the absorption spectra. Difference spectra were obtained by subtracting hemin signals from those of hemin–peptide samples.

Electron paramagnetic resonance (EPR) spectroscopy

To obtain EPR spectra, Kv1.4-IP or Kv1.4-IP-mt (1 mM) was mixed with hemin (1 mM). The samples were then transferred to a quartz EPR tube, frozen in liquid helium at 4 K and tested on a Bruker ESP 300E X-band spectrometer.

2.2.6 Channel expression and electrophysiological measurements in *Xenopus* oocytes

For synthesis of capped mRNA, the plasmids with wild-type or mutant genes were linearized with respective restriction endonucleases (Table 1 & 2). Capped mRNA was synthesized *in vitro* using the mMessage mMachine kit, according to manufacturer's instructions (Ambion, Austin, TX, USA). Oocytes were surgically removed from the ovarian tissue of female *Xenopus laevis* which had been anesthetized by immersion in ice water/tricaine. The oocytes were defolliculated, and healthy stage V and VI *Xenopus* oocytes were isolated and

microinjected with 50 nl of RNA (~10 ng mRNA per oocyte) and incubated at 18 °C for 24 to 48 hrs. The removal of vitelline membrane was carried out by enzymatic treatment for 2-3 min as described by Wang (Wang et al., 2004). Electrophysiological measurements were carried out at 2-4 days after injection. Inside-out patch-clamp experiments were carried out in *Xenopus* oocytes at room temperature by using a patch-clamp amplifier EPC-9 operated with PatchMaster software (both HEKA Elektronik, Lambrecht, Germany). The macroscopic currents were measured using aluminum silicate glass pipettes with resistances of 1-2 MΩ. Changing of intracellular solutions in patch-clamp experiments was done using a multi-channel perfusion system and the patch was placed directly in the middle of the streaming solution (Fig. 6A).

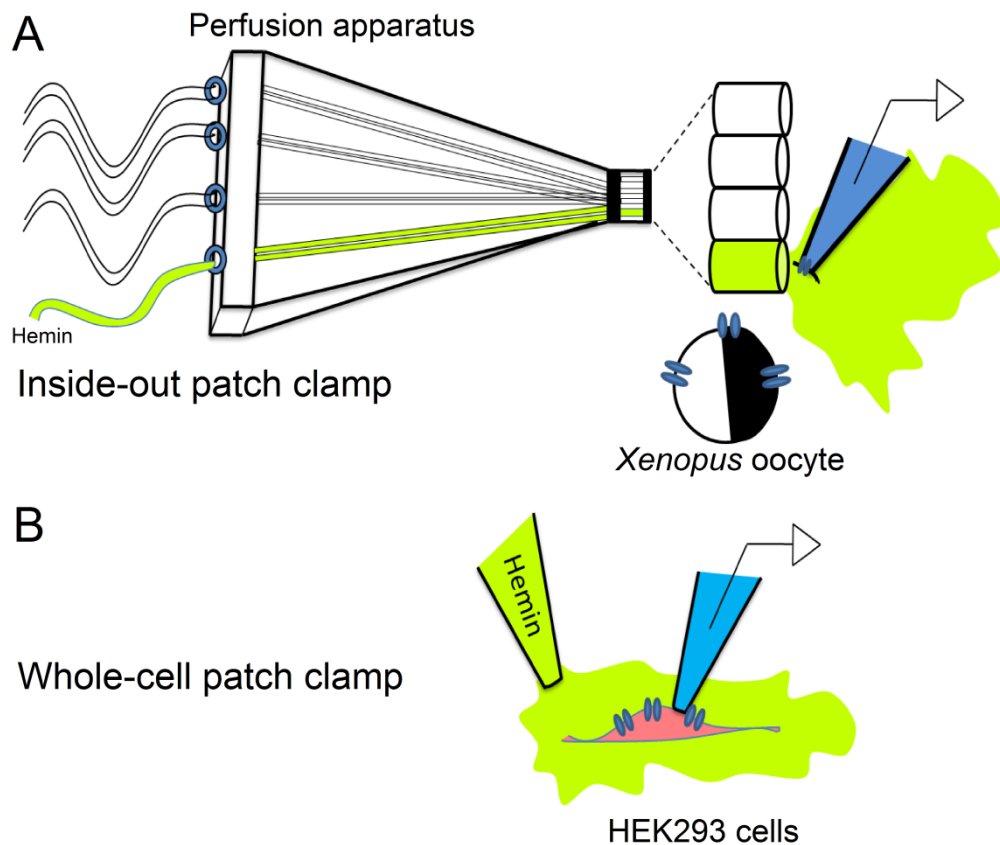


Fig. 6: Overview of the patch-clamp methods used in this study. (A) Cartoon illustrates the inside-out patch-clamp method using *Xenopus* oocytes as expression system. Changing of intracellular solutions was done using a multi-channel perfusion system. (B) Cartoon illustrates the whole-cell patch-clamp method using HEK293 cells as expression system. Application of hemin was performed with a patch pipette with broken tip.

Two-electrode voltage-clamp recordings from *Xenopus* oocytes were performed using a TurboTEC 10 CD amplifier (NPI electronics, Tamm, Germany). Electrodes had resistances of 0.4-0.9 MΩ.

2.2.7 Channel expression and electrophysiological measurements in mammalian cells

HEK293 cells were transfected with DNA of interest by the SuperFect method (Qiagen, Hilden, Germany). The expressed channel currents were measured in the whole-cell patch-clamp configuration 20-48 hrs after transfection. The recordings were performed using an EPC9 (HEKA Elektronik, Lambrecht, Germany) patch-clamp amplifier. Pulse protocol generation and data acquisition was controlled with the program PatchMaster (HEKA Elektronik). Series resistance errors were compensated in the range of 70-80%. Patch pipettes were fabricated from Kimax-51 glass (Kimble Glass, Vineland, NJ) and were of 1-3 MΩ resistance. All experiments were performed at 19-20 °C. The application of compounds was performed with an application pipette (Fig. 6B).

2.2.8 Data acquisition and analysis

The data were analyzed using FitMaster (HEKA Elektronik) and Igor-Pro (Wave-Metrics, Lake Oswego, OR, USA) software. Data were expressed as mean ± SEM. Two-tailed t-tests were used to evaluate the significance of the difference between means ($P < 0.05$).

2.2.8.1 Analysis of Kv1.4 and Kv1.1/Kvβ1.1 current measurements

Degree of fast inactivation

The degree of inactivation was assayed by measuring the peak current as well as the mean current level between 180 and 220 ms after the start of the depolarization, expressed as relative inactivation: $R_{\text{Inact}} = I_{(0.2 \text{ s})} / I_{(\text{max})}$. The ratio R_{Inact} gives an estimate of how many channels do not inactivate after opening; a value of zero represents complete inactivation; a value of one, no inactivation.

The inactivation time constant (τ_{Inact}) was derived from a monoexponential fit to the decay phase of the current.

$$I(t) = I_0 - (I_0 - I_\infty) \left(1 - e^{-\frac{t}{\tau}}\right) \quad (1)$$

I_0 and I_∞ are the current amplitudes at time t_0 and at time t_∞ (Fig. 7).

Time course of inactivation removal

The time course of hemin-induced loss of inactivation was monitored by measuring R_{Inact} elicited to +40 mV at an interval of 10 s (R). The R_{Inact} was plotted as a function of time (t) and fit with the following function:

$$R(t) = R_0 + (R_\infty - R_0) \left(1 - e^{-\frac{t-t_0}{\tau}}\right) \quad (2)$$

with the ratio before hemin application, R_0 , the time of hemin application start, t_0 , the time constant, τ . The ratio after hemin-induced removal of inactivation equilibration is R_∞ (Fig. 7).

Calculation of the EC_{50}

Concentration dependence for hemin-induced removal of inactivation was measured by plotting the R_{Inact} at +40 mV as a function of hemin concentration. The concentration dependence was described with the Hill equation

$$R_{\text{Inact}}([Hemin]) = \frac{R_0 + (R_\infty - R_0)}{1 + (EC_{50}/[Hemin])^h} \quad (3)$$

Where [Hemin] is the hemin concentration, EC_{50} provides a measure for the concentration of half-maximal inactivation inhibition and h is the Hill coefficient (Fig. 9).

2.8.8.2 Analysis of hEAG1 current measurements

Time course of hEAG1 current reduction

The time course of hemin-induced loss of hEAG1 current reduction was monitored by measuring the peak current from pulses elicited to +40 mV at an interval of 10 s. To quantify the time course of onset of hemin-induced block, a monoexponential function was employed.

$$I(t) = I_0 - (I_0 - I_\infty) \left(1 - e^{-\frac{t-t_0}{\tau}}\right) \quad (4)$$

I_0 and I_∞ are the current amplitudes before hemin application (at time t_0) and after hemin-induced block equilibration, respectively. τ is the time constant of onset of block (Fig. 29A & B).

The time course of DTNB-induced loss of hEAG1 current reduction was monitored by measuring the peak current from pulses elicited to +40 mV at an interval of 10 s. To quantify

the time course of onset of DTNB-induced block a double-exponential function was employed.

$$I(t) = I_0 - I_0 r_f \left(1 - e^{-\frac{t-t_0}{\tau_f}} \right) - I_0 (1 - r_f) \left(1 - e^{-\frac{t-t_0}{\tau_s}} \right) \quad (5)$$

I_0 is the current amplitudes before DTNB application (at time t_0), r_f and $1-r_f$ are the fraction of first and slow exponential components after DTNB-induced block equilibration. τ_f and τ_s are the corresponding time constants of onset of block for these components (Fig. 20B).

Calculation of the IC_{50}

Concentration dependence for hemin-induced inhibition of hEAG1 channels was measured from the asymptotic values of mono-exponential fits to $I_{hemin}/I_{control}$ and then fitted to Hill equation

$$\frac{I_{hemin}}{I_{control}}(+40 \text{ mV}) = \frac{1}{1 + ([Hemin]/IC_{50})^h} \quad (6)$$

Where $[Hemin]$ is the hemin concentration, IC_{50} provides a measure for the concentration of half-maximal hemin-induced inhibition, and h is the Hill coefficient (Fig. 29C).

Current–voltage relationships

From a holding potential of -120 mV test depolarizations (50 ms) in the range of from -120 to $+80$ mV were applied at 10-s intervals. The peak currents were measured and plotted as a function of test voltage. The control data were then fitted with an activation curve assuming four independent gating units and a single-channel conductance obeying the Goldman–Hodgkin–Katz equation:

$$I_{peak}(V) = \frac{I_{max}(V)}{(1 + e^{-(V-V_m)/k_m})^4} \quad (7)$$

$$I_{max}(V) = \Gamma V \frac{1 - e^{-(V-E_{rev})/25 \text{ mV}}}{1 - e^{-(V/25 \text{ mV})}}$$

V_m is the voltage of half-maximal gate activation and k_m the corresponding slope factor. Γ is the maximal conductance of all channels and E_{rev} the reversal potential (Fig. 30B).

Noise analysis

Fluctuations in the macroscopic current signal provide information on the unitary current size (i) and the number of channels (N_C). Non-stationary noise analysis was performed from sets

of at least 200 successive current sweeps containing responses to depolarizations of -20 , 0 , 20 , 40 , and 80 mV, compiling the mean current (I). Ensemble variances (σ^2) were compiled from differences of neighboring records, using an algorithm described by Heinemann and Conti (1992) and variance-current plots of the activating current phases were simultaneously fitted for all voltages according to Starkus et al. (2003), using the following equation:

$$\sigma^2 = \sigma_b^2 + iI - I^2/N_C \quad (8)$$

Where σ_b^2 is the background variance. The maximal open-channel probability (P_{open}) was estimated by analyzing the peak macroscopic current using the parameters of Eq. 8.

3. Results

3.1 Intracellular hemin impairs inactivation of A-type potassium channels

Kv1.4 channels give rise to A-type potassium currents and they are influenced by cysteine oxidation. The fast N-type inactivation of Kv1.4 channels has been shown to be sensitive to redox modulation; oxidizing agents remove the fast inactivation by modifying the cysteine residue C13 in the N-terminal inactivation ball domain, and reducing agents can reverse this effect (Ruppersberg et al., 1991; Stephens et al., 1996). In order to avoid potential confounding with secondary oxidation caused by hemin, we carried out all experiments in a reduced GSH environment.

3.1.1 Effects of intracellular hemin on Kv1.4 channel inactivation

To examine whether heme can acutely regulate the Kv1.4 channel function, we heterologously expressed rat Kv1.4 (rKv1.4) channels in *Xenopus* oocytes and assayed them using the excised inside-out configuration of the patch-clamp method. In this configuration, membrane patches containing the channels are physically isolated from the rest of the cell, cytoplasmic factors are largely absent, and hemin can be applied to the cytosolic side of the channel protein.

From a holding potential of -80 mV, channels were activated by repeated 1-s depolarizations to $+40$ mV. Intracellular application of hemin (Fe^{3+} protoporphyrin IX chloride) at 200 nM concentration consistently and significantly removed fast inactivation of Kv1.4 channels (Fig. 7) and the effect of hemin was partially reversible upon washing with reduced GSH (Fig. 7C). Hemin (200 nM) significantly increased the R_{Inact} from 0.09 ± 0.01 to 0.54 ± 0.02 ($P < 0.001$, Fig. 7B). The time course of onset of removal of inactivation was fitted with a monoexponential function (Eq. 2) that yielded a time constant of 51 ± 7 s ($n = 13$).

Hemin increased the inactivation time constant of Kv1.4 channels; τ_{Inact} was 50 ± 2 ms under control condition and changed to 240 ± 20 ms in presence of hemin ($P < 0.001$, Fig. 8D). Hemin apparently impaired the transition from the open state to the inactivated state ($O \rightarrow I$). To test for the hemin effect on the recovery transition back to the open state ($I \rightarrow O$), we measured the recovery rate of Kv1.4 channels with a two-pulse protocol (Fig. 8A). An initial 0.4-s pulse (P1) from -100 to $+40$ mV was followed by a second pulse (P2) after an interval 0.1 to 25 s, between each two-pulse trial there was a gap of 60 s in order to ensure complete recovery of the currents. The ratio current elicited by P1 and P2 pulses ($I_{\text{peak, P1}}/I_{\text{peak, P2}}$) is

plotted against pulse interval to show the recovery from inactivation (Fig. 8B). Under control condition the time constant of recovery from inactivation was 4.6 ± 0.2 s and after application of 200 nM hemin it only reduced to 3.5 ± 0.4 s ($P = 0.06$, Fig. 8C), suggesting that recovery from inactivation was not significantly altered upon application of hemin.

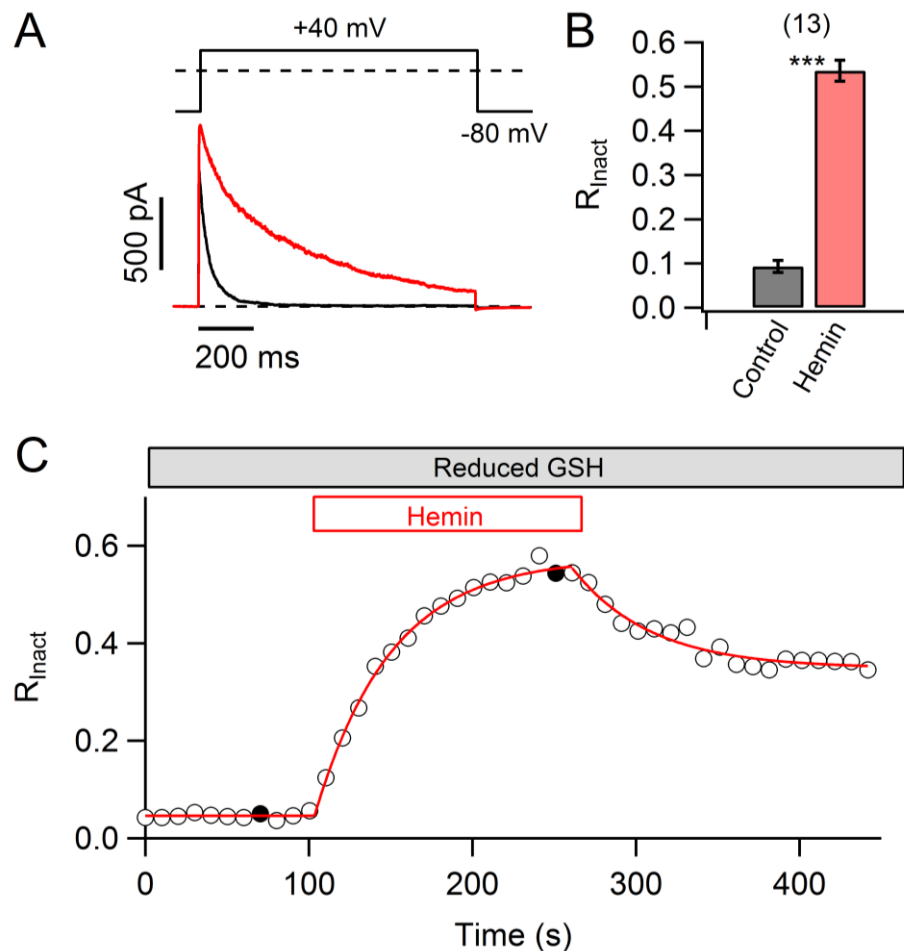


Fig. 7: Hemin removes inactivation of Kv1.4 potassium channels. (A) Pulse protocol (top) and superposition of current responses in inside-out patches from *Xenopus* oocytes expressing channels under control conditions (black), 150 s after application of 200 nM hemin (red). (B) Analysis of R_{Inact} at +40 mV, before and after application of 200 nM hemin. (C) The time course of onset of removal of inactivation with superimposed monoexponential function (Eq. 2). In the presence of 1 mM reduced glutathione (GSH), the inside-out patch was exposed to 200 nM hemin and then followed by washing with hemin-free solutions. Filled symbols denote data points from traces shown in (A).

Hemin removed Kv1.4 inactivation in a concentration-dependent manner. Cells were exposed to each concentration of hemin and cumulative concentration-response curves were acquired. The concentration dependence of inactivation removal was obtained by plotting the R_{Inact} versus the hemin concentration (Fig. 9). The half-maximal effective concentration (EC_{50}) of hemin-mediated removal inactivation was 24.6 ± 3.5 nM with a Hill coefficient (h) of 2.1 ± 0.5 (Fig. 9).

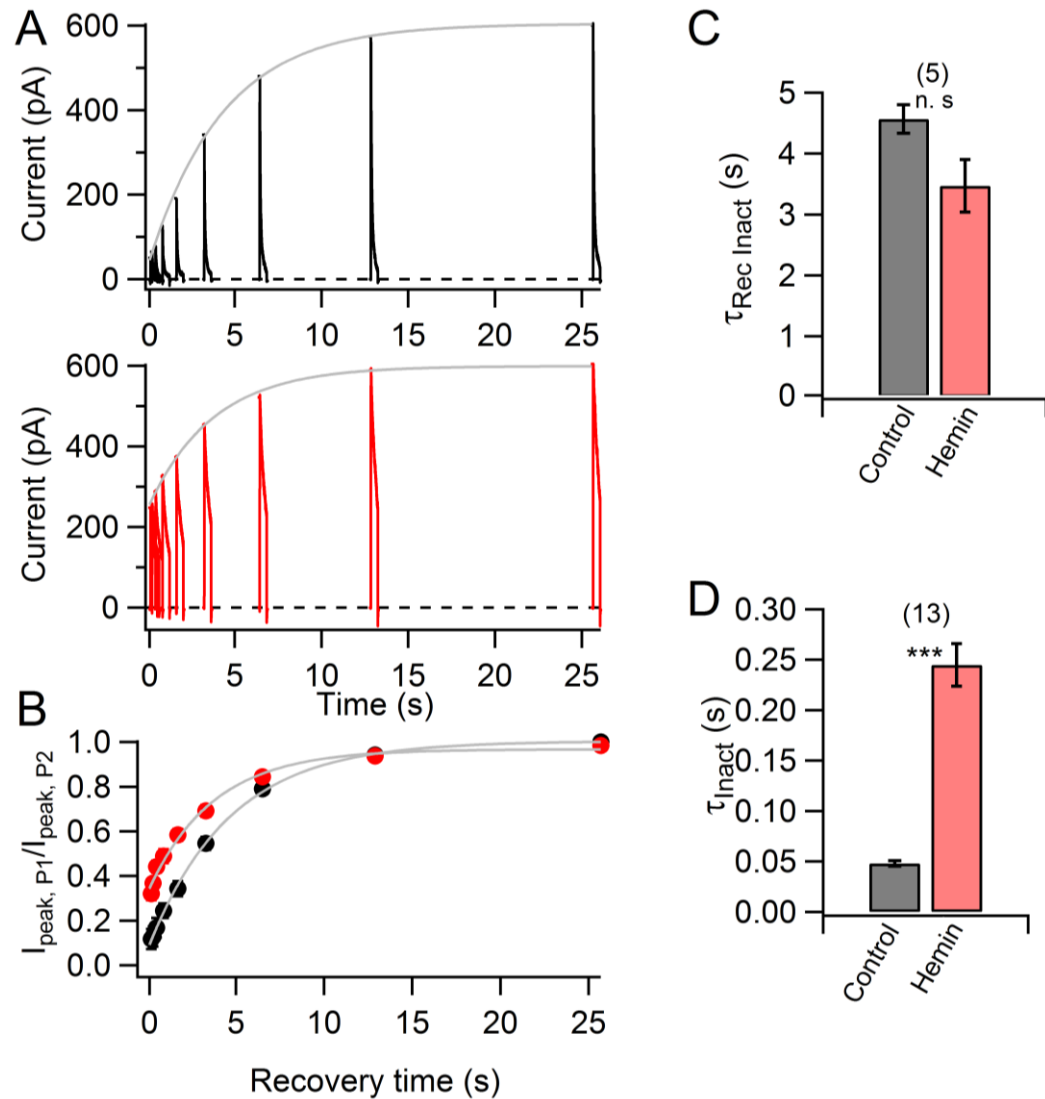


Fig. 8: Effect of hemin on Kv1.4 inactivation time constants. (A) Time course of recovery from inactivation of Kv1.4 channels at -100 mV under control conditions (black) and after application of 200 nM hemin (red). The continuous lines are monoexponential functions fitted to the peak current. (B) The fraction of channels recovered was plotted as a function of recovery time and fitted to a single exponential function (mean \pm SEM of five experiments). (C) Time constants of recovery from inactivation derived from experiments as in (A). (D) Inactivation time constants at +40 mV derived from experiments as in (Fig. 7A).

This indicates that hemin potently inhibits Kv1.4 channel inactivation. This potent acute removal of Kv1.4 inactivation by hemin was evident because the inhibition of inactivation occurred spontaneously without any exogenously added enzyme or cofactor; and the effect of hemin significantly sustained its application duration and was only very slowly reversed by wash, indicative of a very stable physical interaction between hemin and the channel protein.

However, the R_{Inact} did not approach to 1.0, suggesting that hemin could not completely remove the inactivation. One possible explanation would probably be C-type inactivation accounting for residual inactivation of Kv1.4 channels after hemin application.

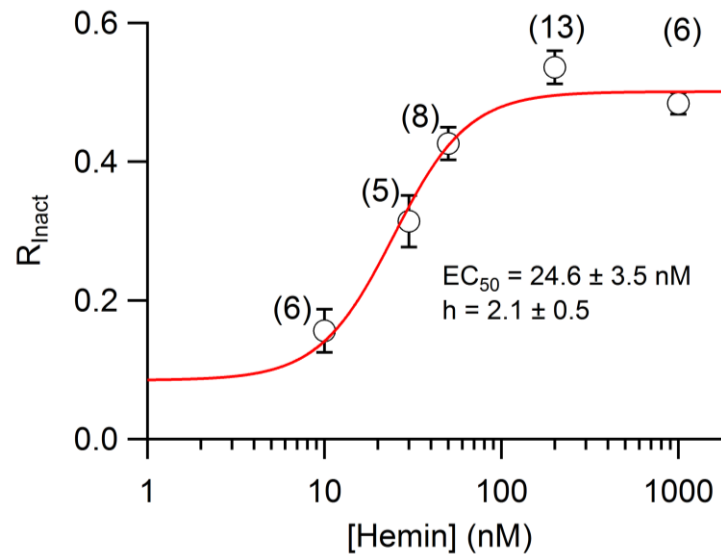


Fig. 9: Concentration dependence of inactivation removal by hemin. R_{Inact} derived from experiments as in Fig. 7 plotted against hemin concentration. Data were fit with the Eq. (3).

3.1.2 Extracellular hemin does not modulate Kv1.4 inactivation

The effects of extracellular hemin on the inactivation were examined using the whole-cell patch-clamp technique. Kv1.4 channels were expressed in HEK293 cells.

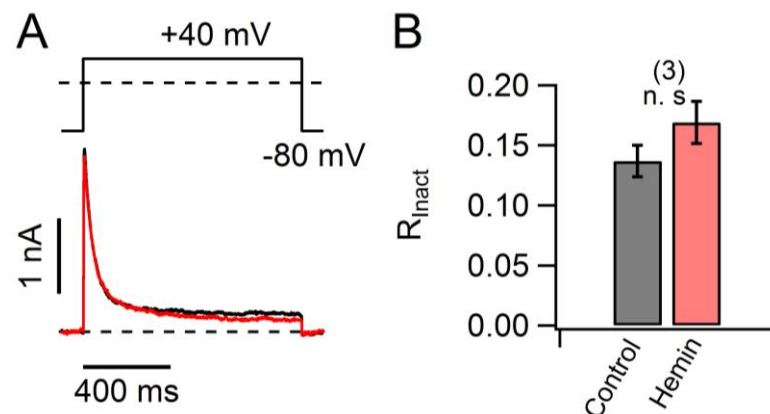


Fig. 10: Effect of hemin on the inactivation of Kv1.4 channels from extracellular side. (A) Pulse protocol (top) and current responses to depolarizations to +40 mV before (black) and 480 s after (red) application of 200 nM hemin. (B) R_{Inact} after 480 s; control, 0.14 ± 0.01 and hemin, 0.16 ± 0.01 .

Extracellular application of hemin 200 nM did not significantly alter Kv1.4 inactivation ($P = 0.22$, Fig. 10). This indicates that the extracellular face of the channel is not responsible for

hemin-mediated inhibition of rapid inactivation. At high hemin ($> 1 \mu\text{M}$) concentration, a peak current reduction could be observed after long waiting periods (not shown).

3.1.3 Effects of heme and heme-related chemicals on Kv1.4 inactivation

The inhibition of rapid inactivation of Kv1.4 channels by hemin was specific. The backbone of heme, i.e. Fe^{2+} ($1 \mu\text{M}$, FeSO_4) and protoporphyrin IX (pp-IX, 50 nM), had no impact on the inactivation (Fig. 11). To ensure that the inhibition of rapid inactivation was specific to free heme, we tested microperoxidase MP-11, a small peptide in which heme remains incorporated after isolation from horse cytochrome *c*. When applied to Kv1.4 channels at a concentration of $2 \mu\text{M}$, no alteration of channel inactivation was observed, indicating that the bound form of heme does not affect Kv1.4 channel inactivation (Fig. 11).

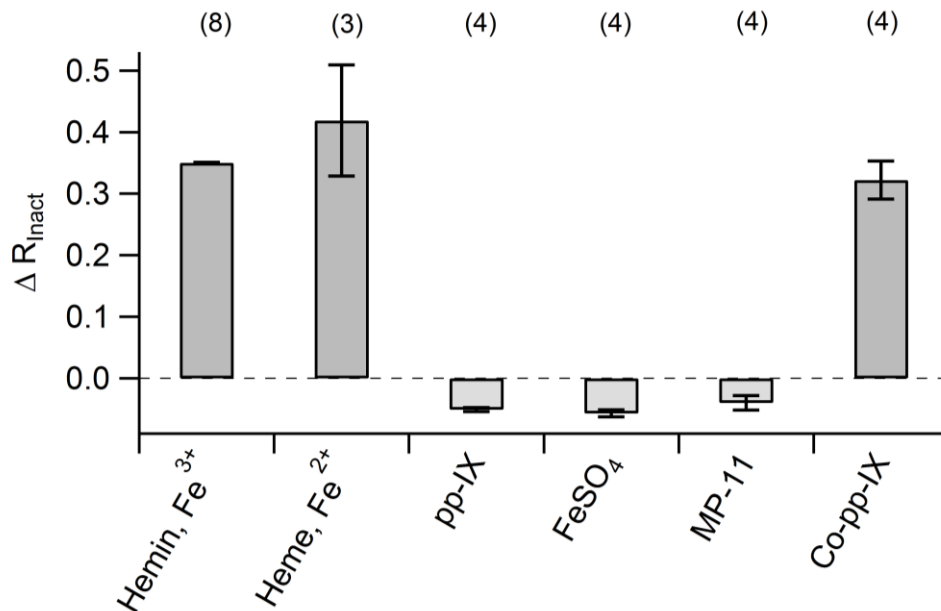


Fig. 11: Effects of heme and heme-related chemicals on Kv1.4 channel inactivation. R_{Inact} obtained at $+40 \text{ mV}$ presented after subtraction of control R_{Inact} , analyzed for hemin (Fe^{3+}), heme (Fe^{2+}) and pp-IX (50 nM), as well as for FeSO_4 ($1 \mu\text{M}$), MP-11 ($2 \mu\text{M}$) and Co-pp-IX (50 nM), indicating a clear preference for hemin, heme and Co-pp-IX.

Reduction of the hemin iron (Fe^{3+} , hemin) to the reduced ferrous form (Fe^{2+} , heme) by sodium dithionite (1 mM) had no impact on the ability to remove Kv1.4 inactivation indicating that the electronic state of the iron center is not crucial (Fig. 11). Another type of metal protoporphyrin IX, cobalt protoporphyrin IX (Co-pp-IX), also inhibited the Kv1.4 inactivation (Fig. 11).

3.1.4 Hemin does not affect C-type inactivation of Kv1.4 channels

Kv1.4 channels possess two types of inactivation: rapid N-type inactivation and slow C-type inactivation (e.g. Rasmusson et al., 1998).

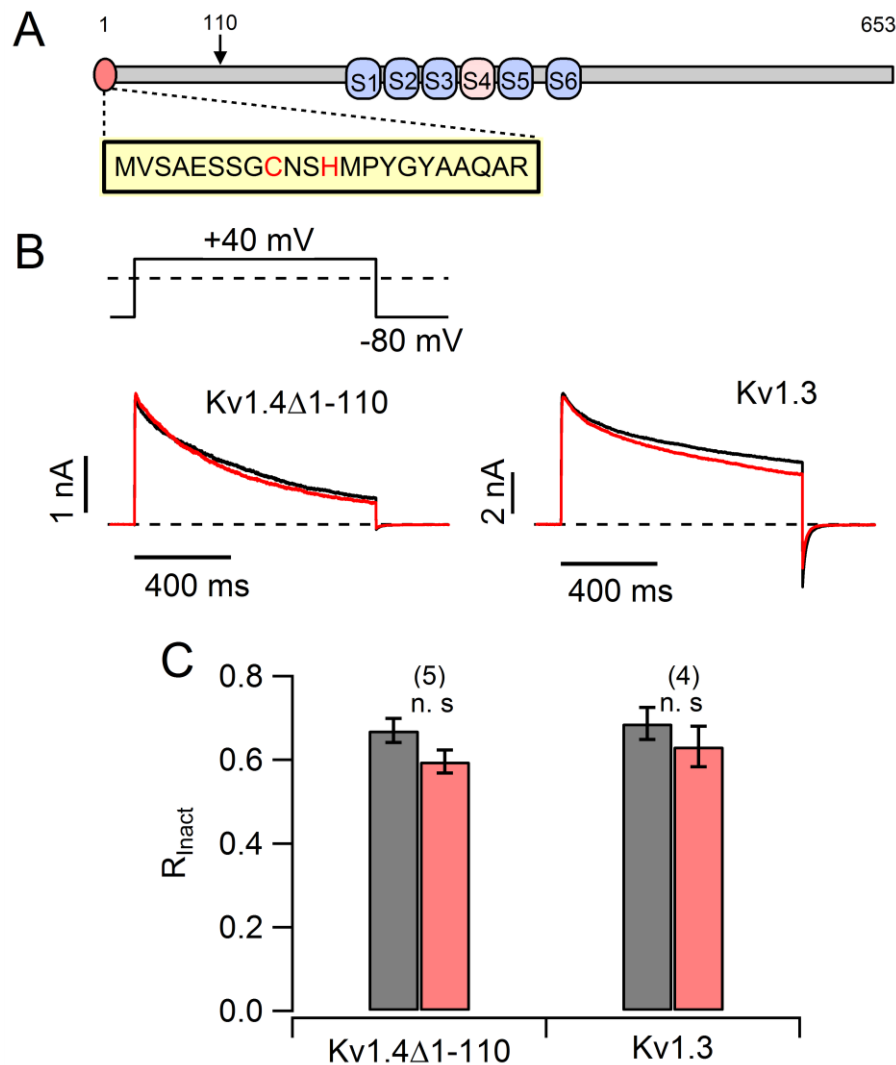


Fig. 12: C-type inactivation is not affected by hemin. (A) Cartoon depicting an overview of an α -subunit of Kv1.4 potassium channels with the sequence of the N-terminal ball domain. The arrow indicates the relevant deletion construct Kv1.4 Δ 1-110. (B) Pulse protocol (top) and superposition of current responses in inside-out patches from *Xenopus* oocytes expressing Kv1.4 Δ 1-110 and Kv1.3 channels under control conditions (black) and 150 s after application of 200 nM hemin (red). (C) R_{Inact} at +40 mV; Kv1.4 Δ 1-110: control, 0.67 ± 0.03 and hemin, 0.56 ± 0.03 ($P = 0.14$); Kv1.3: control, 0.69 ± 0.03 and hemin, 0.63 ± 0.04 ($P = 0.41$).

To judge which type of inactivation was affected by intracellular hemin, we used a deletion construct in which amino acid residues 1-110 were deleted from the N-terminus (Kv1.4 Δ 1-110) (Fig. 12A). This deletion construct has been shown to possess C-type inactivation only (Heinemann et al., 1996). Intracellular application of 200 nM hemin to Kv1.4 Δ 1-110 channels

did not show a noticeable effect on the inactivation time course and also had no effect on the current amplitude (Fig. 12B & C). This finding suggests that hemin does not influence C-type inactivation of Kv1.4 channels. It further supports that the remaining inactivation in Fig. 9 reflects C-type inactivation rather than an incomplete removal of N-type inactivation.

To further corroborate this finding we tested the effect of hemin on the potassium channel Kv1.3, which possesses only C-type inactivation (Panyi, 2005). As shown in Fig. 12B & C, it is evident that the Kv1.3 channel was insensitive to hemin. These results suggest that hemin only affects N-type inactivation.

3.1.5 Elucidation of the molecular loci required for the heme action on Kv1.4 channels

On the basis of the results presented so far, the loss of Kv1.4 channel inactivation is probably mediated by binding of hemin to the Kv1.4 ball domain. The ball domain of Kv1.4 channels harbors a cysteine and a histidine residue (CxxH) (Fig. 12A). In many heme proteins including cytochromes, hemoglobin, myoglobin, and soluble guanylyl cyclase (sGC), heme is bound or coordinated in part by an amino-acid sequence typically containing a histidine or cysteine residue, which acts as an axial 5th ligand (Paoli et al., 2002). To determine whether hemin mediates slowing of Kv1.4 fast inactivation by a mechanism involving cysteine and histidine, we tested the involvement of the cysteine and histidine residues in the ball domain for heme coordination by site-directed mutagenesis. Replacement of cysteine at position 13 to serine (C13S) significantly reduced the sensitivity of the Kv1.4 channels to hemin. Hemin (200 nM) increased R_{Inact} from 0.06 ± 0.002 to 0.42 ± 0.01 (Fig. 13A & B), a smaller effect in comparison to the effect of hemin on wild-type Kv1.4 channels ($P < 0.05$). Replacement of histidine residues at position 16 by alanine (H16A) did not reduce the sensitivity of the Kv1.4 channels to hemin. Hemin (200 nM) increased R_{Inact} from 0.11 ± 0.01 to 0.52 ± 0.02 (Fig. 13A & B), vs wild-type ($P = 0.71$). Interestingly, when mutation C13S was combined with the H16A (C13S/H16A), the hemin sensitivity was completely absent. Hemin (200 nM) had no impact on the inactivation (0.2 ± 0.03 , under control conditions and 0.15 ± 0.02 , under application of hemin) (Fig. 13A & B), vs wild-type ($P < 0.001$). This observation suggests that the high-affinity binding of hemin in Kv1.4 channels is mediated by coordination between the cysteine at 13 and the histidine at 16. The finding that single point mutations of the C13 or H16 residue in the ball domain do not completely eliminate the hemin sensitivity of the inactivation process suggests that other residues might be involved to compensate for one of these critical residues.

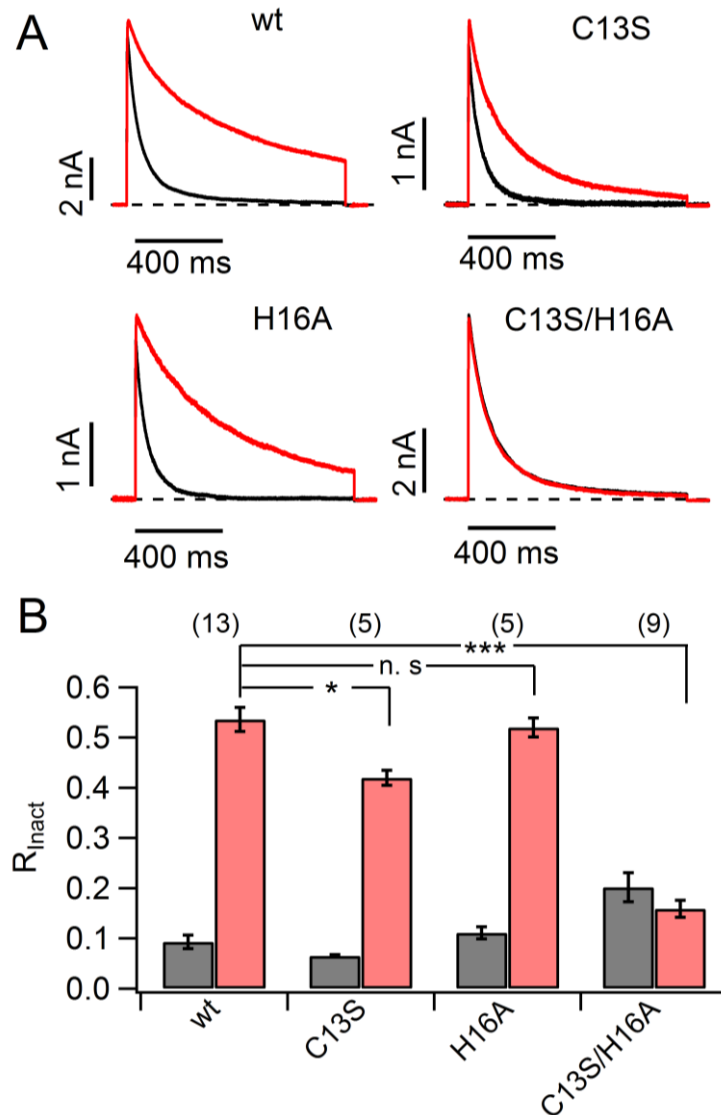


Fig. 13: Effect of hemin on Kv1.4 mutants. (A) Superposition of current responses in inside-out patches from *Xenopus* oocytes expressing indicated Kv1.4 channel mutants under control conditions (black) and 150 s after application of 200 nM hemin (red), measured at +40 mV and holding potential of −80 mV. (B) R_{inact} of indicated channel types.

3.1.6 Hemin interacts with the Kv1.4 inactivation peptide

Hemin-mediated removal of ball-and-chain N-type inactivation of Kv1.4 channels suggests that it may exert its effect by preventing the ball from reaching its receptor. To study this, the ball-hemin interaction was probed with a synthetic ball-domain peptide from Kv1.4. We synthesized a 22-residue synthetic peptide (Kv1.4-IP) encompassing the putative ball-domain located at residues 5–26 of the Kv1.4 channel protein (Fig. 14A). It has been reported that ball peptides derived from Kv1.4 are able to induce inactivation in delayed rectifier K⁺ channels (Antz and Fakler, 1998). Intracellular application of 100 μ M Kv1.4-IP rapidly inactivated delayed rectifier Kv1.1 potassium channels (Fig. 14C). Co-application of 100 μ M Kv1.4-IP

with 100 μ M hemin significantly reduced fast inactivation (Fig. 14C & E, $P < 0.01$). This result suggests that hemin potentially interacts with the Kv1.4 inactivation ball peptide and probably prevents the ball from reaching its receptor.

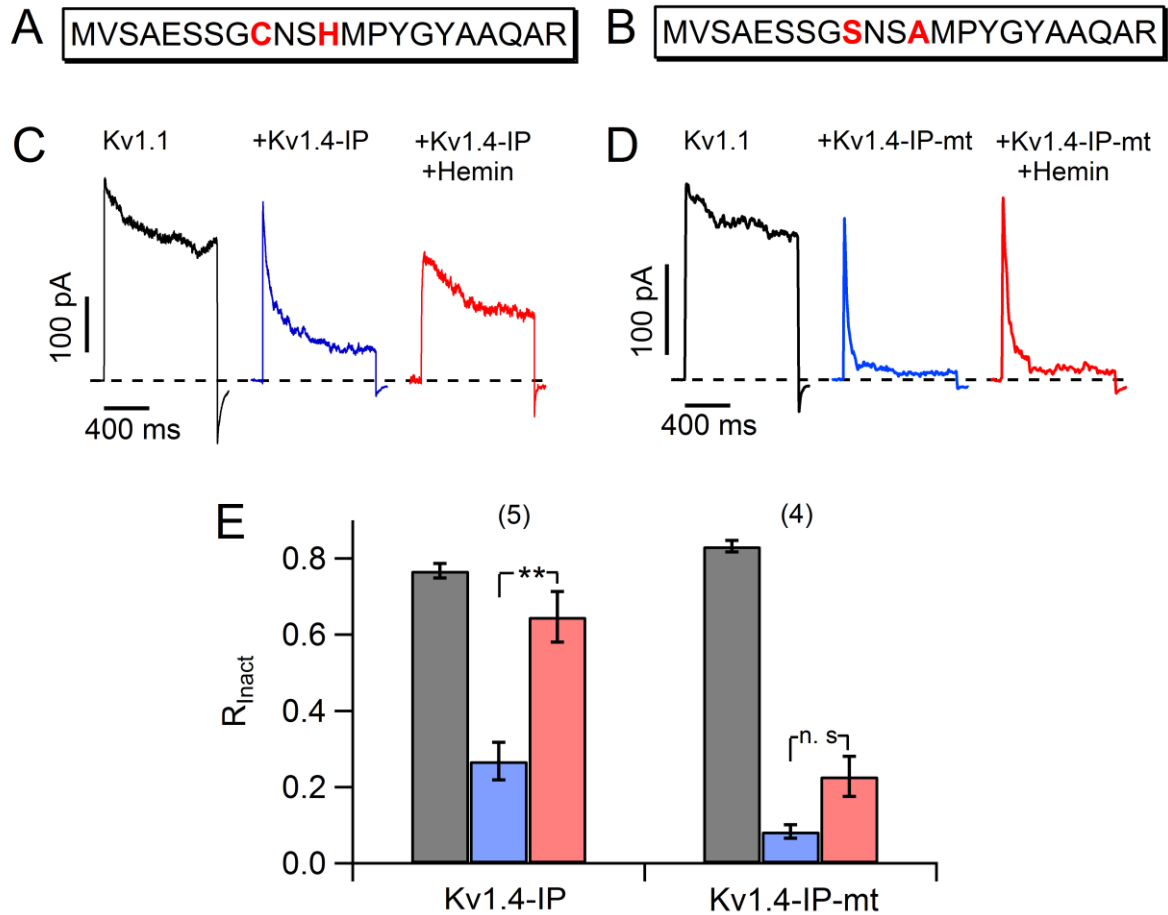


Fig. 14: Hemin prevents Kv1.4-IP to occlude the pore of the channel. (A, B) Representation of Kv1.4 ball peptide sequence of wild-type channel (Kv1.4-IP) and mutant channel where cysteine and histidine are replaced by serine and alanine (Kv1.4-IP-mt). (C, D) Superposition of current traces in inside-out patches from *Xenopus* oocytes expressing Kv1.1 channels, measured at +40 mV and holding potential of -80 mV. Kv1.1 channels were inactivated by Kv1.4-IP and Kv1.4-IP-mt; (ball peptide, 100 μ M) before (black) and after (blue) and co-application of hemin (100 μ M) and ball peptide (100 μ M) (red). (E) R_{Inact} derived from experiments as in (C & D).

To test whether the interaction of hemin with the Kv1.4-IP ball peptide was mediated by cysteine and histidine residues, we synthesized a mutant synthetic peptide (Kv1.4-IP-mt) in which C13 and H16 were replaced with serine and alanine respectively, and examined the sensitivity to hemin (Fig. 14B). Intracellular application of 100 μ M Kv1.4-IP-mt rapidly inactivated delayed rectifier Kv1.1 potassium channels (Fig. 14D) and the potency of inducing inactivation was significantly stronger than for Kv1.4-IP ($P = 0.016$). Co-application of 100 μ M Kv1.4-IP-mt with 100 μ M hemin did not significantly alter fast inactivation (Fig.

14D & E, $P = 0.06$), suggesting that heme potentially interacts with the C13 and H16 residues of Kv1.4-IP.

3.1.7 Spectroscopic characterization of heme-Kv1.4-IP interaction

To further characterize Kv1.4-IP interaction with heme in detail, we used the UV-VIS spectroscopy technique and analyzed the changes in the absorption spectrum of heme after mixing with the peptide. The spectrum shown in Fig. 15A shows two peaks at 410 nm, 540 nm. The principal peak at 410 nm comprises the Soret band. The Kv1.4-IP absorption spectrum in the presence of heme closely resembled that of a cytochrome-*c*-derived undecapeptide, MP-11, in which heme remains covalently bound to the amino acid sequence CAQCH (Fig. 15A). Furthermore, the mutant peptide in which the cysteine and histidine residues were mutated to serine and alanine (Kv1.4-IP-mt), did not show the absorption maxima (Fig. 15A) indicating that cysteine and histidine residues are responsible for interaction of heme with Kv1.4-IP.

The heme-binding site on the Kv1.4-IP was titrated with increasing amounts of heme (Fig. 15B). The absorbance at 410 nm increased with heme concentration. Hill plot analysis of the Kv1.4-IP Soret band signal gave a Hill coefficient of ~ 2 , indicating that a stoichiometry of 2. However, it is not possible to discern an exact stoichiometric relationship between heme and the peptide from the results of this experiment because of the considerably low affinity of heme for the peptide, as revealed by the presence of absorption due to free heme (high spin type spectrum) even at a heme:peptide ratio of less than unity. Since protoheme is known to undergo dimerization or to form higher aggregates in a neutral solution (Brown et al., 1970), the effective heme concentration for the binding should be significantly lower when it is assumed that only the heme monomer binds to the site.

The heme-Kv1.4-IP interaction was also analyzed by electron paramagnetic resonance (EPR) spectrometry (Fig. 15C). The EPR spectrum of heme-Kv1.4-IP showed a signal characteristic of low spin state of ferric iron with Landé factors of: $g_x = 2.43 \pm 0.03$ (279.0 mT), $g_y = 2.26 \pm 0.001$ (299.3 mT) and $g_z = 1.87 \pm 0.001$ (361.5 mT). However, no interaction of heme was observed with Kv1.4-IP-mt. This observation further supports the previous findings that the Kv1.4 ball domain functionally interacts with heme and that this inactivation is mediated by the CxxH motif in the ball domain. (EPR spectrometry was performed by Dr. Manfred Friedrich, University of Jena).

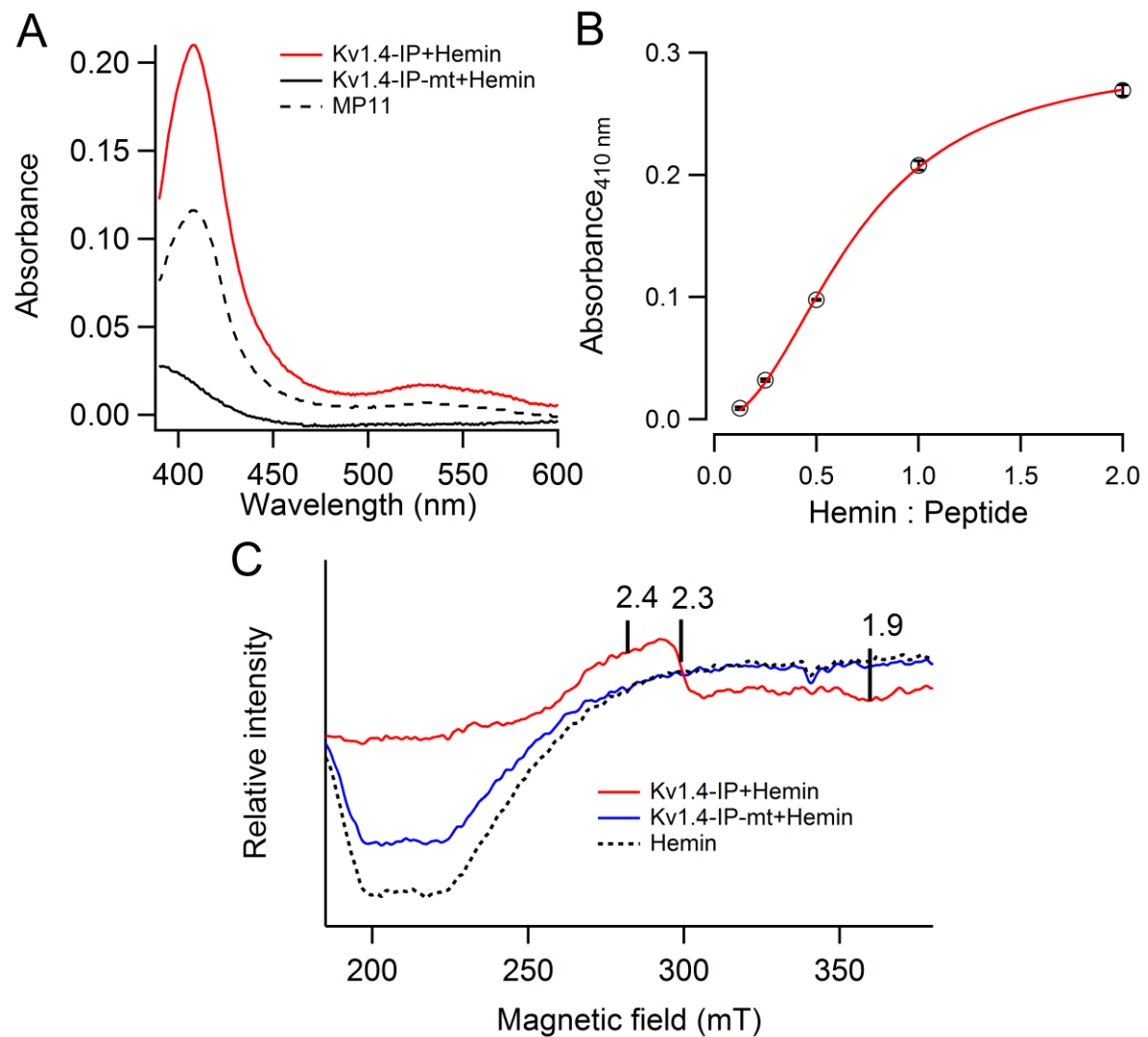


Fig. 15: Hemin binding to Kv1.4-IP. (A) Ultraviolet–visible light spectra of Kv1.4-IP (20 μ M) + hemin (20 μ M), Kv1.4-IP-mt (20 μ M) + hemin (20 μ M), and MP-11 (15 μ M). Data were presented after subtraction of hemin spectrum. (B) Titration of heme-binding activity of Kv1.4-IP. The peptide (20 μ M) in 0.01 M sodium phosphate buffer (pH 7.4) was mixed with increasing amounts of hemin. The spectra were recorded from 650 to 300 nm for each sample, and the binding was assessed by measuring the absorbance increment at 410 nm. Data were fitted with a Hill equation and are presented in triplicates (mean \pm SEM). (C) EPR spectrum of 1 mM Kv1.4-IP and 1 mM Kv1.4-IP-mt with 1 mM hemin. Lines indicate the Landé factors.

3.1.8 Effect of hemin on rapid N-type inactivation induced by Kv β subunits

The results presented above show that C13 and H16 in the ball domain of Kv1.4 represent a heme binding motif being responsible for the exquisite sensitivity of the channel to hemin. It is highly probable, therefore, that other A-type potassium channels with fast N-type inactivation and similar CxxH motifs in the ball domain region may be modulated by hemin as well. It is well established that some Kv β -subunits (such as Kv β 1) can confer the N-type

inactivation mechanism to some otherwise non-inactivating Kv channels such as the “delayed rectifier” type Kv1.1 or Kv1.5 (Rettig et al., 1994).

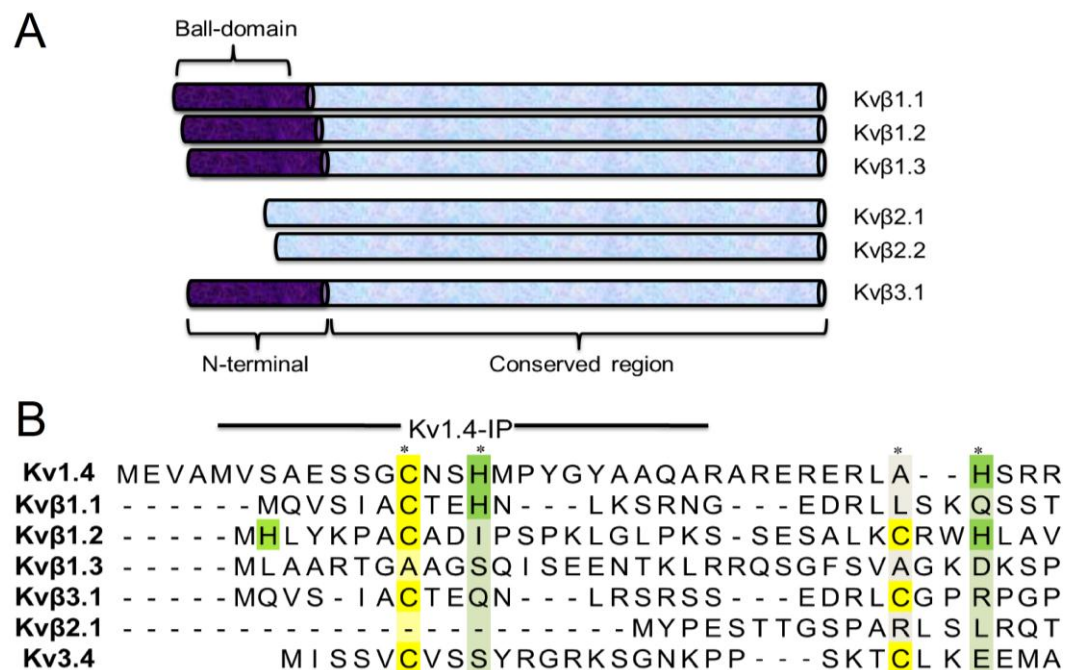


Fig. 16: Sequence comparison of Kva and various Kvβ subunits. (A) Representation of three mammalian genes encoding Kvβ-subunits: Kvβ1, Kvβ2, and Kvβ3, indicating variable N-terminal regions, which consist of a ball domain. **(B)** Alignment of ball-domain sequences of Kvβ subunits and N-terminus of Kv1.4 and Kv3.4 α-subunits ball-domain sequence, highlighted cysteine (yellow) and histidine (green) residues.

In the mammalian genome, three genes encode Kvβ-subunits: Kvβ1, Kvβ2, and Kvβ3. The Kvβ1 gene gives rise to splice variants resulting in Kvβ1 proteins with different NH₂-terminal sequences (70–90 amino acids; Kvβ1.1–1.3). Kvβ2, which lacks an inactivating N-terminal domain, does not induce inactivation (Rettig et al., 1994; Pongs et al., 1999). Protein sequence alignment of Kvβ family members showed that Kvβ proteins generally display variant N-terminal sequences which are responsible for N-type inactivation. The variant NH₂-terminal is followed by a highly conserved protein core sequence (~330 amino acids) with more than 80% sequence identity (Fig. 16A). Inspection of Kvβ ball domain sequences revealed that Kvβ1.1 and Kvβ1.2 bear cysteine and histidine residues, while Kvβ1.3 does not contain cysteine and histidine residues (Fig. 16B). Another A-type potassium channel, Kv3.4, also harbors a cysteine inside the ball domain.

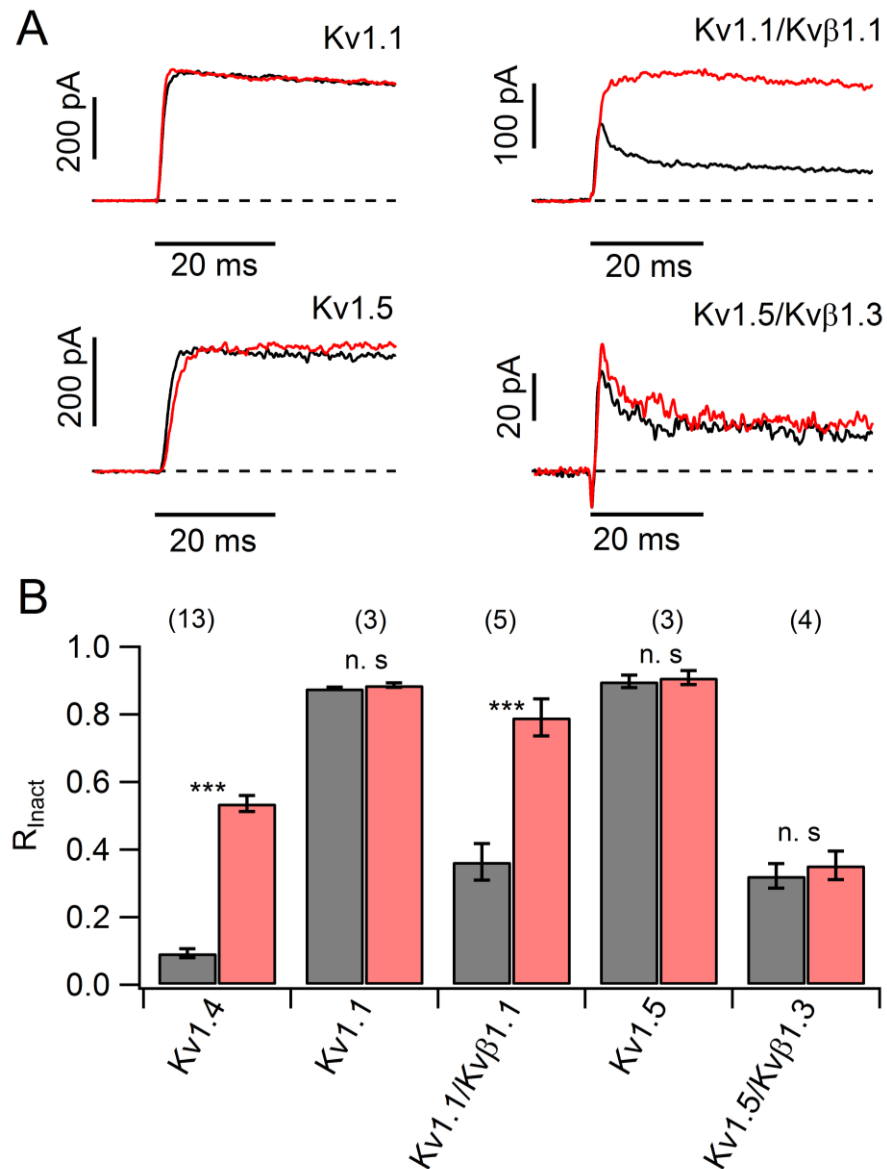


Fig. 17: Kvβ subunits confer hemin sensitivity. (A) Superposition of current responses in inside-out patches from *Xenopus* oocytes expressing indicated channels under control conditions (black) and 150 s after application of 200 nM hemin (red). Oocytes were clamped at -80 mV and depolarized to +40 mV. (B) R_{Inact} of indicated channel types: Kv1.4, control, 0.09 ± 0.01 and hemin, 0.54 ± 0.02 ; Kv1.1, control, 0.88 ± 0.003 and hemin, 0.89 ± 0.005 ($P = 0.4$); Kv1.1/ Kvβ1.1, control, 0.36 ± 0.05 and hemin, 0.79 ± 0.05 ; Kv1.5, control, 0.89 ± 0.02 and hemin, 0.90 ± 0.02 ($P = 0.7$) and Kv1.5/ Kvβ1.3, control, 0.32 ± 0.04 and hemin, 0.35 ± 0.04 .

Therefore, experiments were designed to test whether hemin would remove fast inactivation of A-type potassium channels induced by Kvβ subunits. When expressed alone in *Xenopus* oocytes, Kv1.1α subunits produce non-inactivating voltage-activated K⁺ currents (black trace, Fig. 17A, top left), while co-injection of Kvβ1.1 with Kv1.1 results in a rapidly inactivating current (black trace, Fig. 17A, top right). Application of 200 nM hemin to delayed rectifier Kv1.1 channels from the intracellular side did not show any effect, while hemin potently

removed the fast inactivation of Kv1.1/Kv β 1.1 channels. Hemin (200 nM) significantly increased R_{Inact} from 0.36 ± 0.05 to 0.79 ± 0.05 (Fig. 17, $P < 0.001$). Comparison of the hemin effect on Kv1.4 channels suggests that cysteine and histidine residues in the ball domain of Kv β 1.1 would probably be responsible for hemin-mediated removal of Kv1.1 inactivation. The effect of hemin was also explored on the fast N-type inactivation induced by Kv β 1.3, not harboring CxxH in the ball domain. Kv β 1.3 is known to induce fast inactivation in Kv1.5 potassium channels (Kwak et al., 1999). Co-expression of Kv1.5 with Kv β 1.3 subunits introduces rapid N-type inactivation (Fig. 17A, lower right). Application of 200 nM hemin to delayed rectifier Kv1.5 channels from the intracellular side did not affect the current. Interestingly, the R_{Inact} of Kv1.5/Kv β 1.3 channels was not affected by hemin either (Fig. 17, $P = 0.5$). This finding indicates that the hemin sensitivity on fast inactivation of A-type channels induced by Kv β subunits probably relies on the presence of cysteine or histidine residues in the ball domain.

3.2 Oxidative modification of hEAG1 potassium channels

The activity of several ion channels is known to be modulated by oxidation of certain amino acid residues such as cysteines (Ruppersberg et al., 1991; Duprat et al., 1995; Stephens et al., 1996; Rozanski et al., 2002). The α -subunits of hEAG1 channels harbor 19 cysteine residues and are distributed throughout the major cytosolic domains such as the PAS domain, the C-linker and the CNG-binding domain. To probe the role of critical cysteines responsible for hEAG1 function, we used cysteine-modifying reagents.

3.2.1 Cytosolic cysteines are responsible for hEAG1 channel function

To test whether the important cysteines for channel function reside at the extracellular side or cytosolic side, we used the thiol-modifying reagent DTNB, a hydrophilic membrane impermeable agent that modifies proteins based on the principle of thiol-disulfide exchange reaction. Extracellular application of 100 μ M DTNB to the hEAG1 channels expressed in HEK 293 cells and activated by repeated depolarization to +40 mV showed a slight increase of hEAG1 current (Fig. 18A). On the contrary, extracellular application of 25 μ M DTNP, a lipophilic membrane permeable thiol-modifying reagent, caused a complete inhibition of macroscopic hEAG1 current (Fig. 18B). Treatment with H_2O_2 (1 mM), a slowly membrane permeable physiological oxidant, also inhibited hEAG1 current ($59 \pm 4\%$ remaining current after exposure for 200 s) (Fig. 18C). These results suggest that intracellular cysteines are responsible for the profound alteration of the hEAG1 channel activity by DTNP and H_2O_2 .

To study the effect of thiol-modifying reagents from the intracellular side, membrane patches expressing hEAG1 channels were excised from *Xenopus* oocytes in the inside-out configuration and the thiol-reactive reagents DTNB, MTSES, or MTSET were applied by exchanging the bath solution. MTSES (–) and MTSET (+) are charged and presumably modify cysteines only accessible from the intracellular side. During reagent application, the membrane was held at –80 mV, and macroscopic hEAG1 currents were evoked by 50 ms test pulses to +40 mV every 10 s. As shown in Fig. 19A, 160 s intracellular application of 100 μ M DTNB, 300 μ M MTSET, and 100 μ M MTSES inhibited hEAG1 current by $72 \pm 3\%$ ($n = 9$), $90 \pm 1\%$ ($n = 6$), and $82 \pm 1\%$ ($n = 6$), respectively. These results suggest that various sulfhydryl-modifying reagents cause rundown of hEAG1 currents.

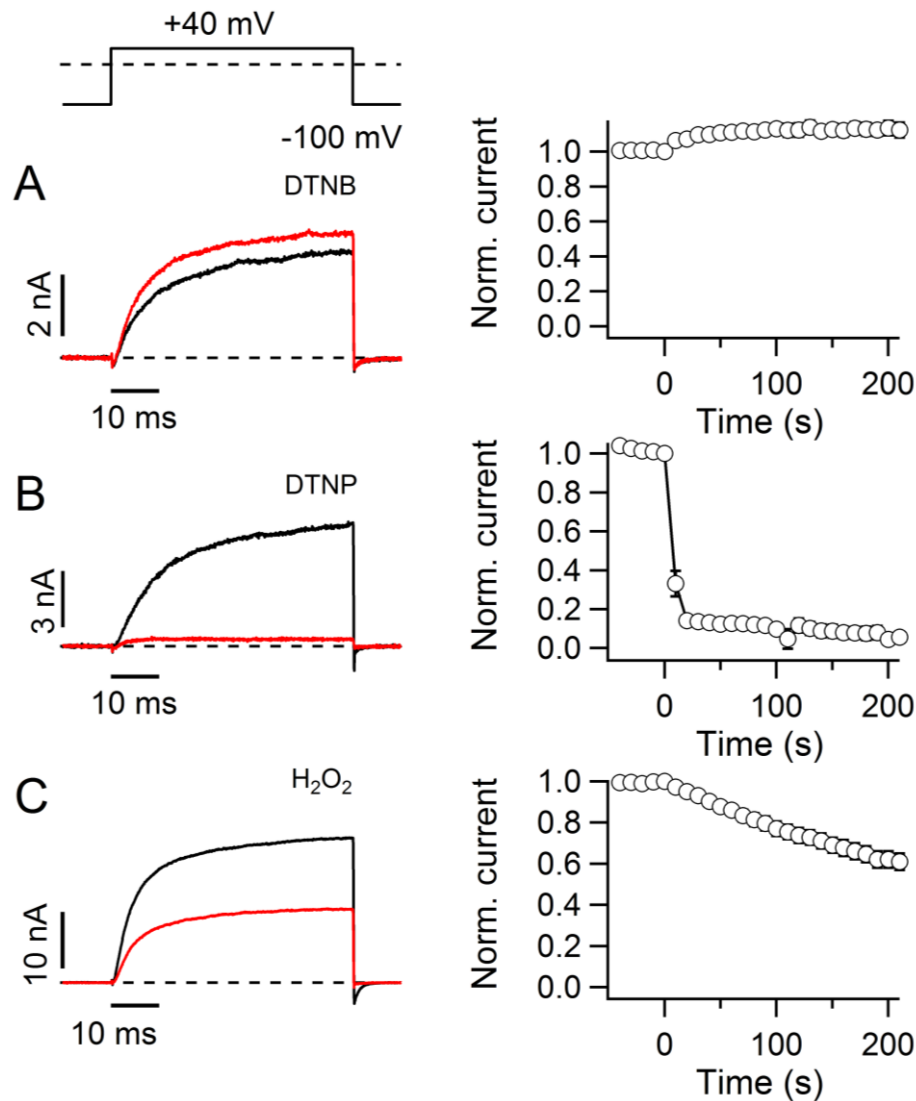


Fig. 18: Intracellular cysteines are susceptible to oxidative modification. Pulse protocol (top). (A) hEAG1 channels were transiently expressed in HEK 293 cells. (left) Superposition of two current traces measured in the whole-cell patch-clamp configuration under control condition (black) and 200 s after application of 100 μ M DTNB (red). (right) Time course of normalized current at +40 mV with application of 100 μ M DTNB ($n = 5$). (B, C) Similar experiments with 20 μ M DTNP (B, $n = 5$) and 1 mM H_2O_2 (C, $n = 6$).

To keep the possibility that hEAG1 channel inhibition was caused by sulfhydryl modification and not due to an unspecific effect on ion channels, we analyzed the action of DTNB on delayed rectifier potassium channels. Fig. 19B & C illustrates the effect of 100 μ M DTNB on Kv1.5 and Kv1.1 channels. We found that Kv1.5 and Kv1.1 channels were insensitive to cysteine modification, demonstrating that the DTNB effect is specific for the hEAG1 channel.

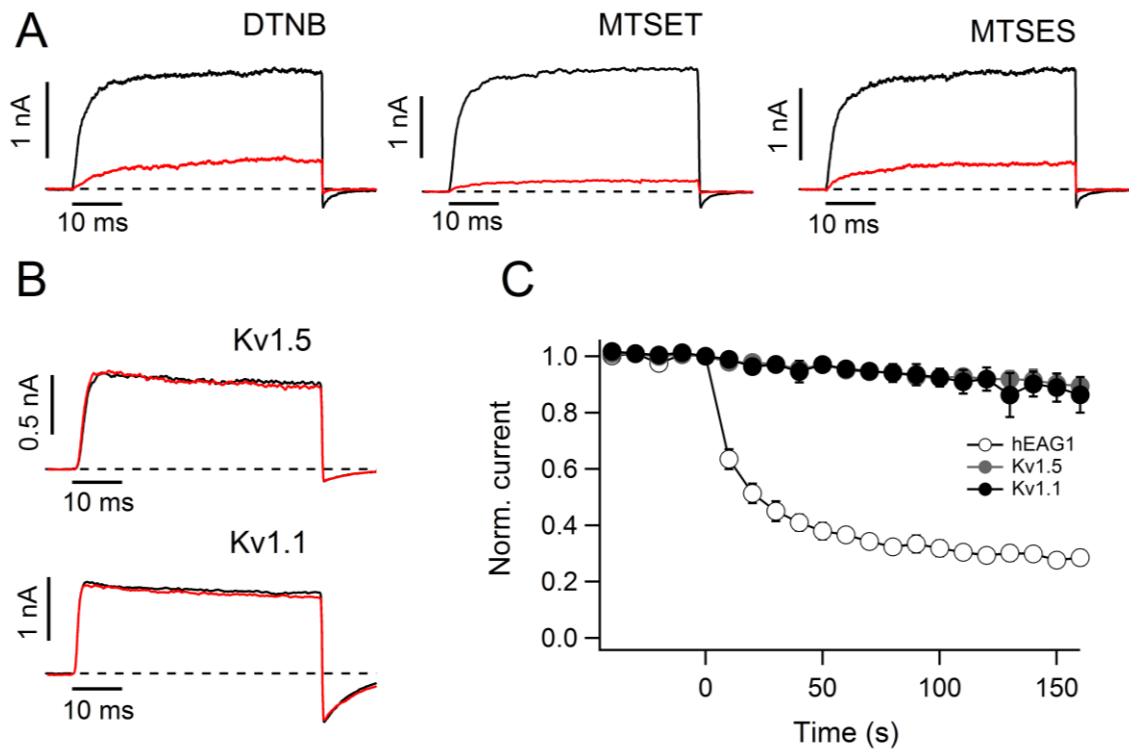


Fig. 19: Effect of sulfhydryl modifying reagents on potassium channels. (A) Current responses of hEAG1 channels recorded from inside-out patches before (black) and 160 s after (red) application of 100 μ M DTNB (left), 300 μ M MTSET (middle), and 100 μ M MTSES (right). Depolarization steps were applied to +40 mV. (B) Current traces of the indicated channel types recorded at +40 mV from inside-out patches before (black) and 160 s after (red) application of 100 μ M DTNB. (C) Mean current at the end of the test depolarizations to +40 mV as a function of time. Relative remaining currents after 160 s were: hEAG1, $28 \pm 3\%$ ($n = 9$), Kv1.5, $90 \pm 3\%$ ($n = 5$), and Kv1.1, $86 \pm 6\%$ ($n = 5$). Solution: standard K-Asp.

3.2.2 Time course of DTNB effect on hEAG1 potassium channels

To characterize the effect of DTNB on hEAG1 current in detail, we measured hEAG1 channels in symmetrical potassium solutions. At +40 mV, application of 20 μ M DTNB from the cytosolic side produced a biphasic current reduction: a fast decrease of hEAG1 current with a time constant (τ_{fast}) of 12 ± 2 s and block of $62 \pm 6\%$ ($n = 5$) and a slow component that gradually blocked the rest of the hEAG1 current with a time constant (τ_{slow}) of 370 ± 91 s ($n = 5$). Fig. 20A & B shows the effect of DTNB on hEAG1 current at -40, +40 and +100 mV. The inhibitory effect was only partially reversible by the application of DTT. Given the lack of complete reversibility under DTT application suggests that either the fast or the slow component of the DTNB effect is irreversible.

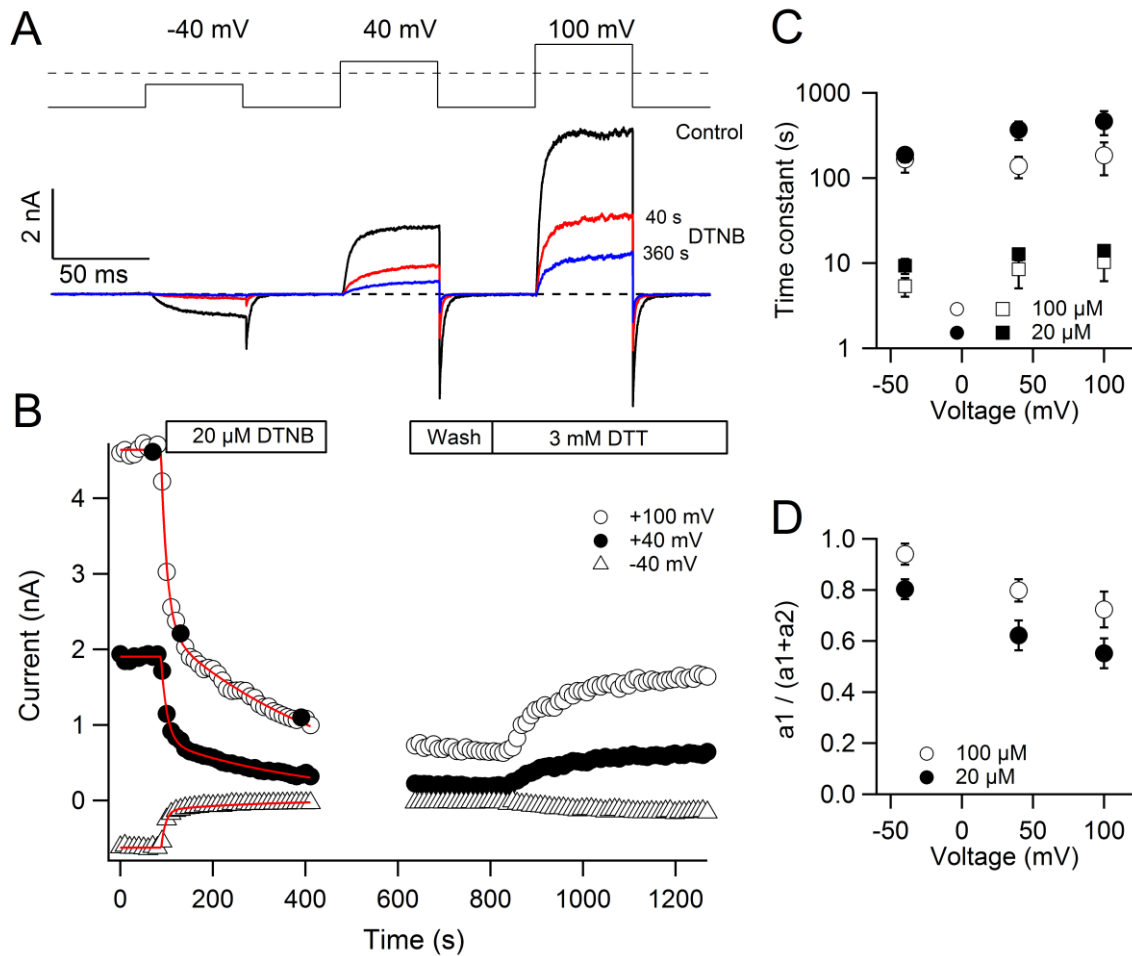


Fig. 20: DTNB inhibits hEAG1 currents via at least two processes. (A) Pulse protocols (top) with current traces before (black) and after 40 s (red) and 360 s (blue) of DTNB (20 μ M) application. (B) Time course of DTNB-mediated current rundown with superimposed double-exponential fit function (Eq. 5), followed by wash and partial reversibility by 3 mM DTT, at 3 voltages (open circle, +100 mV, dense circle, +40 mV and triangle, -40 mV) of a single experiment. (C, D) Analysis of inhibitory kinetics: time constants (C) and relative fast fraction (D) at 3 voltages and with 2 different concentrations (dense, 20 μ M and open, 100 μ M). There were two time constants: fast time constant (rectangle) and slow time constant (circle), obtained by fitting the data with double-exponential fit function ($n = 5$).

From the analysis of inhibitory kinetics, we observed two interesting facts: first, the time constant of current reduction becomes faster at negative voltages. Fig. 20C demonstrates the time course of inhibition at 20 μ M and 100 μ M DTNB (dense and open) at three different voltages. τ_{fast} of the rapid decrease (rectangle) was 9 ± 2 s (20 μ M) and 5 ± 1 s (100 μ M) s at -40 mV and it became slower at depolarizing voltages 12 ± 2 , 14 ± 2 s (20 μ M) and 8 ± 3 , 10 ± 4 s (100 μ M) at +40 and +100 mV, respectively. τ_{slow} of the slow effect (circle) were $(187 \pm 34, 370 \pm 91, 462 \pm 144$ s (20 μ M) and $166 \pm 50, 138 \pm 39, 184 \pm 86$ s (100 μ M) at -40, +40 and +100 mV, respectively). Second, from the relative fast fraction of the DTNB effect (Fig. 20D), it is evident that the inhibitory effect becomes weaker at negative voltages ($80 \pm 4\%$ (20

μM) and $93 \pm 4\%$ ($100 \mu\text{M}$) at -40 mV), whereas the effect becomes stronger at depolarizing voltages (62 ± 6 , $55 \pm 6\%$ ($20 \mu\text{M}$) and 79 ± 4 , $72 \pm 7\%$ ($100 \mu\text{M}$) at $+40$ and $+100 \text{ mV}$). This observation implies that there is a voltage dependence of the DTNB effect on hEAG1 potassium channels.

3.2.3 DTNB alters the gating of hEAG1 potassium channels

The observation that DTNB decreases hEAG1 currents could be interpreted to indicate that DTNB is a simple pore blocker of the hEAG1 channel.

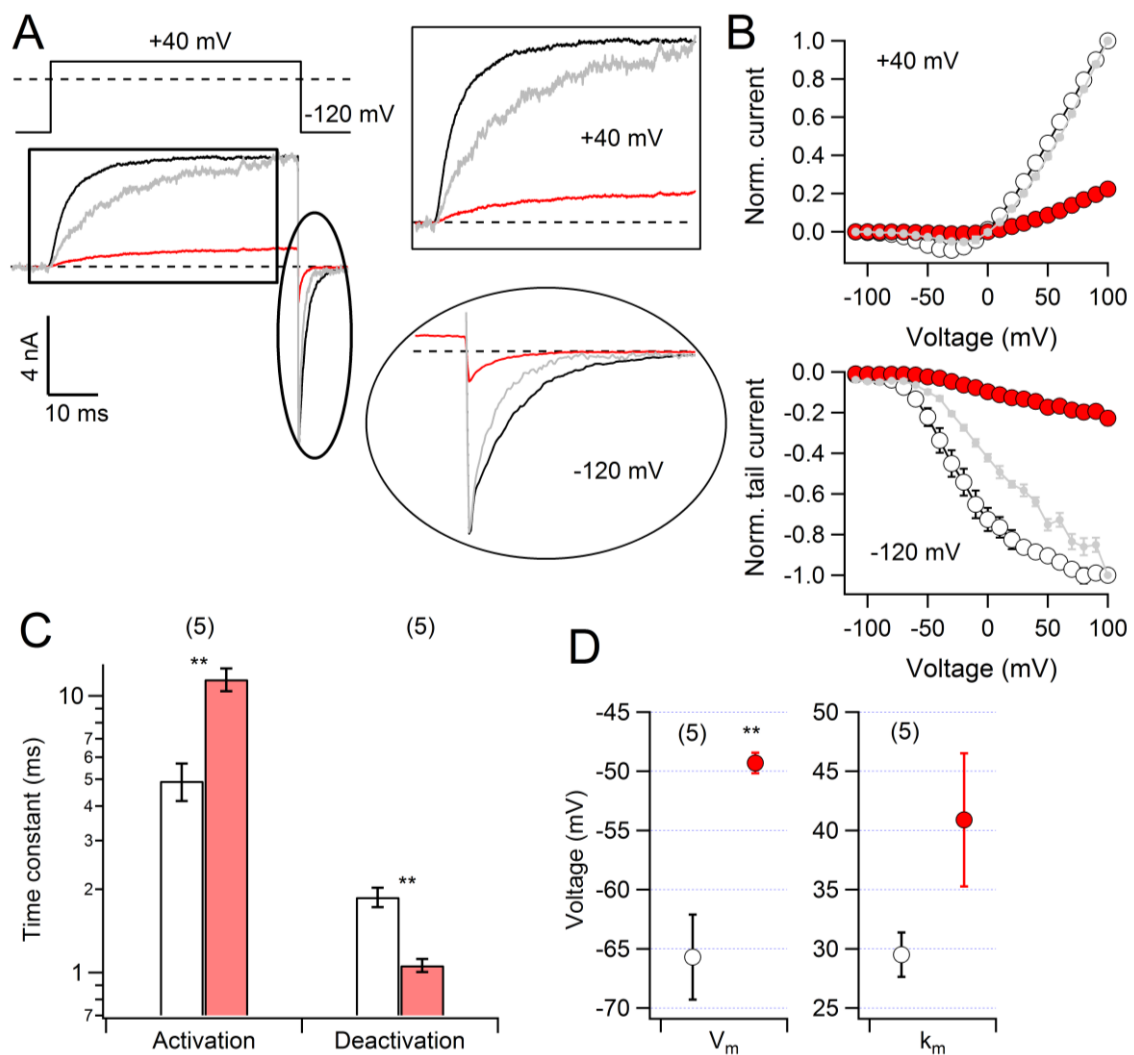


Fig. 21: Voltage dependence of DTNB-induced hEAG1 inhibition. (A) DTNB slows the activation kinetics at $+40 \text{ mV}$ and accelerates the deactivation kinetics at -120 mV (rectangle and oval). Superposition of current traces recorded from inside-out patches, before (black) and after (red) application of $20 \mu\text{M}$ DTNB. The gray circles are scaled DTNB traces to match the maximal control current. (B) Mean current measured at the end of the test depolarizations (top) and tail currents at -120 mV (bottom) as a function of voltage, before (black) and after (red) application of $20 \mu\text{M}$ DTNB. The gray circles are normalized to maximum current ($n = 5$). (C) Time constant of channel activation and deactivation, before (black) and 200 s after (red) application of $20 \mu\text{M}$ DTNB. (D) Half-activation

voltage (V_m) and slope factor (k_m) before (black) and 200 s after (red) application of 20 μ M DTNB. Data were obtained by fitting the current-voltage relationships (as in panel B) curve with the Goldman-Hodgkin-Katz equation (Eq. 7).

However, several lines of evidence collectively show that DTNB is a gating modifier of the hEAG1 channel. For example, DTNB modifies the activation and deactivation kinetics of the hEAG1 channel (Fig. 21A). Intracellular application of 20 μ M DTNB slows the activation kinetics at +40 mV (rectangle) and accelerates the deactivation kinetics at -120 mV (oval). Quantitatively, the activation time constant significantly slowed down from 4.9 ± 0.7 to 11.5 ± 1.0 ms (Fig. 21C, $P < 0.01$) and the deactivation time constant significantly accelerated from 1.9 ± 0.1 to 1.0 ± 0.06 ms (Fig. 21C, $P < 0.01$). From the current-voltage relationship it was evident that DTNB shifts the voltage dependence of activation towards the right (Fig. 21B). The half-activation voltage (V_m) was shifted from -66 ± 3 to -49 ± 0.8 mV (Fig. 21D, $P < 0.01$) and the slope factor (k_m) from 29 ± 2 to 40 ± 5 mV (Fig. 21D). These results show that the voltage-sensitivity of the channel was markedly altered by DTNB.

3.2.4 Effects of DTNB on single-channel activity

Macroscopic hEAG1 currents are a function of the number of functional hEAG1 molecules in the membrane (N), the hEAG1 unitary current (i), and the open probability (P_{open}) of the channels. In principle, a change in any of these three components could account for the effect of thiol reagents on the macroscopic hEAG1 current.

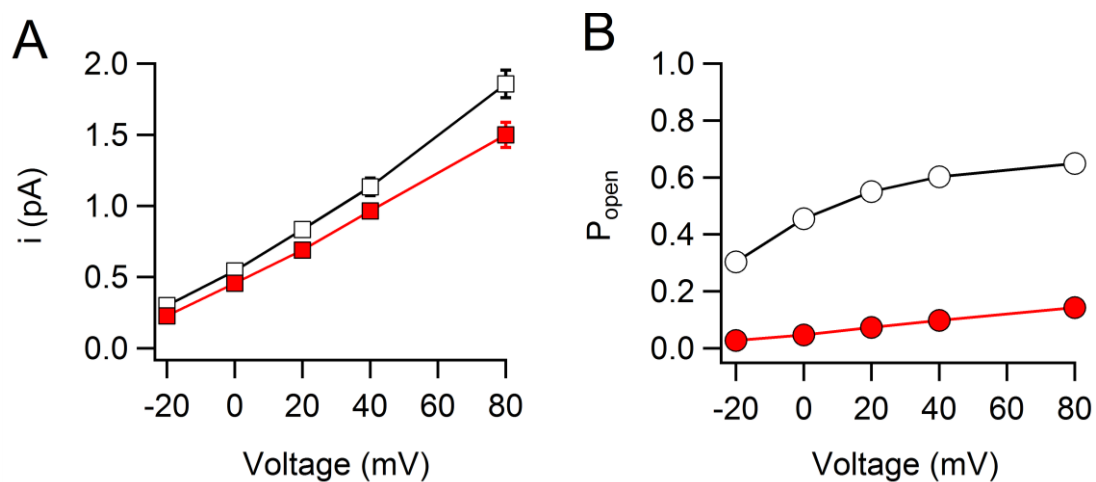


Fig. 22: DTNB modifies hEAG1 channel at single channel level. (A) Single-channel current and (B) open probability of hEAG1 channels were extracted via non-stationary noise analysis (Eq. 9), from inside-out recording at five different voltages, before (black) and after (red) application of 20 μ M DTNB ($n = 3$). The number of channels was kept constant.

Therefore, non-stationary noise analysis was performed in the inside-out configuration. Ensemble current and ensemble variance were measured for five different 50-ms depolarization voltages in parallel. From the analysis of the mean current and the variance (σ^2) of 200 consecutive traces, we found that there is a small reduction in single-channel current, while the channel open-probability potentially reduced upon application of 20 μ M DTNB (Fig. 22). At +40 mV, the single-channel current was reduced by ~14% and the P_{open} by ~83%. This observation indicates that cysteine modification induced by DTNB alters the gating properties of the channel.

3.2.5 Critical cysteines responsible for thiol-dependent modulation of hEAG1 channels

To further explore the mechanisms underlying the inhibition of hEAG1 by thiol-reactive agents, we used a site-directed mutagenesis approach to identify critical cysteine residues. As already pointed out, 19 cysteine residues in the hEAG1 sequence are located in the predicted transmembrane segments or cytosolic amino and carboxyl terminal parts of the channel and 16 cysteine residues are potentially facing the intracellular side (Fig. 23A). We examined the effects of DTNB on mutant constructs of hEAG1 that lacked one or more cysteines. Initially, we screened several constructs in which multiple cysteines were replaced by alanine. When all 19 cysteines were replaced, channels expressed poorly and were impossible to study. However constructs lacking 5 cysteines in the N terminus (Cysless-N) or lacking 11 cysteines in the C-terminus (Cysless-C) or lacking 16 cysteines in both N and C- terminus (Cysless-NC) expressed macroscopic currents. Testing the effects of DTNB on these constructs, we found that Cysless-N does not show the fast component of the DTNB effect and was slowly blocked ($80 \pm 5\%$ remaining current after 200 s) with τ_{slow} of 404 ± 73 s, whereas Cysless-C did not exhibit the slow component of the DTNB effect and was rapidly blocked ($32 \pm 3\%$ remaining current after 200 s) with τ_{fast} of 20 ± 7 s. Removing 16 cysteines together (Cysless-NC) produced a completely DTNB insensitive channel (Fig. 23B & C). The membrane-spanning S1-S6 domain possesses 3 cysteine residues but they are unlikely to be accessible from the cytosolic side and the mutant Cysless-T (C303A-C357V-C368V) showed sensitivity towards DTNB which was indistinguishable from that of the wild type (not shown).

From this observation, it is clear that N-terminal cysteines play a major role in DTNB-mediated hEAG1 inhibition. To assess the functional importance of the 5 cysteine residues in the N-terminus, each cysteine was mutated to alanine and assayed for DTNB effect. Fig. 24 describes the effect of 100 μ M DTNB on the individual cysteine mutants. Mutants C145A

and C214A showed the least DTNB sensitivity with ~66% of the remaining current. Mutations C50A, C67A and C128A showed ~ 28, 48 and 52% of the remaining current (Fig. 24). This result indicates that C145 and C214 are probably the major targets of DTNB-mediated inhibition.

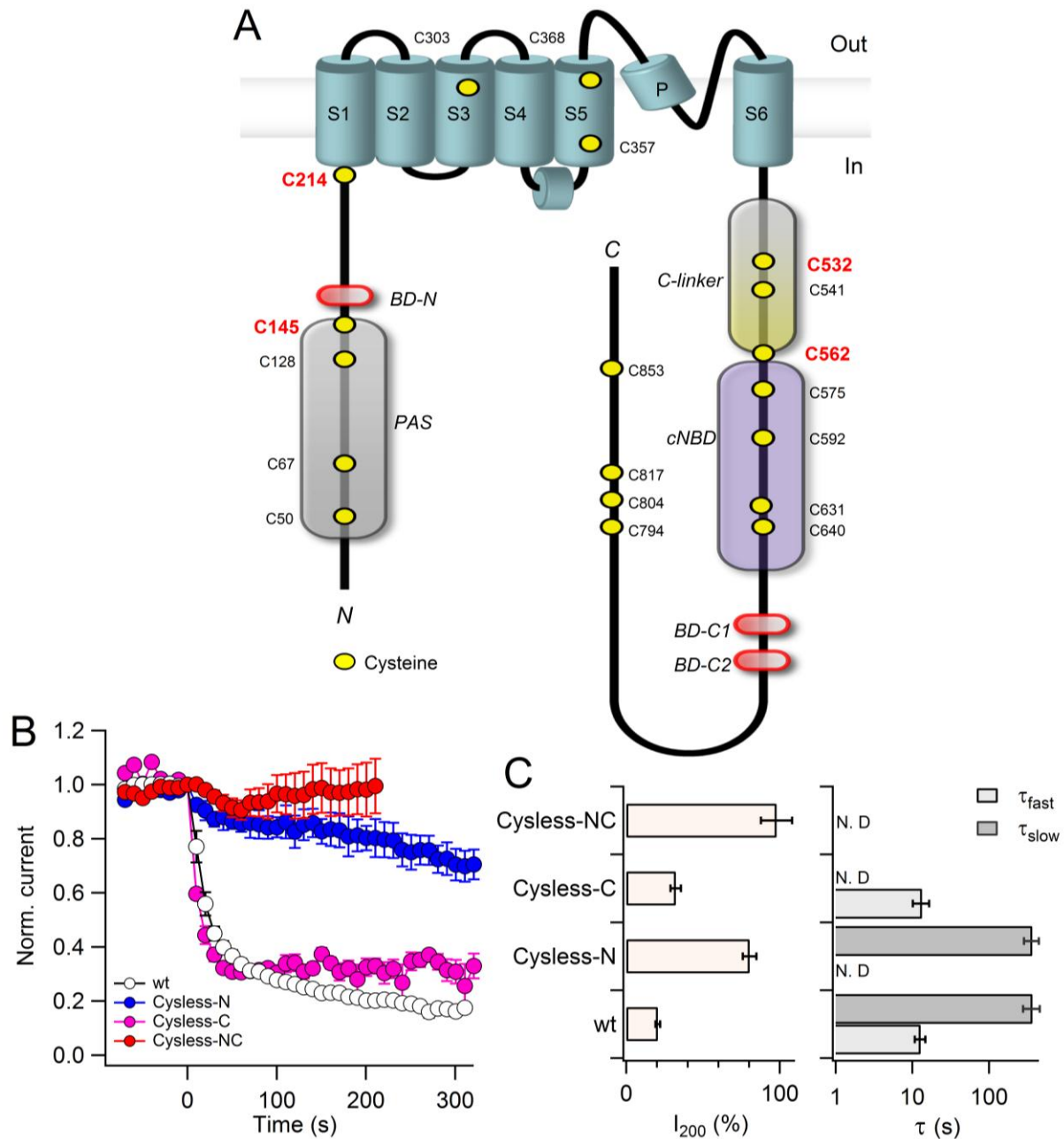


Fig. 23: Identification of critical cysteines responsible for the DTNB effect. (A) Topological model of an hEAG1 subunit indicating cysteine residues (yellow). (B) Time course of current reduction induced by intracellular application of 20 μ M DTNB to hEAG1 channels and the indicated mutants (n = 4-5). (C) (left) Relative remaining currents (I_{200}) 200 s after 20 μ M DTNB application to indicated channels (n = 4-5). (right) Time constants of onset of DTNB mediated current reduction at +40 mV were derived from Fig. 23B by fitting with double exponential fit functions (Eq. 5). Solution: symmetrical high K-Asp.

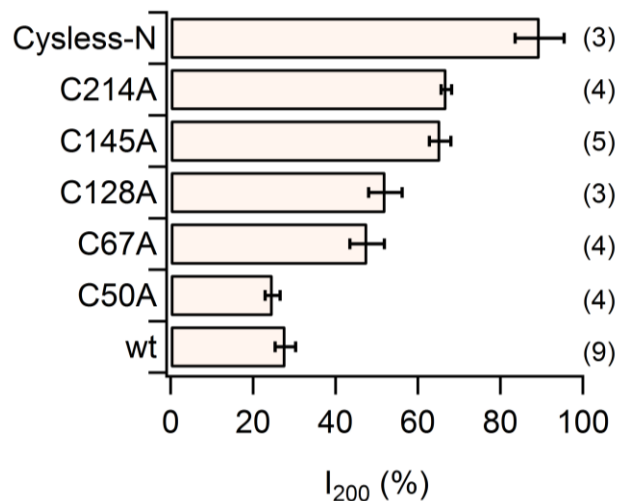


Fig. 24: Effect of DTNB on the individual cysteine mutants in the N-terminus: Relative remaining currents 200 s after 100 μ M DTNB application to individual cysteine mutants in the N-terminus. Solution: standard K-Asp.

3.2.5.1 Concurrent mutation of C145, C214, C532 and C562A removes the oxidative sensitivity

The major cytosolic domains of hEAG1 channels such as the C-linker and CNG-binding domain are conserved in the EAG family. A study from our group (Kolbe et al., 2010) has found that C723 and C740 of hERG1 channels are responsible for oxidative modification and mutation of these cysteine residues rendered the hERG1 channel less sensitive to reactive oxygen species. The homologous position in hEAG1 channels are C532 and C562. When we combined these two cysteines with the two critical cysteines in the N-terminus C145 and C214, DTNB (20 μ M) had least effect on hEAG1 current ($76 \pm 6\%$ current remaining after 200 s) ($n = 6$, Fig. 25A & B). To assess the relative contributions of N-terminal and C-terminal critical cysteines in DTNB-mediated current rundown, we assayed the effect of the DTNB on the double mutants C145-214A of the N-terminus and C532-C562A of the C-terminus. We found that mutant C145-214A removed the fast component and decreases current ($43 \pm 2\%$ remaining current after 200 s) with a time constant of 175 ± 20 s ($n = 7$), while the mutant C532-562A abolished the slow component and decreases current ($24 \pm 2\%$ remaining current after 200 s) with a time constant of 15 ± 2 s ($n = 5$) (Fig. 25A & B).

Furthermore, we analyzed the impact of DTNB on the gating of these mutant channels and found that the mutant C145-214A of the N-terminus exhibited no shift in V_m and a small change in $k_m \sim 5$ mV (Fig. 24C), whereas mutant C532-562A of the C-terminus shifted V_m by ~ 20 mV and changed in k_m by ~ 15 mV (Fig. 24B). The combination mutant C145-214-532-

562A of the N- and C-terminus has no shift in V_m and a slight change in k_m by ~ 2 mV (Fig. 24C). From this experiment, it appears that the V_m of mutants C145-214A and C145-214-532-562A were significantly right shifted in comparison to hEAG1 wt ($P < 0.01$) but the k_m was not significantly affected. This might be the reason for the mutants being insensitive to DTNB modification. However, this finding reveals that DTNB inhibits hEAG1 channels via two distinct processes: first, DTNB changes the gating property of the hEAG1 by interacting with cysteines C145 and C214 of the N-terminus and, second, DTNB inhibits hEAG1 current by interacting with cysteines of C532 and C562 of the C-linker region of the C-terminus.

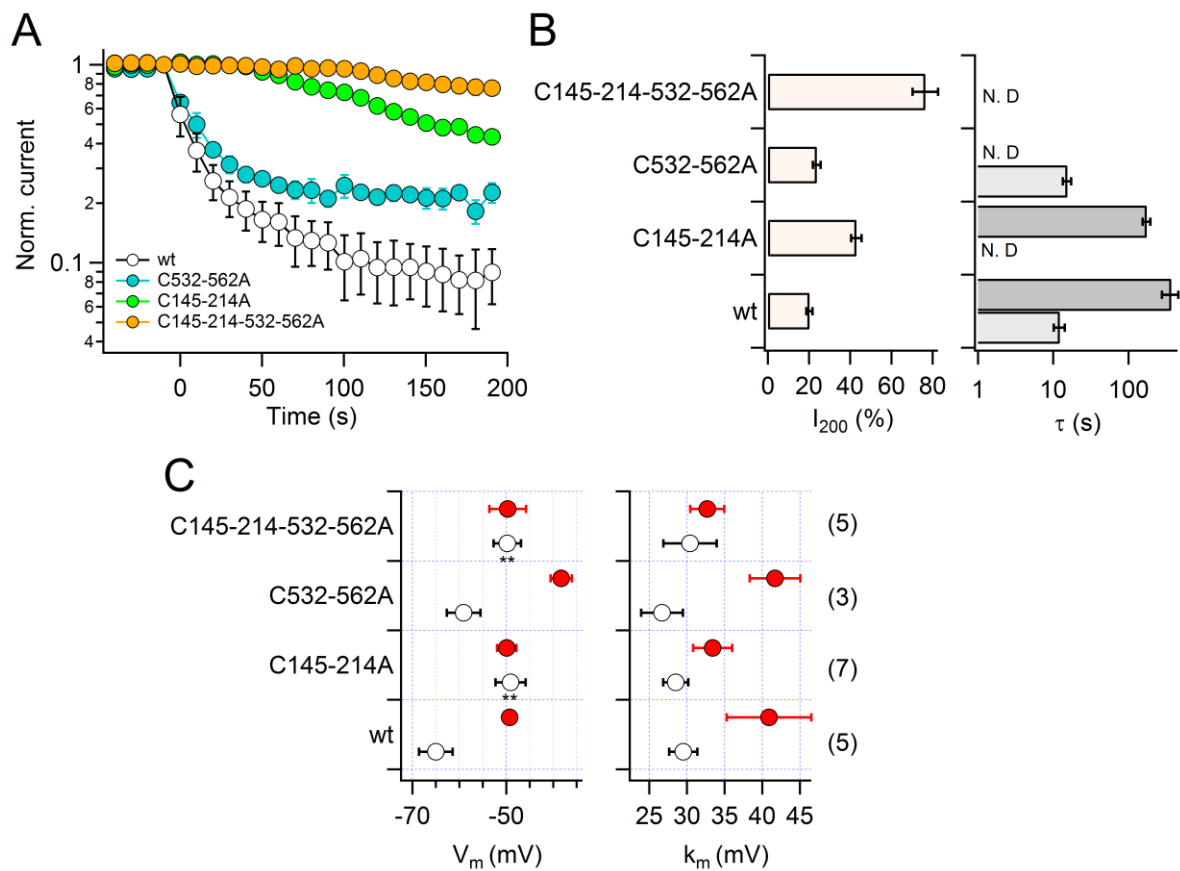


Fig. 25: Four cysteines in the N- and C-terminus of hEAG1 channels are susceptible to oxidation. (A) Time course of current rundown induced by intracellular application of 20 μ M DTNB to hEAG1 channels and the indicated mutants at +40 mV ($n = 5-7$). (B) (left) Relative remaining currents 200 s after 20 μ M DTNB application to indicated channels ($n = 5-7$). (right) Time constants of onset of DTNB mediated current reduction were derived from Fig. 25A by fitting with double exponential fit functions (Eq. 5). (C) Half-activation voltage (V_m) and slope factor (k_m) before (black) and after (red) application of 20 μ M DTNB of indicated channels. Solution: symmetrical high K-Asp.

3.2.5.2 Evaluation of critical cysteines via a knock-in approach

To further evaluate the role of four critical cysteines in DTNB-mediated hEAG1 modulation, we used a knock-in approach where the critical cysteines were reintroduced in the background

of Cysless N- and C-terminus (Cysless-NC) and assayed for the DTNB effect. This approach is particularly interesting because we can assign the role of critical cysteines in DTNB-mediated current rundown of the hEAG1 channel.

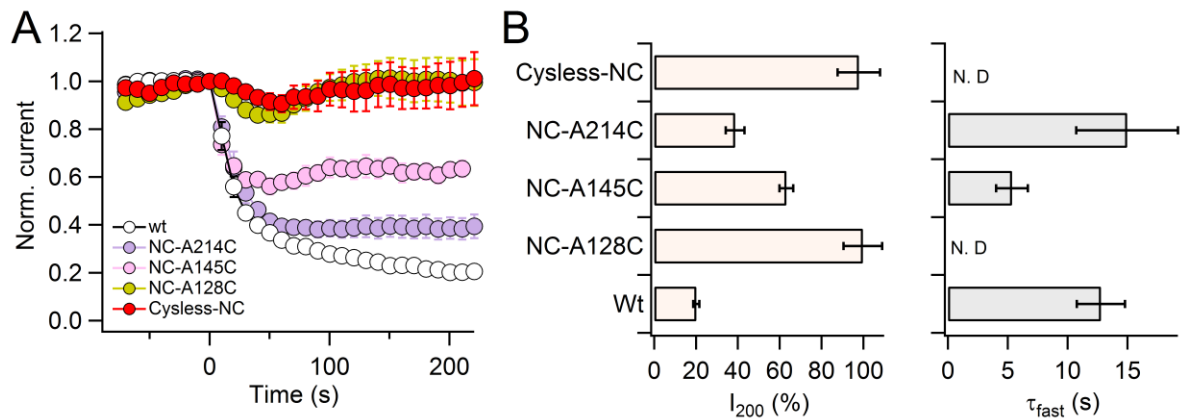


Fig. 26: Impact of DTNB on the critical cysteine knock-in mutants in the N-terminus. (A) Time course of current reduction at +40 mV, induced by application of 20 μ M DTNB to indicated knock-in mutants ($n = 4-5$). (B) (left) Relative remaining currents 200 s after 20 μ M DTNB application to knock-in mutants in the N-terminus. (right) Time constants (τ_{fast}) of onset of DTNB mediated current reduction, were derived from Fig. 26A by fitting with double exponential fit functions ($n = 4-5$).

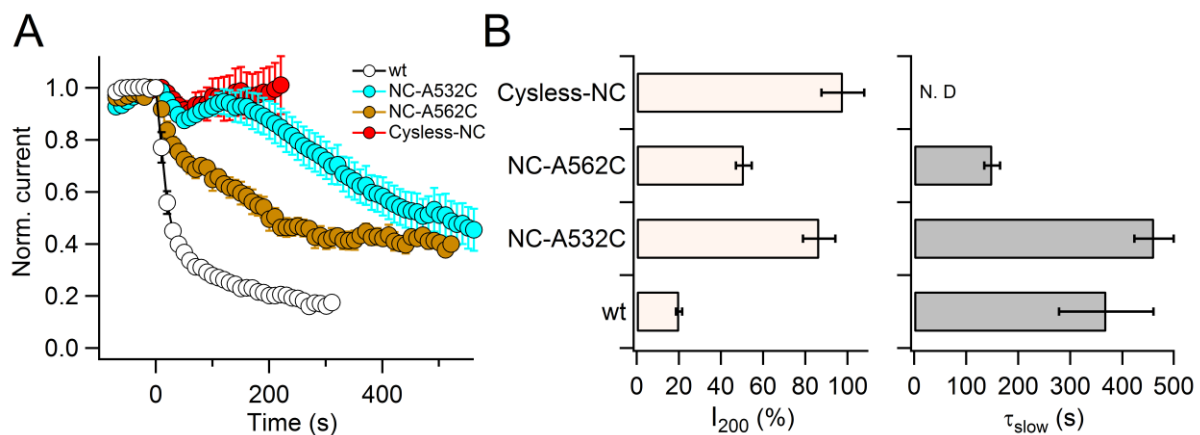


Fig. 27: Impact of DTNB on the critical cysteine knock-in mutants in the C-terminus. (A) Time course of current reduction at +40 mV, induced by application of 20 μ M DTNB to indicated knock-in mutants. (B) (left) Relative remaining currents 200 s after 20 μ M DTNB application to knock-in mutants in the C-terminus. (right) Time constants (τ_{slow}) of onset of DTNB mediated current reduction, were derived from fig. 27A by fitting with double exponential fit functions ($n = 4-5$).

Reintroduction of cysteine at position C214 and C145 gained the fast DTNB effect. Fig. 26A displays the effect of 20 μ M DTNB on the knock-in NC-A214C and NC-A145C mutants. DTNB inhibited these channels (~ 39 and 63% of the remaining current after 200 s) with a time constant of τ_{fast} of 15 ± 4 and 5 ± 1 s, respectively (Fig 26B & C). However, no DTNB effect was observed in case of NC-A128C knock-in mutants. These results provide evidence

that the fast component of DTNB effect is mediated by two critical cysteines C145 and C214 in the N-terminus. Furthermore, we performed a similar study with knock-in mutants in the C-linker region of the C-terminus. Fig. 27A displays the effect of DTNB on knock-in NC-A532C and NC-A562C mutants. Reintroduction of cysteine at position C532 and C562 gained the slow DTNB effect (Fig. 27A), ~86 and 51% of the remaining current after 200 s with a time constant of τ_{fast} of 507 ± 36 and 150 ± 15 s, respectively (Fig 27B & C). These results provide evidence that C-linker cysteines contribute to the slow DTNB effect.

3.3 Heme is a potent inhibitor of EAG potassium channels

3.3.1 Effect of hemin on delayed rectifier potassium channels

From the preceding study we found that A-type potassium channels with heme binding motifs (CxxH) in the N-terminal ball-domain are modulated by heme. This observation raised the logical question whether other channels are similarly regulated by heme/hemin. Therefore, we studied the impact of hemin on delayed rectifier potassium channels.

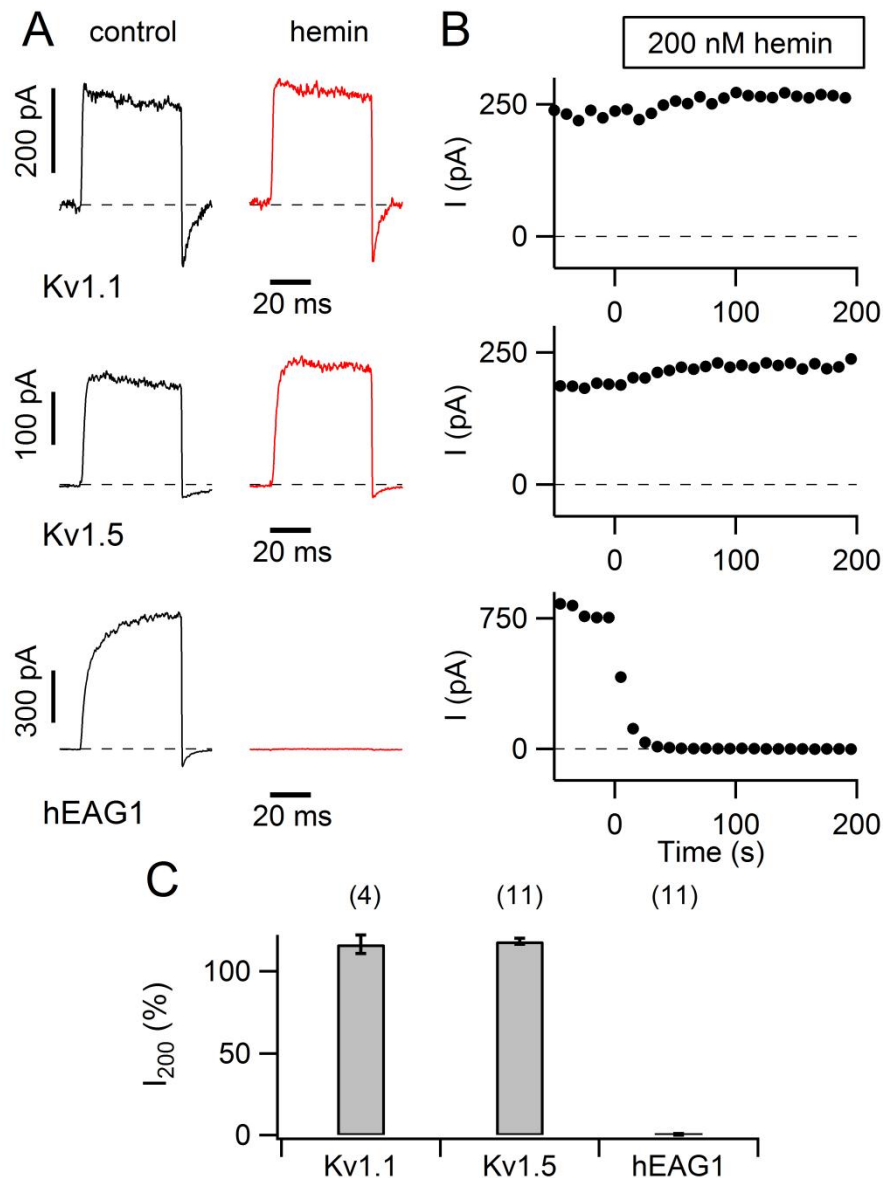


Fig. 28: Effect of hemin on voltage-gated potassium channels. (A) Current responses of the indicated channel types expressed in *Xenopus* oocytes, recorded from inside-out patches before (black) and 200 s after (red) application of 200 nM hemin. (B) Maximal currents measured at +40 mV as a function of time. The application of 200 nM hemin is indicated. (C) Relative remaining current upon application of 200 nM hemin after 200 s for the indicated channel types.

Fig. 28 shows the effect hemin on delayed rectifier potassium channels Kv1.1, Kv1.5 and hEAG1, expressed in *Xenopus* oocytes. To assay the action of hemin, repetitive 50-ms depolarizations to +40 mV were applied and currents were measured at the end of the test pulses. Intracellular application of 200 nM hemin caused a slight increase in Kv1.1 and Kv1.5 current. On the contrary, hemin efficiently inhibited hEAG1 channels to $0.8 \pm 0.5\%$ remaining current after 200 s (Fig. 28). This observation implies that hemin is an inhibitor of hEAG1 channels. However, hemin did not have any noticeable effect when applied to the channels from the extracellular side (data not shown), suggesting that the intracellular side of the channel is responsible for the hemin effect.

3.3.2 Hemin reduces K^+ currents through hEAG1 potassium channels

In order to understand the effect of hemin on hEAG1 current in detail, we measured hEAG1 channels in symmetrical potassium solutions.

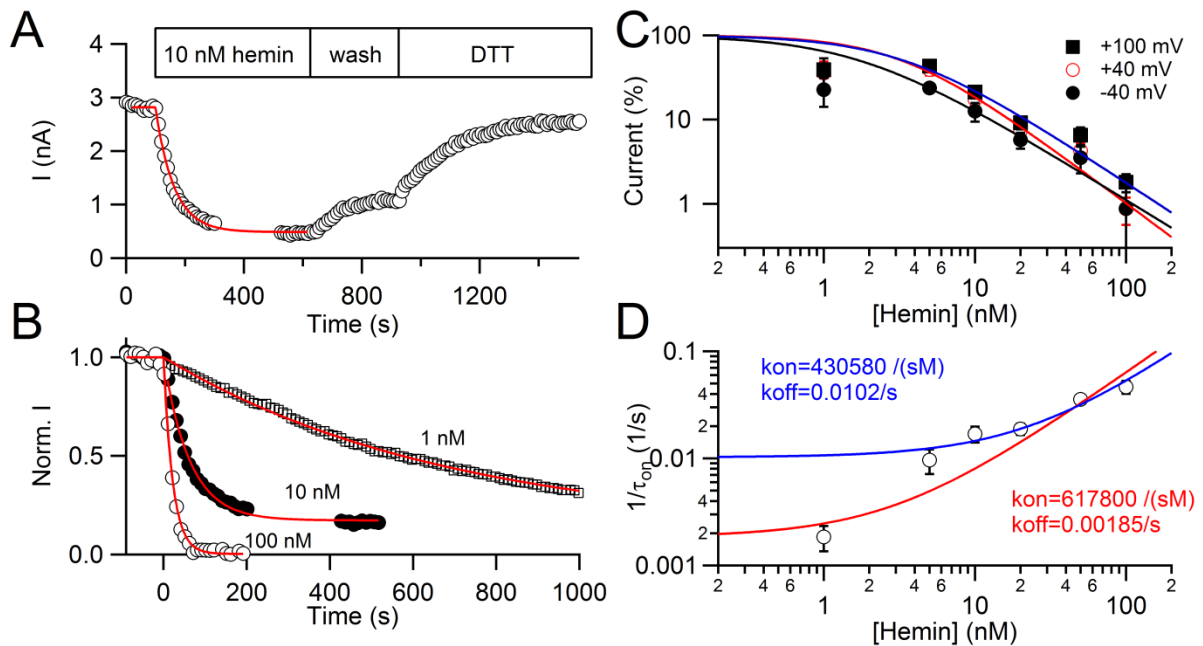


Fig. 29: Concentration dependence of hEAG1 inhibition by hemin. (A) Time course of hemin effect on hEAG1 channels in an inside-out patch. Currents were elicited by +40 mV depolarization at an interval of 10 s. Upon equilibration of the hemin effect, control solutions were applied (wash); finally, the inside-out patch was exposed to control solution with 3 mM DTT. The continuous curve is a single-exponential data fit to characterize the onset of current inhibition. (B) Example of onset of hemin-induced current inhibition for the indicated hemin concentrations at +40 mV with superimposed single-exponential fits. (C) Concentration dependence of the equilibrium current inhibition at -40, +40, and +100 mV. The continuous curves represent fits with a Hill equation (Eq. 6). (D) Inverse of the time constant of hemin-induced current inhibition ($1/\tau_{on}$) as a function of hemin concentration. The continuous line is the result of a data fit assuming a single molecular reaction (blue and red lines are fits without and with 1 nM data, respectively), i.e. $\tau_{on} = \frac{1}{[Hemin]k_{on}+k_{off}}$ and $K_d = k_{off} / k_{on}$.

Application of 10 nM hemin from the cytosolic side consistently and markedly reduced the macroscopic hEAG1 K⁺ current amplitude to ~15% of the control, following an exponential time course (Fig. 29A). This potent inhibitory action of hemin was direct because the inhibition occurred spontaneously without any exogenously added enzyme or cofactor; and the effect of hemin significantly outlasted its application duration and was only very slowly and partially reversed by wash, indicative of a very stable physical interaction between hemin and the channel protein. The reversibility was accelerated by the application of DTT.

Hemin decreases hEAG1 currents in a concentration dependent manner. A lower concentration of hemin, 1 nM, was also effective (Fig. 29B) but the time course of development of the inhibition was slower. The observation that 1 nM hemin progressively decreased current suggests that even picomolar concentrations of hemin, given enough time, are effective. Fig. 29B shows the impact of hemin on hEAG1 at 3 different concentrations. The magnitude of the responses was dependent on [hemin]_i with half-maximal inhibitory concentration of 1.7 ± 0.3 nM, 3.3 ± 0.5 nM and 3.4 ± 0.5 nM at -40, +40 and +100 mV, and a Hill coefficient of ~1 (Fig. 29C). However, data for 1 nM did not fit to a Hill function; it can be interpreted such that the slow inhibitory effect of 1 nM hemin might be the mixture of the current rundown and hemin effect or the hEAG1 channel may harbor more than one hemin binding site.

We determined the kinetics of the inhibitory interaction between the hEAG1 channel and hemin at various hemin concentrations. Our results suggest that the “on” kinetics (rate of association) follows a single exponential time course, consistent with the idea that binding of one hemin molecule to the channel is sufficient to alter the characteristic of the channel. The “on” kinetics appears concentration dependent, becoming faster with increasing concentrations of hemin (Fig. 29D). The rate of association $k_{on} = \sim 4.3 \times 10^5 \text{ s}^{-1} \text{ M}^{-1}$. The “off” kinetics (rate of dissociation) is more difficult to measure because washout does not rapidly restore the current size (Fig. 29A). Nevertheless, our results appear to suggest that the “off” kinetics is very slow and independent of hemin concentration, rate of dissociation $k_{off} = \sim 0.01 \text{ s}^{-1}$. The apparent dissociation constant (K_d) was ~24 nM. When we included the 1 nM hemin data, the k_{on} became $\sim 6.2 \times 10^5 \text{ s}^{-1} \text{ M}^{-1}$ and k_{off} became extremely slow $\sim 0.002 \text{ s}^{-1}$, suggesting that hemin might be interacting with more than one binding site; therefore, hemin dissociation from the channel became slower. The apparent K_d became ~3 nM which was approximately the same as the IC₅₀ value at +40 mV. This observation indicates that the effect of 1 nM hemin on hEAG1 channel is not the combined effect of hemin and rundown. However, the tentative findings that rate of dissociation \ll rate of association and the half-effective

concentration is on the range of 1 nM may have the consequence that every channel is essentially fully bound with hemin at ≥ 10 nM.

3.3.3 Hemin inhibits hEAG1 channels in a voltage-dependent manner

The fact that hemin decreases hEAG1 currents could be annotated to indicate that hemin is a simple pore blocker of the hEAG1 channel.

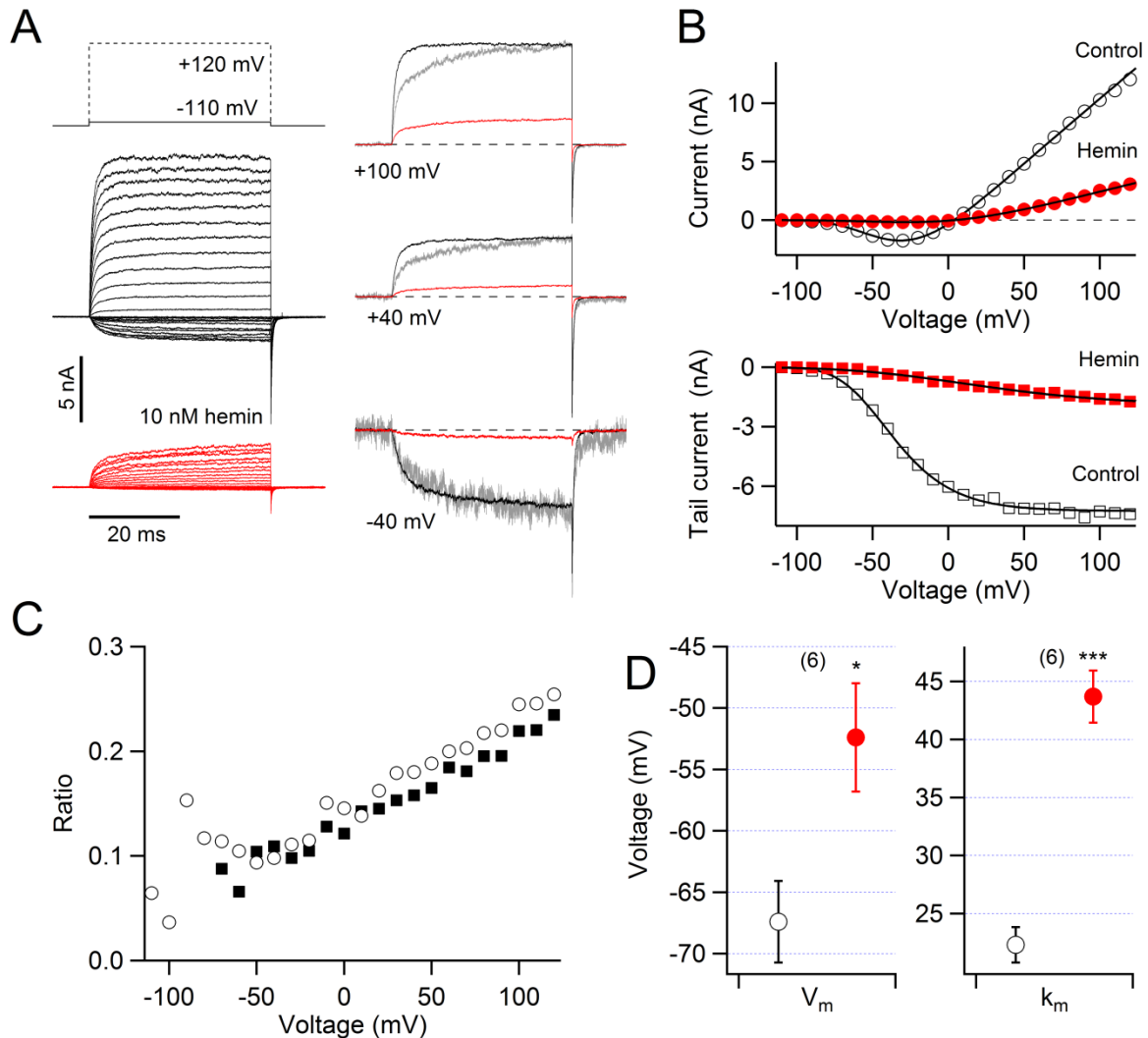


Fig. 30: Voltage dependence of hemin-induced hEAG1 inhibition. (A, left) Superposition of current traces recorded from inside-out patches according to the indicated pulse protocol in which depolarizations range from -110 to $+120$ mV before (black) and after (red) application of 10 nM hemin. (A, right) Sample current traces from the experiment shown on the left for the indicated voltages before (black) and after (red) hemin application. The gray traces are scaled hemin traces to match the maximal control current. Scale factors applied: -40 mV: 10.7; $+40$ mV: 5.2; $+100$ mV: 3.92. (B) (top) Mean current measured at the end of test depolarizations, (bottom) tail currents at -140 mV as a function of test voltage with superimposed data fits according to Eq. 7 ($n = 6$). (C) Voltage dependence of relative current remaining after application of 10 nM hemin determined from test currents (B, top) (circles) and from tail currents (B, bottom) (squares) indicating an almost linear voltage dependence of the hemin-mediated current reduction. (D) Half-activation voltage (V_m) and slope factor (k_m) before (black) and 200 s after (red) application of 10 nM hemin. Data were obtained by fitting I-V curves with the Goldman-Hodgkin-Katz equation (Eq. 7).

However, our results collectively show that hemin is a gating modifier of the hEAG1 channel. For example, hemin slows the activation kinetics at positive voltages and accelerates the deactivation kinetics (Fig. 30A, right). Additionally, hemin shifts the half-activation voltage (V_m) to the positive direction from -67 ± 3 mV to -52 ± 4 mV ($P = 0.02$) and the slope factor (k_m) from 22 ± 1 to 43 ± 3 mV ($P < 0.001$) (Fig. 30B & D). From the relative fraction of the hemin effect it is evident that the inhibitory effect becomes stronger at negative voltages and the effect becomes weaker at depolarizing voltages (Fig. 30C). This observation implies that hemin modifies the voltage dependence of hEAG1 channels.

3.3.4 Effects of heme and heme-related chemicals on hEAG1 channels

In order to unravel whether the inhibitory effect of hemin is specific or due to components of hemin, we tested the impact of Fe^{3+} (FeSO_4) and protoporphyrin IX (pp-IX) on hEAG1 channels. Fig. 31 describes the averaged relative remaining hEAG1 current after 200 s. FeSO_4 (1 μM) and pp-IX (50 nM) had no impact on the hEAG1 current, indicating the specificity of hemin-induced hEAG1 current reduction (Fig. 31).

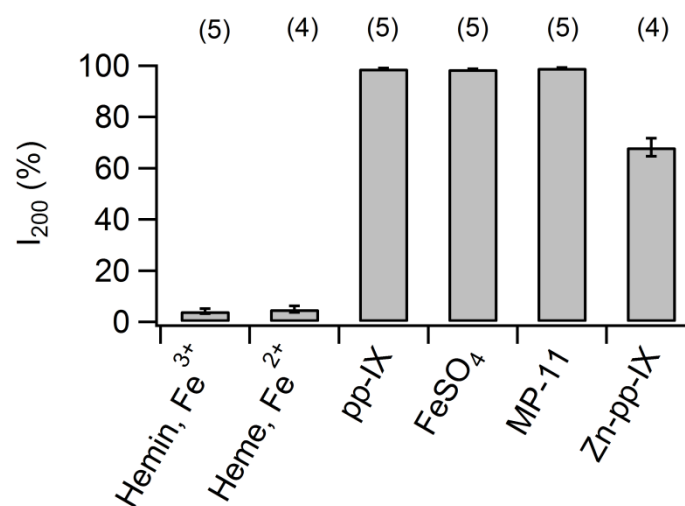


Fig. 31: Specificity of hemin effect on hEAG1 channels. Effects of heme and heme-related chemicals on hEAG1 currents in inside-out patches, measured at +40 mV. Averaged relative remaining current upon application of hemin (Fe^{2+}), heme (Fe^{3+}), pp-IX (50 nM), as well as for FeSO_4 (1 μM), MP-11 (2 μM), and Zn-pp-IX (50 nM).

We tested microperoxidase MP-11, a small peptide isolated from horse cytochrome *c* in which heme remains incorporated. When applied to hEAG1 channels at a concentration of 2 μM , no alteration of channel current was observed, indicating that the bound form of heme does not affect hEAG1 channels. Reduction of the heme iron to the reduced ferrous form (Fe^{2+}) by sodium dithionite (1 mM) did not alter the current inhibition efficacy, indicating that the electronic state of the iron center is not crucial. Another type of metal protoporphyrin IX,

Znic protoporphyrin IX, also inhibited the hEAG1 channel, although it was less effective than hemin (Fig. 31).

3.3.5 Pull-down assay for hemin binding to hEAG1 channels

To evaluate whether hemin can directly interact with hEAG1, hemin-agarose pull-down assays, essentially as described by Lee (1992), were performed. We prepared crude cell lysates containing hEAG1 from HEK 293 cells heterologously expressing human EAG1 channels and tested the ability of the hemin-agarose affinity resin to precipitate the plasma membranes by binding to hEAG1 in them.

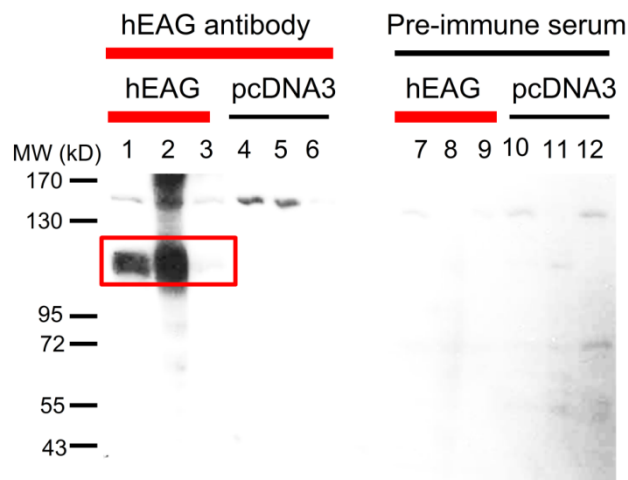


Fig. 32: Hemin pull-down assay.

1-6: probed with polyclonal hEAG antibodies.

7-12: probed with pre-immune serum.

1, 7: hEAG1 cell sample.

2, 8: hEAG1 cell sample and hemin-agarose beads.

3, 9: first wash flow through of hEAG1 lysate + hemin beads.

4, 10: pcDNA3 only cell sample.

5, 11: pcDNA3 only cell sample and hemin-agarose beads.

6, 12: first wash flow through of pcDNA3 only cell sample and hemin-agarose beads.

The hEAG1 bands are boxed. The polyclonal antibodies may recognize other proteins, one of which is around ~150 kD.

Essentially the same purification protocol was successfully used in our previous studies examining the direct physical interaction between the channel and calmodulin (Schönherr et al., 2000; Ziechner et al., 2006) and S100B (Sahoo et al., 2010). hEAG1 antibodies against the distal C-terminus sequence (⁸⁰⁵AKRKSWARFKDACGK⁸¹⁹) of hEAG1, prepared by a commercial service (Antagene), was used to recognize hEAG1. A representative data set is shown in Fig. 32. The antibodies recognize hEAG1 (~110 kD in size; lane 1) in the hEAG1-expressing cell lysate and the sample containing hemin agarose beads pre-incubated with hEAG1-expressing cell lysate (lane 2 vs. 3). However no non-specific bands appeared when

hemin agarose beads were pre-incubated with cell lysate containing mock pcDNA3.1 vector (lane 4-6). Similar experiments were carried out with pre-immune serum and also no nonspecific bands appeared, indicating the specificity of the hEAG1 antibody (lane 7-12) (Fig. 32). This result suggests that hemin directly interacts with the hEAG1 channel.

3.3.6 Annotation of the molecular loci required for the hemin-channel interaction

We hypothesize that the hEAG1 channel has heme binding pockets, into which heme can fit and remain bound in a stable manner in part by the ligation of the iron center with the channel protein.

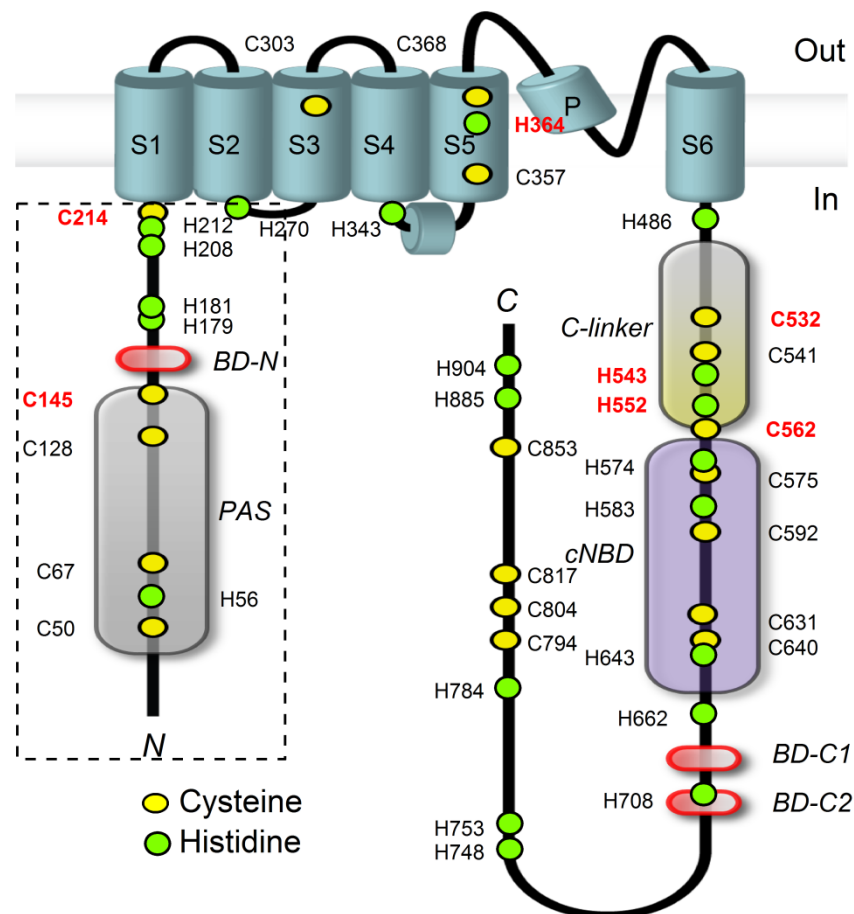


Fig. 33: Schematic illustration of an hEAG1 subunit. Topological model indicating cysteine and histidine residues and the deletion of N-terminus (dashed rectangle) introduced to hEAG1. Cysteine and histidine residues of particular importance are highlighted (red). Characteristic domains are: PAS: Per-Arnt-Sim domain; cNBD: cyclic nucleotide binding domain; BD-N, BD-C1 and BD-C2: calmodulin binding sites.

In order to reveal the molecular loci within hEAG1 required for the hemin effects, we used multiple approaches: deletion mutagenesis, systematic cysteine mutagenesis, histidine mutagenesis, and chimeric approaches. The hEAG1 channel has large N and C termini (Fig. 33). The N-terminus of hEAG1 channels bears a PAS domain and it has been reported that

heme can bind to the PAS domain of many proteins (Gilles-Gonzalez and Gonzalez, 2004). In order to reveal whether the PAS domain of hEAG1 channels plays a role in heme sensitivity, we used a deletion construct that lacks the PAS domain, 189-residues of the N-terminus (hEAG1 Δ N), and tested for hemin effect. It has been shown that the activation threshold of the hEAG1 Δ N channel was shifted by about -75 mV and the deactivation was slow. As a result, these channels were constitutively open around the normal resting potential of an excitable cell and Ca^{2+} /calmodulin insensitive (Ziechner et al., 2006). However, our result show that 200 nM hemin completely inhibited hEAG1 Δ N channels (Fig. 34). This finding demonstrates that the PAS domain of the hEAG1 channel is not responsible for the hemin effect.

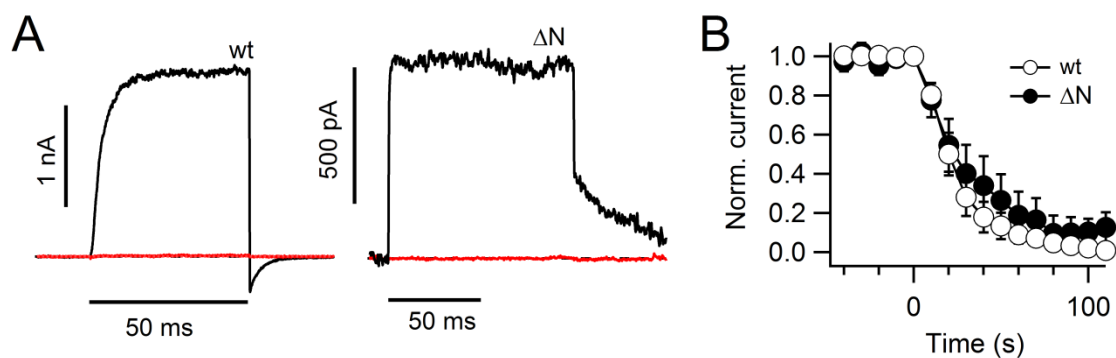


Fig. 34: hEAG1 N-terminus is not responsible for hemin sensitivity. (A) Superposition of current traces recorded from inside-out patches of indicated channel types at $+40$ mV before (black) and 150 s (wt), 90 s (Δ N) after (red) application of 200 nM hemin. (B) Time course of current reduction upon application of 200 nM hemin for the indicated channel types: hEAG1 wt ($n = 8$) and hEAG1 Δ N ($n = 4$), holding potential for hEAG1 was -80 mV and for hEAG1 Δ N -120 mV.

Our previous studies on heme modulation of Kv1.4 channels and the studies about the heme regulation of BK channels (Tang et al., 2003) suggest that heme is dependent on cysteine residues. Following this example, it may be hypothesized that hemin binding to the hEAG1 channel would require cysteine in the channel as a potential target for heme-mediated oxidation. This hypothesis is particularly attractive because we observed that the hEAG1 channel activity is inhibited by treatment with select cysteine modifiers. The possible involvement of cysteine oxidation is also suggested by our finding that the reducing agent DTT accelerates recovery from the hemin effect (Fig. 29A). We tested the hypothesis that hemin binding promotes cysteine oxidation, which in turn leads to the observed electrophysiological consequences, using mutant hEAG1 channels wherein one or more cysteine residues are replaced with alanine. As mentioned in Section 3.2, an hEAG1 subunit possesses 19 cysteine residues and a construct lacking 16 cysteines in both N- and C terminus (Cysless-NC) produced oxidation insensitive channels. We tested this constructs for the hemin effect. Our results show that the hEAG1 Cysless-NC channel remains sensitive to

intracellular hemin (200 nM). The membrane-spanning S1–S6 domain possesses three cysteine residues but they are unlikely to be accessible from the cytosolic side. Our results indicate that mutation of cysteines in the S5 transmembrane region (C357V and C368V) retains sensitivity to hemin (Fig. 35). Replacement of cysteines in the S3 transmembrane region (C303A) showed hemin sensitivity but the time course of development of the inhibition was slower. The impact of hemin on C303A was significantly less ($53 \pm 4\%$ remaining current after 50 s, $P < 0.001$, $n = 3$) than the wild-type ($12 \pm 5\%$ remaining current after 50 s, $n = 8$) (Fig. 35). This result suggests that C303 could play a role in hemin-induced hEAG1 channel inhibition.

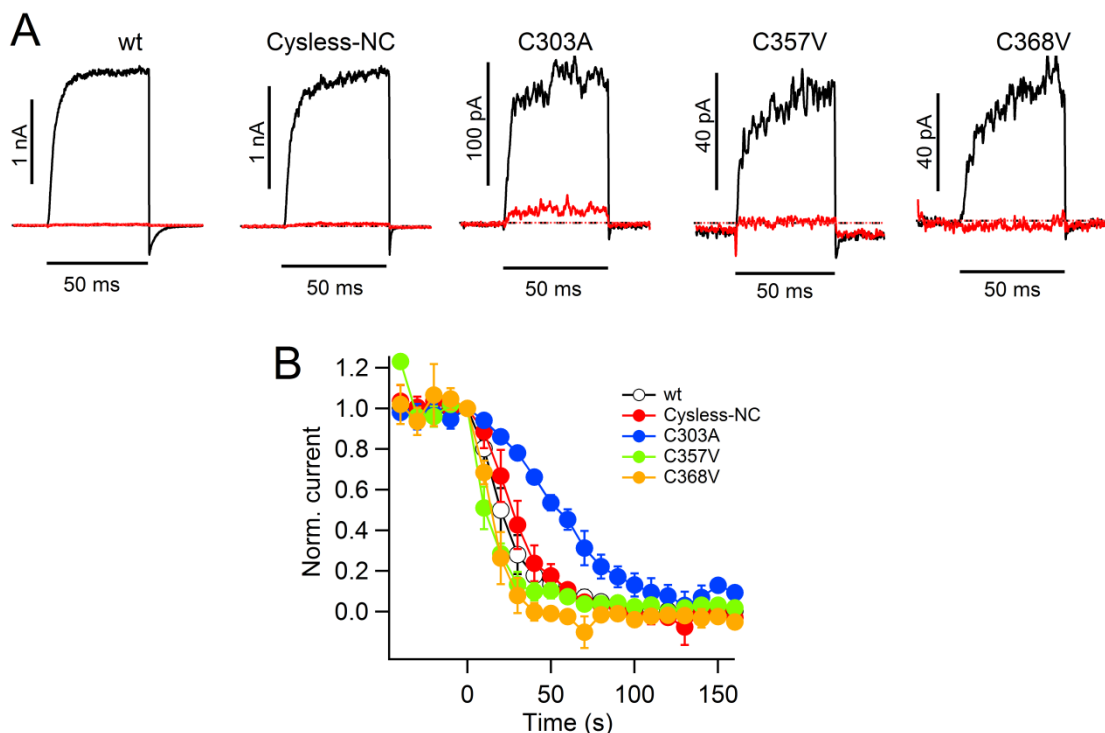


Fig. 35: Impact of hemin on cysteine residues on hEAG1 channels. (A) Superposition of current traces recorded from inside-out patches of the indicated channel variants at +40 mV before (black) and 150 s after (red) application of 200 nM hemin. (B) Time course of current reduction upon application of 200 nM hemin for the indicated channel types: hEAG1 wt ($n = 8$); Cysless-NC ($n = 5$); C303A ($n = 3$); C357V ($n = 2$); C368V ($n = 5$).

Our next strategy was to systematically mutate histidine residues in the hEAG1 channel. In numerous heme proteins, histidine acts as an important axial ligand to the heme iron center (Reedy and Gibney, 2004), suggesting that histidine in hEAG1 may be also important. Accordingly, we systematically mutated each histidine to arginine in hEAG1 and assessed whether any of the mutations alters the hemin sensitivity. hEAG1 contains 21 histidine residues: 5 in the N terminus, 3 in the transmembrane segments and 13 in the C terminus (Fig. 33). Initially, we screened several constructs in which multiple histidines were replaced by arginine. A simultaneous replacement of all 21 histidines and 13 histidines of the C-terminus

yielded an electrophysiologically non-functional protein. Furthermore, analysis of each individual histidine mutant revealed that H364R in the S5 region and H543R and H552R in the C-linker region produced non-functional channels. However, constructs lacking 2 histidines in transmembrane region (H270-343R), 6 histidines in the distal C-terminus (H708-904R), and individual histidine mutants in the cNBD segment (H486R, H574R, H583R, H640R, and H662R) expressed macroscopic currents. These constructs were assayed for the hemin sensitivity.

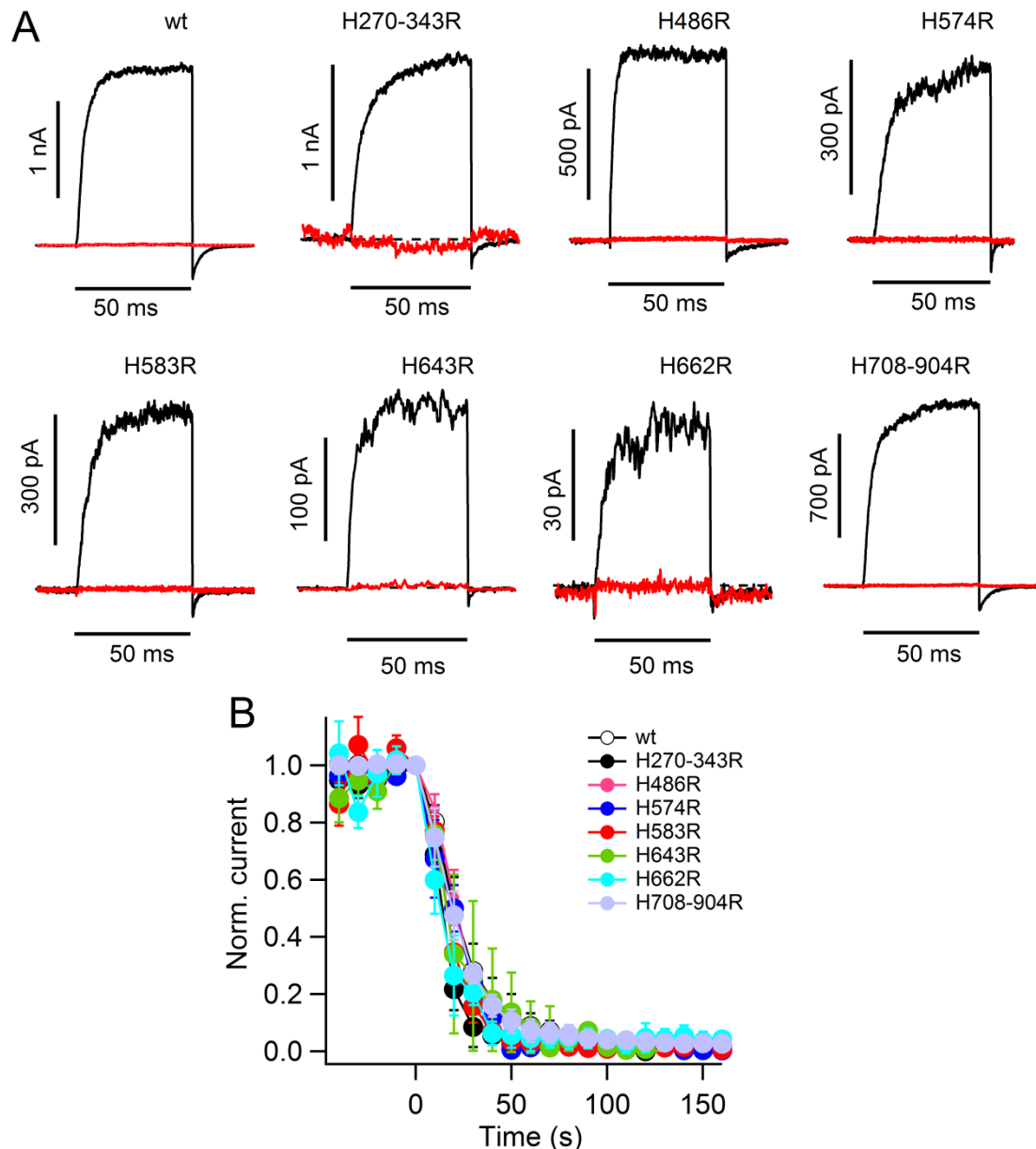


Fig. 36: Impact of hemin on histidine mutants of hEAG1 channels. (A) Superposition of current traces recorded from inside-out patches of indicated channel types at +40 mV before (black) and 150 s after (red) application of 200 nM hemin. (B) Time course of current reduction upon application of 200 nM hemin for the indicated channel types: hEAG1 wt (n = 8); H270-343R (n = 4); H486R (n = 3); H574R (n = 4); H583R (n = 3); H643R (n = 3); H662R (n = 3); H708-904R (n = 4). Mutant label

“H708-904R” denotes the combination of 6 histidine mutants: H708R-H748R-H753R-H784R-H885R-H904R.

Our result shows that none of the histidine mutants abolished hemin sensitivity (Fig. 36). In order to unravel the importance of histidine residues in channel function, we used histidine modifying reagents. Intracellular application of histidine modifier diethyl pyrocarbonate (DEPC, 7 mM), which reacts with the histidine nitrogen atoms, caused a complete inhibition of hEAG1-mediated current (data not shown). This observation indicates that histidines are essential for channel function and raised the possibility that the 3 histidines (H364 in the S5 region and H543 and H552 in the C-linker region) could play a role in hemin-mediated sensitivity.

3.3.6.1 Histidine 364 in the S5 region and histidine 543 and 552 in the C-linker region may represent heme binding sites in hEAG1 channels

From the preceding results we speculated that two areas of the hEAG1 channel may be particularly critical for the hemin sensitivity: the S5 segment and the C-linker segment of the cytoplasmic domain connecting to the S6 segment.

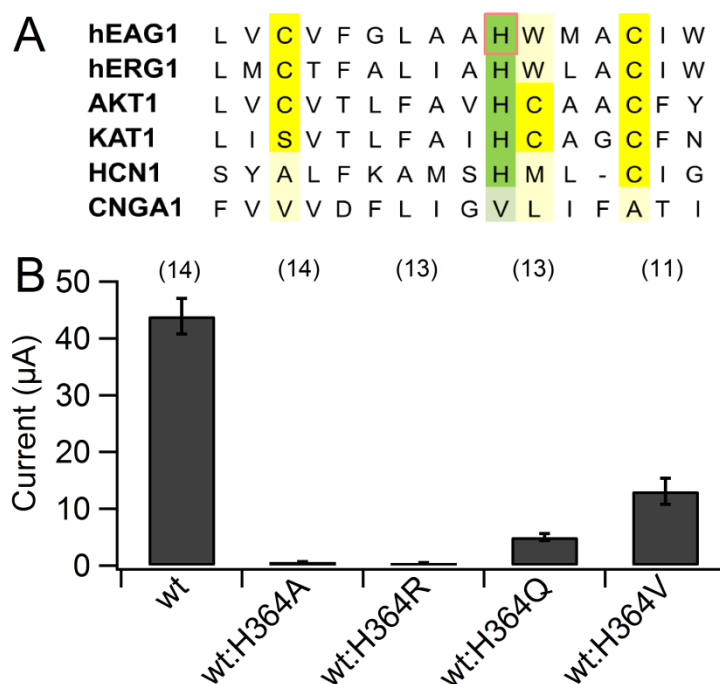


Fig. 37: Representation of S5 histidines. (A) Multiple sequence alignment of S5 segment of cNBD family of channels. Red box indicates the H364 of hEAG1 channels, might be responsible for hemin binding. (B) Mean current measured at the end of test depolarizations +40 mV, measured in two-electrode voltage clamp configuration. hEAG1 wt was co-expressed with four different histidine substituted mutants in 1:1 ratio and measured after 4th day of mRNA injection.

The S5 segment of hEAG1 channels has a histidine at position 364 and is conserved throughout the hEAG1 family and cNBD family of channels. Alignment of the S5 region also revealed that the plant potassium channels KAT1 and AKT1 harbor a classical cytochrome *c* heme binding motif but in opposite order HCxxC (Fig. 37A). A synthetic peptide consisting of 5 amino residues (HCAAC) of the S5 region of AKT1 potassium channels functionally interacts with hemin, as revealed by UV-Vis spectroscopy method. Mutant peptides where histidine is replaced by arginine (RCAAC), did not interact with hemin, suggesting that histidine of S5 region could contribute in hemin mediated sensitivity of hEAG1 channels (this study was performed by Dr. Diana Imhof, University of Jena, Germany).

H364 of hEAG1 channel was mutated to 4 different amino acids alanine, arginine, glutamine, and valine. All of the mutants produced an electrophysiologically non-functional protein. In addition, these mutants were found to function as a dominant negative mutation when coexpressed with wild-type (Fig. 37B), indicating that H364 is a key player in channel function.

The C-linker segment is one of the high-priority target areas because in the previous section we found that cysteines at position C532 and C562 of hEAG1 channels and C723 and C740 of hERG1 channels (Kolbe et al., 2010) in the C-linker region confer oxidation sensitivity to the channels.

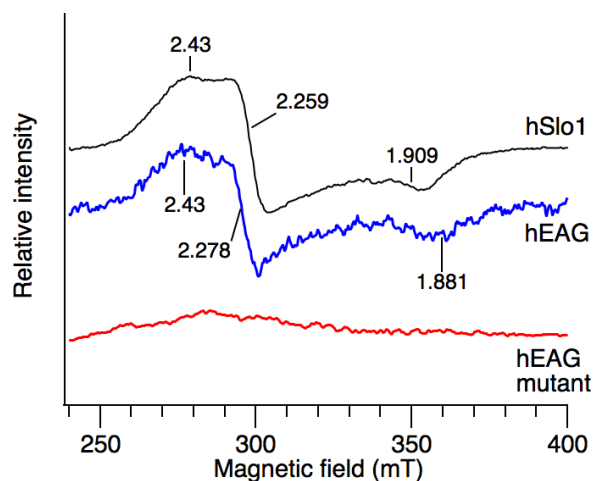


Fig. 38: EPR measurements using a model channel peptide in the presence of hemin. Equal concentrations of the peptides and hemin were subjected to EPR at 15 K. hSlo1: a heme binding peptide (23 residues) derived from the Slo1 BK channel (Tang et al., 2003), hEAG1: “C-linker peptide”, hEAG1 mutant: a “C-linker” peptide in which two histidine residues (H543R/H552R) are replaced with arginine. The Landé factors calculated are shown (experiment was carried out by Prof. S.H. Heinemann and Dr. R. Kappl, Universität des Saarlandes, Homburg).

Here we showed that mutation of H543 and H552 of C-linker region to arginine or alanine resulted non-functional channels indicating the functional importance area. Based on this observation, we speculate that the C-linker segment may be critical for hemin regulation of

the hEAG1 channel. Therefore, we synthesized a 22-mer peptide with a sequence corresponding to the C-linker segment and subjected it to EPR measurements (Fig. 38). When incubated with hemin, the C-linker hEAG1 peptide showed a rhombic signal typical for low-spin Fe^{3+} and the signal closely resembled that obtained with the Slo1 hemin binding protein used in study by Tang et al. (2003). Importantly, mutation of the two histidine residues in the peptide (equivalent to H543 and H552 in the channel) to arginine abolished the rhombic signal (Fig. 38). This observation demonstrates that hemin interacts with hEAG1 channels via C-linker histidines H543 and/or H552.

3.3.6.2 Chimeric approach to identify molecular loci required for the hemin-channel interaction

The result presented above suggests that the C-linker peptide consisting of relevant histidines interact with hemin and the S5 region histidine may functionally interact with hemin. However, it was not possible to show the interaction by the patch-clamp method, because the mutants produced an electrophysiologically non-functional protein. A chimeric approach could be a strategy of choice for solving this problem.

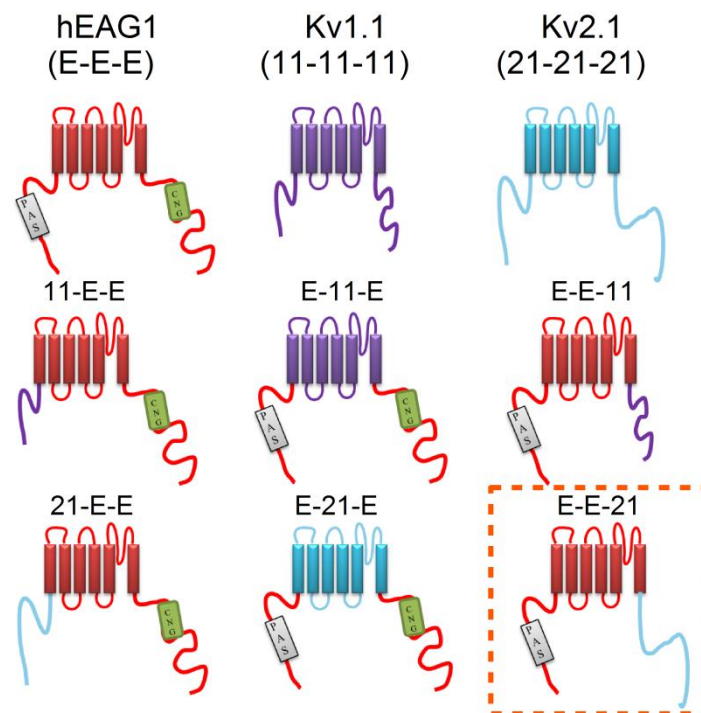


Fig. 39: Chimeric constructs involving hEAG1 (hemin inhibits the channel), Kv1.1 (hemin insensitive) and Kv2.1 (hemin opens the channel). Each construct is named for its N terminus, transmembrane area, and C terminus. For example, “E-E-E” represents wild type hEAG1 and “11-E-E” has a Kv1.1 N-terminus, an hEAG1 transmembrane domain, and an hEAG1 C-terminus. hEAG1 parts are shown in red, Kv1.1 in violet, and Kv2.1 in blue. The orange box indicates the only functional chimera “E-E-21” that produced macroscopic current and was suitable for inside-out patch-clamp measurements.

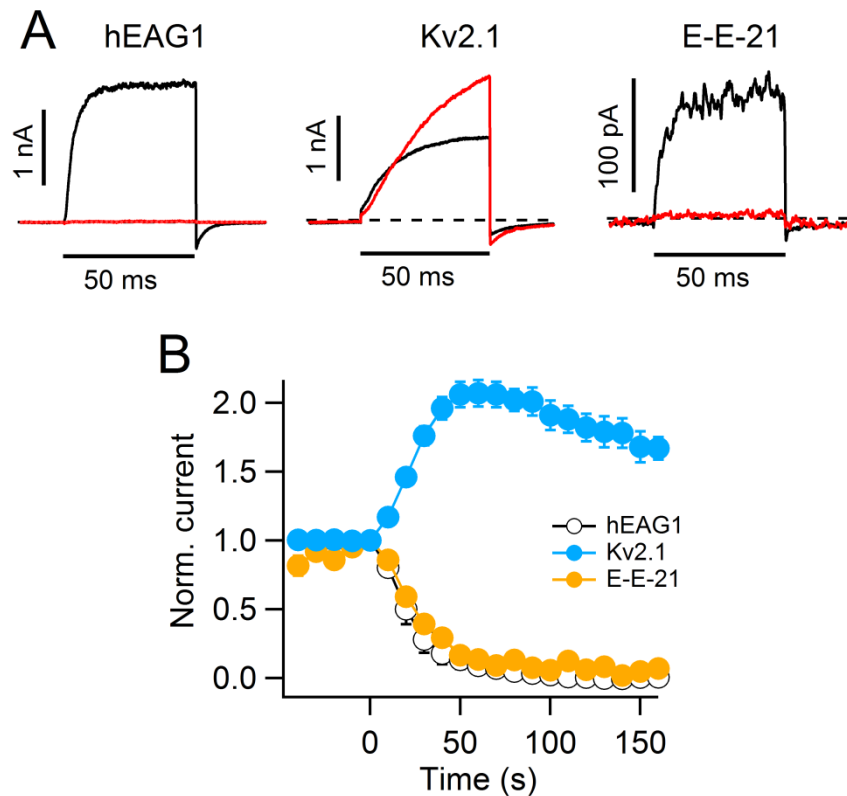


Fig. 40: Effect of hemin on E-E-21 chimera. (A) Superposition of current traces recorded from inside-out patches of indicated channel types at +40 mV before (black) and 150 s after (red) application of 200 nM hemin. (B) Time course of current reduction upon application of 200 nM hemin for the indicated channel types: hEAG1 wt (n = 8), Kv2.1 (n = 5), and E-E-21 (n = 4).

We found that hemin opens Kv2.1 channels. As shown in Fig. 40, intracellular application of 200 nM hemin increased Kv2.1 currents of about 2-fold. Following this observation, we constructed chimeric channels involving 3 genes: hEAG1 (hemin inhibits the channel), Kv1.1 (hemin remains insensitive), and Kv2.1 (hemin opens the channel) (see Fig. 39; red – EAG, violet – Kv1.1, and blue – Kv2.1). In this chimeric strategy, we have initially divided each channel into three areas: N-terminus, transmembrane area, and C-terminus. We produced a set of 6 chimeric constructs (Fig. 39). Out of 6 constructs only 2 chimeras “E-E-21” (i.e., hEAG1 N-terminus, hEAG1 transmembrane area, and Kv2.1 C-terminus), and “E-E-11” (i.e., hEAG1 N-terminus, hEAG1 transmembrane area, and Kv1.1 C-terminus) were functional. However, only for chimera “E-E-21” it was possible to measure current in the inside-out patch-clamp configuration. E-E-21 lacks the C-linker histidines (H543 and H552) but still harbors the S5 histidine (H364). Our results show that intracellular application of 200 nM hemin completely inhibited E-E-21 channels (Fig. 40). This finding demonstrates that C-linker histidine may play a minor role in the hemin sensitivity of hEAG1 channels. Likewise, it argues for an involvement of the S5 segment as a potential functional heme binding site.

4. Discussion

4.1 Heme is a potent non-genomic modulator of ion channels

Conventionally, heme was viewed as a stable protein cofactor, often conferring gas sensitivity as exemplified in cytochromes, hemoglobin, myoglobin, and soluble guanylyl cyclase (sGC). Emerging evidence, however, suggests a new paradigm of heme function; intracellular free heme may be a potent non-genomic acute signaling molecule capable of directly regulating membrane proteins such as ion channels. The large-conductance Ca^{2+} - and voltage-gated (Slo1 BK) K^+ channels inaugurated the role of heme as an acute non-genomic regulator of ion channel function (Tang et al., 2003). Heme applied to the cytoplasmic side acutely and dramatically decreased Slo1 BK current in cell-free membrane patches with a high affinity ($\text{IC}_{50} \sim 70 \text{ nM}$). Detailed analysis of the biophysical action of hemin on the Slo1 BK channel demonstrated that hemin is a potent modulator of the allosteric gating mechanism of the channel (Horrigan et al., 2005). Mutagenesis studies identified the sequence CKACH located in the cytoplasmic C-terminus to play a critical role (Tang et al., 2003; Jaggar et al., 2005). It was also observed that heme oxygenase-2 (HO2) modulates calcium-sensitive BK channels. In normoxia, the BK channel activity was enhanced (Williams et al., 2004) while in hypoxia, the BK channel activity was inhibited, suggesting that HO2 acts as an oxygen sensor for BK channels (Hoshi & Lahiri, 2004) and heme in direct regulation of BK channels acts as a signaling molecule at the level of the plasma membrane.

Another study by Wang et al. (2008) showed that epithelial sodium channels (ENaCs) in mouse cortical-collecting duct cells were inhibited by application of nanomolar concentrations of hemin to the cytoplasmic surface of the membrane ($\text{IC}_{50} \sim 24 \text{ nM}$). However, when hemin was co-applied with NADPH (permitting activity of hemeoxygenase), the activity of ENaC was stimulated under normoxic conditions (when hemeoxygenase would be active) but was inhibited under conditions of hypoxia. Furthermore, application of CO, a product of hemoxygenase activity, stimulated ENaC activity, mimicking the effects of hemin when co-applied with NADPH under normoxic conditions. These findings demonstrated a potent, O_2 -sensitive mechanism for regulation of ENaC, in which hemeoxygenase acts as the O_2 sensor, its substrate, heme and its degradation product, CO inhibiting and stimulating the activity of ENaC.

This observation, however, raised the logical question whether other channels are similarly regulated by heme. This is an important question because free heme and heme degradation

products, many of which are putative signaling molecules themselves, are now implicated in multiple diseases, such as delayed cerebral vasospasm following brain hemorrhage (Clark and Sharp, 2006) and cerebral malaria (Hunt and Stocker, 2007; Pamplona et al., 2007). In these devastating disorders, the exact effectors of heme and heme degradation products are not known and it is plausible that ion channels could be affected. Yet, no information exists whether ion channels other than Slo1 BK channels and ENaC channels are regulated by heme and heme degradation products. In this study we identified two additional classes of potassium channels to be modulated by heme: A-type and EAG potassium channels.

We found that heme/hemin removes fast inactivation of A-type channels. A-type potassium currents (e.g. mediated by Kv1.1/Kv β 1.1 or Kv1.4) are quickly inactivating with importance in the initial notch of repolarization in cardiac cells and the fast-spiking behavior of some neurons (Connor and Stevens, 1971). For detailed characterization of hemin modulation we used Kv1.4 potassium channels. Hemin applied to the cytoplasmic side potently inhibited N-type inactivation of Kv1.4 channels. Hemin strongly slowed down channel inactivation with a half-maximal effect at ~24 nM and we found that this effect was mediated by hemin binding to C13 and H16 in the ball domain of the Kv1.4 channel protein.

hEAG1 voltage-gated K⁺ channels are even more sensitive to hemin. EAG channels are depolarization-activated K⁺ channels expressed abundantly in neuronal tissues, including the cerebral cortex and the hippocampus, and contributing to modulation of action potential firing pattern. We found that application of hemin to the intracellular side profoundly inhibited K⁺ currents through hEAG1 elicited by depolarization. Only a few nanomolar of hemin were sufficient to exert a full inhibition. The hEAG1 channel is in fact far more sensitive to hemin than epithelial sodium channels (ENaCs), Kv1.4, and Slo1 Ca²⁺-dependent K⁺ channels, by 10-40 folds (IC₅₀ ~2 nM).

The high sensitivity to hemin found in hEAG1 and Kv1.4 channels is not shared by all other voltage-gated K⁺ channels. We found that Kv1.1, Kv1.3, and Kv1.5 channels are essentially unaffected by hemin. The insensitivity of the Kv channels suggests that the presence of a functional voltage sensor domain alone is not sufficient to confer heme sensitivity.

4.2 Free heme concentration inside the cell

As discussed above, intracellular free heme acts as a potent non-genomic acute signaling molecule, capable of directly regulating ion channels. In this context, one of the open questions to be addressed, what is the exact concentration of intracellular free heme? The

major portion of all heme in a cell is generally bound to hemoproteins, but it would be reasonable to assume that there exists a modest amount of free heme, which may have regulatory functions (Ponka, 1999).

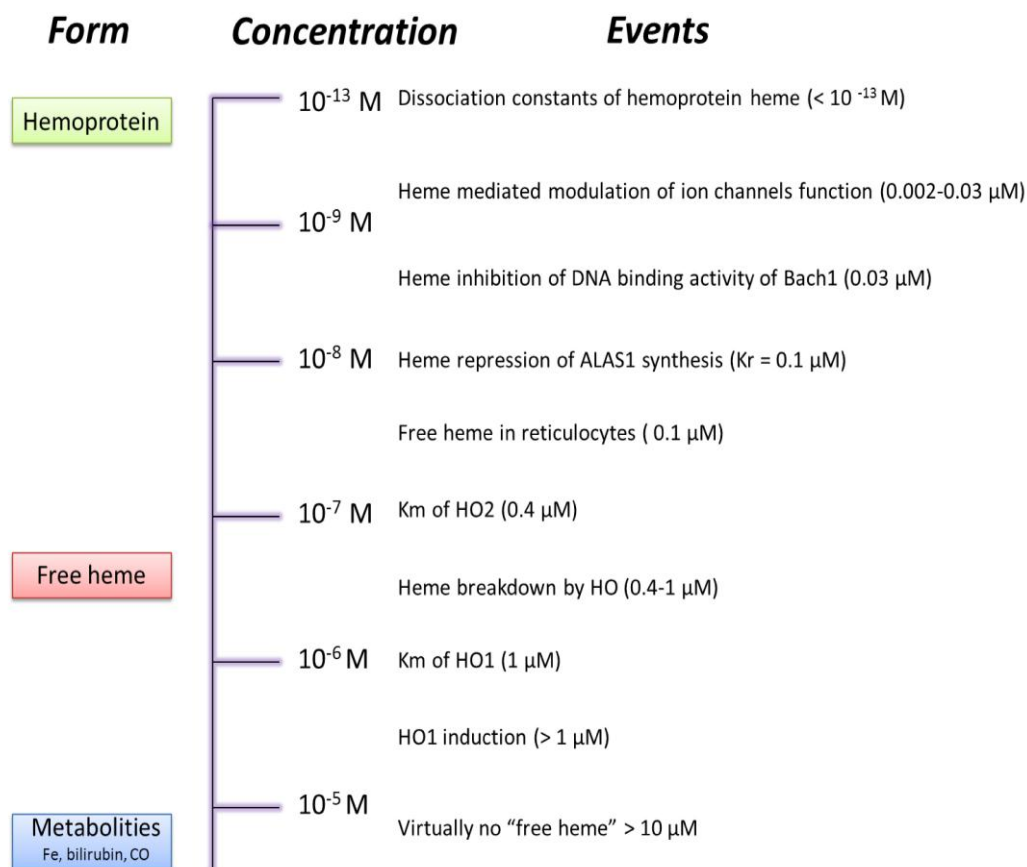


Fig. 41: "Free heme" concentrations in the cell. Free heme exerts distinctive regulatory functions at low and high concentrations. At submicromolar concentrations such as < 0.001 – 0.03 μ M, it is involved in modulation of ion channel function, as well as in controlling gene expression for both heme metabolism and biosynthesis. At high concentration such as > 1 μ M, heme is degraded by HO to release three metabolites: iron, bilirubin and CO. Free heme > 10 μ M was found only in abnormal cells e.g. in inherited HO1 deficiency, sickle cell disease, malaria, and ischemia reperfusion (adopted from Sassa, 2004).

Exact concentrations of heme in the cytoplasm are not known, as technical limitations preclude high-resolution measurements of free intracellular heme concentrations. One study suggests that the concentration may reach at least ~ 100 nM in reticulocytes (Garrick et al., 1999). This estimate is in line with the presence of heme-sensitive transcription factors such as Bach1 that respond to hemin in the 100 nM range in vitro (Ogawa et al., 2001). However, reported values for total cellular heme vary considerably. For spleen cells the reported value is 13 nmol/mg protein (equivalent to ~ 163 μ M), whereas, in olfactory receptor neurons 1.5 nmol/mg protein (~ 18.8 μ M) (Ingi et al., 1996; Wang et al., 2009) was reported. Another

study by Trakshel et al. (1986) reported that the K_m values for heme of HO1 and HO2 are 1 μM and 0.4 μM . These observations suggest that the physiologically important concentration of free heme in the cell must be below 1 μM (Fig. 41). The comparison of these values in the low nanomolar range hemin sensitivity of hEAG1 and Kv1.4 channels suggests that heme could be sufficient to regulate native hEAG1 and A-type K^+ channels.

4.3 Physiological and pathophysiological role of free heme

For heme to have a regulatory role in cells, it should occur in the cell in a “free” form. Once free heme is released to both intra- and extracellular milieu, it may work as a double-edged sword, displaying both protective and deleterious actions. Among the protective effects, free heme can influence the expression of several genes, including enzymes involved in its own synthesis (Arruda et al., 2005). Through this ability, free heme regulates neuronal differentiation in rat pheo-chromocytoma (PC12) cells, a model system for studying neuronal differentiation (Zhu et al., 2002). Heme deficiency induced by succinyl acetone, a potent inhibitor of ALA dehydratase and the second enzyme involved in heme synthesis, potently reduces the number and length of NGF-induced neurites (Zhu et al., 2002). The effect of succinyl acetone on neurite outgrowth is reversed by the addition of heme, suggesting that heme deficiency is responsible for the effect of succinyl acetone on neurite outgrowth. Heme deficiency appeared to have a less severe effect on uninduced than on differentiated PC12 cells (Sengupta et al., 2005). Moreover, heme shortage interferes with neuronal gene expression. Under normal heme concentrations, NGF induces the expression of neuron-specific genes in PC12 cells, many of which encode signal transducers and important structural functions (Gage et al., 1990). Upon inhibition of heme synthesis, the induction of these genes is abolished, which may explain why heme deficiency interferes with neuronal differentiation. Microarray gene expression analysis showed that more than 20 neuronal key genes that were induced by NGF were suppressed by succinyl acetone. Such genes with important structural functions in neurons, whose expression is modulated by heme, include survival motor neuron protein, synaptic vesicle protein (SVOP), nicotinic acetylcholine receptor, dopadecarboxylase, neural adhesion molecule, neuropeptide Y precursor, and neurofilament protein (Zhu et al., 2002; Sengupta et al., 2005).

Heme deficiency may be a factor in the mitochondrial and neuronal decay observed in aging and Alzheimer's disease (Atamna et al., 2002). Heme deficiency induced with N-methyl protoporphyrin IX, a selective inhibitor of ferrochelatase, in two human brain cell lines, SH-SY5Y (neuroblastoma) and U373 (astrocytoma), as well as in rat primary hippocampal

neurons, markedly decreases mitochondrial complex IV, activates nitric oxide synthase, alters amyloid precursor protein, and corrupts iron and zinc homeostasis. The metabolic consequences resulting from heme deficiency seem similar to dysfunctional neurons in patients with Alzheimer's disease (Atamna et al., 2002).

Heme deficiency or imbalance in free heme homeostasis may also influence ion channel function. A recent study suggests that heme deficiency induced by succinyl acetone and N-methyl protoporphyrin IX in cortical neurons from mice resulted in the lowered expression of NMDA receptor (NMDAR), a non-selective cation channel which allows Ca^{2+} , Na^+ , and K^+ to pass into the cell, and neurofilament light peptide (NF-L). In heme depleted cells exogenous application of 100 nM heme rescued the expression of these neuron-specific genes, suggesting a protective action of free heme (Chernova et al., 2006). The same group also reported that inhibition of heme synthesis causes neurodegeneration via NMDAR-dependent suppression of the ERK1/2 pathway (Chernova et al., 2007). Electrophysiological recordings of NMDAR showed that the neurodegeneration is accompanied by reduced NMDAR currents and Ca^{2+} influx, as well as reduced voltage-gated sodium currents. However, the Ca^{2+} influx through NMDAR was entirely reestablished by exogenous heme. The electrophysiological data also suggested that heme replacement caused very significant increases in $[\text{Na}^+]_i$. It is currently unclear whether this is attributable to a direct effect of heme signaling or secondary to NMDAR signaling (Chernova et al., 2007).

While heme deficiency has deleterious consequences, also high amounts of free heme can be extremely dangerous to the organism, catalyzing non-enzymatic generation of reactive oxygen species (ROS), and leading to oxidative stress. ROS created in the presence of heme are capable of damaging proteins, lipids and DNA (Vercellotti et al. 1994). Free heme can also intercalate in membranes and alter the dynamics of cellular structures (Ryter & Tyrrel, 2000). High levels of free heme (up to 20 μM) are found in pathological states of increased hemolysis, such as sickle cell disease, malaria, and ischemia reperfusion. Under these conditions, the physiological mechanisms of removing free heme from the circulation collapse, especially its binding to hemopexin, thereby allowing nonspecific heme uptake and heme-catalyzed oxidation reactions (Muller-Eberhard and Fraig, 1993). Heme is a lipophilic molecule that can easily cross cell membranes and gain entry to cells (Kumar and Bandyopadhyay, 2005). *In vitro* and *in vivo*, cells accumulate exogenous heme which results in the synergistic amplification of damage and cytotoxicity of oxidants present in the cell (Balla et al., 1991). Heme-mediated inflammation has been implicated in the pathogenesis of

several diseases, including arteriosclerosis, renal failure, and heart transplant failure (Kumar and Bandyopadhyay, 2005). The oxidative potential of heme is neutralized by heme detoxification systems. Several detoxification–defense mechanisms exist in humans. They consist of heme oxygenase systems (HO1, HO2, HO3) (Castellani et al., 2000) and extra-HO systems (hemopexin, albumin, etc.). HO is a heme-degrading enzyme that plays a significant role in protecting cells from heme-induced oxidative stress. It breaks down the porphyrin ring to yield equimolar amounts of biliverdin, free iron (Fe^{2+}), and carbon monoxide (CO) (Fig. 2). There is a wide range of physiological functions attributed to the heme oxygenase system (see review, Maines, 1997, 2000, 2005).

4.4 Mechanism of heme modulation of A-type potassium channels

Our experiments demonstrate that the inactivation gate of a mammalian A-type K^+ channel is regulated by direct action of heme/hemin. The main findings are: hemin specifically inhibits N-type inactivation of K^+ channels encoded by Kv1.4; a peptide corresponding to the inactivation ball domain of the N-terminus of Kv1.4 interacts with hemin *in vitro*; specific cysteine and histidine residues within this region are important hemin targets, mediating removal of N-type inactivation; and concurrent substitution of these residues abolishes hemin-mediated removal of N-type inactivation; differential hemin sensitivities of Kv β 1.1 and Kv β 1.3.

4.4.1 The effect of hemin on N-type inactivation is specific

In the present study, we have provided evidence to suggest that hemin selectively disrupts the N-type inactivation of Kv1.4 and Kv1.1/Kv β 1 channels. The N-type inactivation utilizes the so-called ball-and-chain mechanism. The ball-chain N-type inactivation of A-type potassium channels is the best understood inactivation mechanism, which occurs on the order of milliseconds to tens of milliseconds (Zagotta et al., 1990). From the observed removal of the fast N-type inactivation by hemin, we propose that hemin binds to the channel inactivation machinery directly. Our results strongly suggest that hemin binds to the inactivation ball. The concept for this result is based upon two observations. First, hemin remained ineffective to the deletion construct Kv1.4 Δ 1-110, which lacks the inactivation ball domain. Second, hemin-mediated removal of inactivation was abolished by mutating cysteine 13 and histidine 16 residue of the Kv1.4 ball domain. This observation clearly indicates that the hemin effect is mediated by the ball domain of the channel.

4.4.2 Identification of hemin target sites that regulate N-type inactivation

Mutagenesis experiments on Kv1.4 channels provided evidence in favor of a direct action of hemin. The regulation of N-type inactivation of Kv1.4 channels was sensitive to mutations that affected cysteine and histidine at positions 13 and 16, respectively. When cysteine 13 was mutated to serine (C13S) the effect of hemin was significantly less. In contrast, the effect on the histidine mutant (H16A) was not significantly reduced, suggesting that hemin may also act through additional auxiliary sites in the absence of H16. The ball domain of Kv1.4 channels harbor another histidine at position 35 (H35) and we suppose that in the absence of H16, H35 may serve as an axial ligand to hemin. However, the double mutation (C13S/H16A) completely abolished hemin-mediated removal of Kv1.4 fast N-type inactivation.

Hemin binding sequences are diverse, and a broad range of specificities has been reported (see review, Schneider et al., 2007). The heme-binding site has the consensus of *c*-type cytochromes, CxxCH (where x represents any amino acid). Previous work on BK channels has demonstrated a *c*-type cytochromes motif CxxCH located between the 2 putative RCK domains (Tang et al., 2003). However, our study revealed another class of motif: CxxH present in α -subunits of Kv1.4. This type of motif is also present in known hemo-proteins such as soluble guanylate cyclases (GCs) and Rieske-type ferredoxin. Soluble guanylate cyclases (GCs) act as a heme sensor that selectively binds nitric oxide (NO) (Boon and Marletta, 2005), triggering reactions essential for animal physiology. Soluble guanylate cyclases were placed in the H-NOX (heme nitric oxide and/or oxygen-binding domain) family that also includes bacterial proteins from aerobic and anaerobic organisms. H-NOX proteins possess either a distal pocket tyrosine required for O₂ binding or a very conserved CxxH motif in the heme-binding domain that is responsible for NO binding (Boon and Marletta, 2005). Rieske ferredoxin is an iron-sulfur protein (ISP) component of cytochrome *bc1* complex and the cytochrome *b6f* complex. Rieske ferredoxins are involved in a wide variety of biological functions. They typically act as electron carriers between different redox partners. Membrane-bound Rieske ferredoxins are found as covalent domains in the cytochrome *bc1*, *b6f* and *bc* respiratory complexes in mitochondria, chloroplasts and bacterial cell walls (Trumpower and Gennis, 1994), as well as in the respiratory chains of archaeal organisms (Schafer et al., 1996). These proteins harbor a CxH and CxxH metal-binding motif. The cysteine and histidine residues in this sequence motif are responsible for liganding the Rieske iron–sulfur center (Schmidt and Shaw, 2001).

Spectroscopic experiments on Kv1.4 channels provided further evidence in favor of a direct action of hemin. The UV-Vis spectrum of the Kv1.4 inactivation ball peptide (Kv1.4-IP)-hemin complex has a single Soret peak centered at 410 nm, while the EPR spectrum showed a signal characteristic of low spin state of ferric iron with g -values of 2.43, 2.26 and 1.87. Kv1.4-IP-hemin complex shares nearly similar g -values as Slo1 BK channels heme binding peptide (HBP23) (Tang et al., 2003) and *P. falciparum* histidine-rich protein 2 (PfHRP2) (Choi et al., 1999), suggesting that one of the axial ligands might be a histidine nitrogen (Brautigan et al., 1977). Mutant peptides where cysteine and histidine residues were replaced (Kv1.4-IP-mt) showed no binding to hemin in spectroscopic experiments.

4.4.3 Different hemin sensitivities of Kv β 1.1 and Kv β 1.3

Although Kv β isoforms introduce N-type inactivation, they differ in intracellular modulation by heme and expression pattern. The variation in the amino-acid sequence of the proximal N termini determines the different hemin sensitivities of Kv β 1.1 and Kv β 1.3. Our results indicate that the Kv1.5/Kv β 1.1 channel was sensitive to hemin, while the Kv1.5/Kv β 1.3 channel was insensitive. Given the fact that there is very little homology between the Kv1.4 N-terminal ball structure and different Kv β ball structures, the hemin sensitivity probably relies on the presence of cysteine and histidine residues in the ball domain. It has been shown that Kv β 1 and Kv β 2 subunits bind to Kv1 α subunits. Kv β 1.1 harbors a cysteine at position 7 and a histidine at position 10, while Kv β 1.3 does not contain any cysteine or histidine in the ball-domain. As pointed out in the alignment (Fig. 16), N-terminal splicing of Kv β 1 produces the Ca²⁺-insensitive Kv β 1.3 isoform that retains the ability to induce Kv1 channel inactivation (Decher et al., 2008). Thus, an important physiological consequence of N-terminal splicing of the Kv β 1 gene might be the generation of rapidly inactivating channel complexes with different sensitivities to hemin and intracellular Ca²⁺. Kv β 1.1 is known to be abundantly expressed in the hippocampal CA1 region and in the striatum (Rettig et al., 1994; Rhodes et al., 1996) and to confer fast inactivation to the otherwise noninactivating delayed rectifier potassium channels such as Kv1.1, Kv1.2, Kv1.3, Kv1.4, and Kv1.5 (Rettig et al., 1994; Bähring et al., 2001; Heinemann et al., 1994, 1996). The loss of Kv β 1.1 caused a reduction in K⁺ current inactivation in hippocampal CA1 pyramidal neurons. This change in K⁺ current inactivation was accompanied by a reduction of frequency-dependent spike broadening and attenuation of the slow afterhyperpolarization (sAHP), without any obvious change in synaptic plasticity (Giese et al., 1998). While, Kv β 1.3 is preferentially expressed in heart (England et al., 1995a, b) and confer fast inactivation to delayed rectifier potassium channels

Kv1.5 (Decher et al., 2008). Apart from Kv β 1.1, other Kv β subunits such as Kv β 1.2 and Kv β 3.1 harbor cysteine and histidine residues inside the ball domain (Fig. 16). It would be interesting to see whether these subunits confer hemin sensitivity; further work is needed to resolve this issue.

4.4.4 A model for hemin action on A-type channels

In a general model of A-type K⁺ channel gating (Zagotta and Aldrich, 1990; Hoshi et al., 1994), voltage-dependent activation is followed by a voltage-independent transition that opens the channel, and subsequent inactivation. According to the “ball and chain” hypothesis (Bezanilla and Armstrong, 1977; Zagotta et al., 1990; Hoshi et al., 1990), the cytoplasmic N-terminus of the channel polypeptide is the inactivation gate (“ball” domain) tethered to the rest of the molecule by a hydrophilic arm. The inactivation ball domains of A-type channels are highly flexible and have no classical secondary structure backbone characteristics in aqueous solution (Antz et al., 1997; Abbott et al., 1998; Wissmann et al., 1999, 2003; Schott et al., 2006). As determined from NMR experiments, Kv1.4 harbors two inactivation ball domains at its N-terminus. Inactivation domain 1 (ID1, residues 1–38) consists of a flexible N-terminus anchored at a 5-turn helix, whereas ID2 (residues 40–50) is a 2.5-turn helix made up of small hydrophobic amino acids (Fig. 42C). Functional analysis suggests that only ID1 may work as a pore-occluding ball domain, whereas ID2 most likely acts as a “docking domain” that attaches ID1 to the cytoplasmic face of the channel (Wissmann et al., 2003). The ID of Kv3.4 was found to exhibit well-defined and compact folding although the backbone lacks secondary structural elements (Antz et al., 1997). In contrast, the ID from Shaker B and the inactivating N-terminus of Kv β 1.1 (amino acids 1–62) showed no unique, folded structure, but rather behaved like random-coil peptides (Abbott et al., 1998; Wissmann et al., 1999).

Heme is known to induce protein folding. Heme incorporation is integral to the protein folding process. Thermodynamically, heme binding provides additional free energy for protein folding. In apo-proteins of low stability, heme incorporation is a major contributor to protein folding, and heme-protein interactions can trigger events such as the condensation of the unfolded state (cyt *c*) or nucleation of secondary structure elements (cyt *b*₅₆₂) (Feng et al., 1994). The interactions of the protein at the iron via ligation as well as at the porphyrin macrocycle by hydrophobic contacts are critical to the structural uniqueness of the hemoprotein native state, regardless of protein fold (Lu et al., 2001).

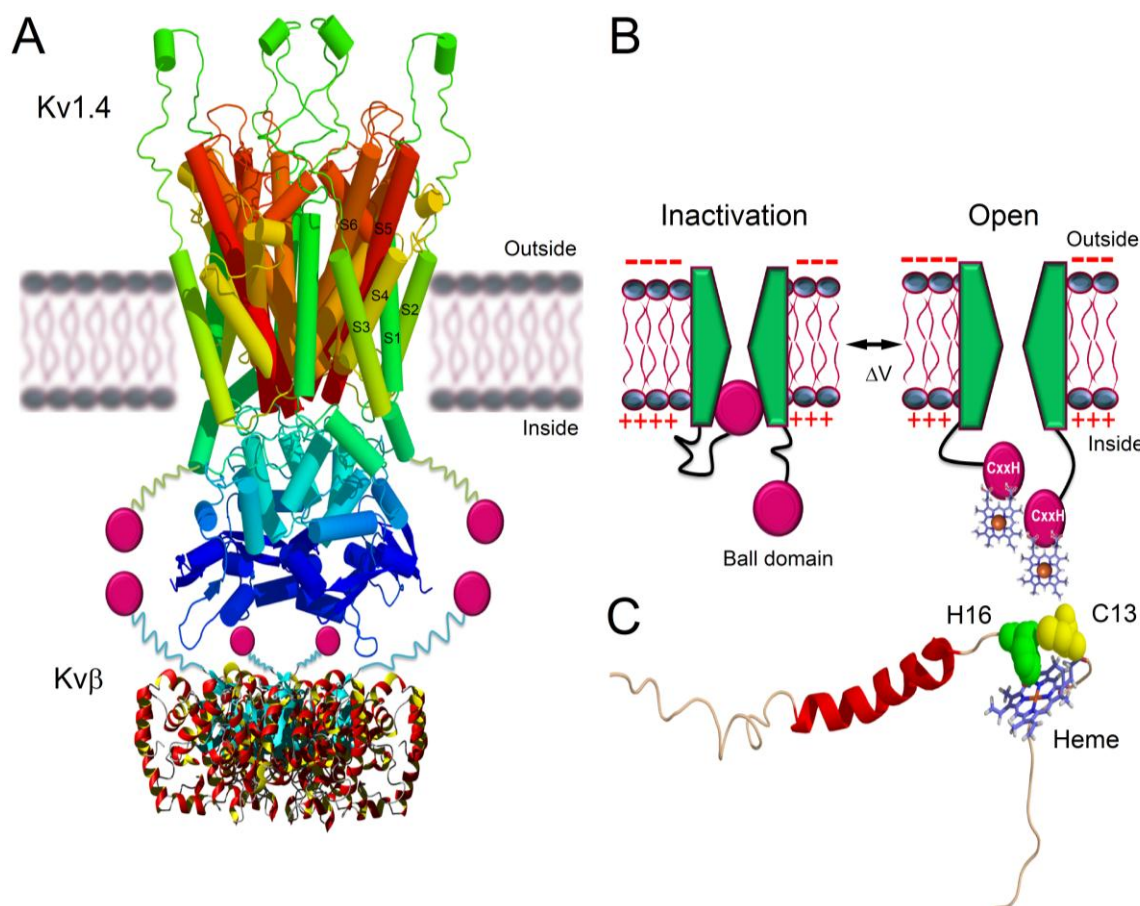


Fig. 42: Proposed model depicting the hemin action on A-type potassium channels. (A) Swiss model homology structures of Kv1.4 channels, aligned to full-length shaker potassium channel Kv1.2 (3LUT) and PDB structure of Kvβ-subunit (KCNAB2, 1ZSX). Cartoons of ball domains are superimposed to the N-terminus of Kv1.4 and Kvβ-subunits structures. (B) Simplified model of hemin-mediated removal of A-type channel fast inactivation. Following membrane depolarization, the flexible ball domain in the N-terminus plugs the pore of the channel which causing fast inactivation. In the presence of hemin, the ball domain probably adopts a partial secondary structure and restricts the mobility of the ball domain which in turn relieves from inactivation. (C) NMR structure of the Kv1.4 ball domain (1KN7) with hypothetical structural representation of heme binding to cysteine (C13, yellow) and histidine (H16, green).

A study by Abbott et al. (1998) found that the synthetic Kv3.4 channel ball peptide adopts a partial β -sheet structure in the presence of the anionic lipids phosphatidylglycerol (PG). In contrast to the wild-type Kv3.4 ball peptide, substitution of the hydrophobic valine residue at position 7 for a negatively charged glutamate residue ablates the ability of the ball peptide to adopt ordered β -structure, regardless of anionic lipids (Abbott et al., 1998). Our results of Kv1.4 ball domain interaction with hemin may be consistent with this model. Binding of hemin to the ball peptides might reduce the flexibility of the ball-and-chain machinery and induce a partial secondary structure of the ball-and-chain machinery, which makes it impossible for the ball peptides to reach their binding sites (Fig. 42).

4.5 Possible physiological role of heme modulation of A-type potassium channels

One of the major features of A-type potassium channels is their fast inactivation, which tends to accelerate repolarization and forces a delay between successive action potentials, thereby shortening the action potential duration and limiting the firing rate. However, during high frequency trains of action potentials, the A-type channel's effects are overcome, since they do not have time to recover from inactivation between spikes. As a result, the presynaptic action potentials widen, allowing more Ca^{2+} influx per spike and potentiating neurotransmitter release (Dodson and Forsythe, 2004). This feature of A-type potassium channels may contribute to hyperexcitability of neurons and could be associated to pathophysiological conditions such as epilepsy or pain. The importance of this activity has recently been demonstrated by Schulte et al. where they reported that, in the hippocampal formation, Lgi1 (leucine-rich glioma inactivated gene 1 protein) and Kv1.1 co-assembled with Kv1.4 and Kv β 1.1 in axonal terminals. Lgi1 selectively prevents N-type inactivation mediated by the Kv β 1.1 subunit. Mutation in the Lgi1 gene results in a protein that is defective in preventing Kv β 1.1-mediated inactivation and is the cause of autosomal dominant lateral temporal lobe epilepsy (ADLTE) (Schulte et al., 2006). From this observation they hypothesized that the Lgi1-mediated removal of fast inactivation of A-type Kv channels associated with the presynaptic bouton causes prolongation of presynaptic action potential (AP) up to 3-fold at high-frequency excitation, a phenomenon known as AP broadening. In the trisynaptic hippocampal network, increased EPSPs in granule and pyramidal cells may lead to an imbalance between excitation and inhibition (McNamara, 1999) that triggers focal epileptic activity in particular in response to high-frequency stimulations such as the “theta-burst activity” or other high-frequency excitations (Geiger and Jonas, 2000). Our studies show that hemin efficiently modulates N-type inactivation in Kv1.4 and Kv1.1/ Kv β 1.1 channels. This modulation may be an alternative mechanism in controlling hyperexcitability of neurons and probably maintains the balance between excitation and inhibition that triggers focal epileptic activity in particular in response to high-frequency stimulations such as the “theta-burst activity” or other high-frequency excitations.

The observation that N-type inactivation induced by the ball domain can be competed off the channel with the small-molecule hemin suggests that the Kv1-ball domain complex of A-type channels may not be permanent. As a recent study has pointed out (Wells and McClendon, 2007), it is in general very difficult to obtain small-molecule compounds that interfere with protein-protein interactions because the interfaces are usually large and extensive. Small

molecule Kv channel disinactivators (compounds that disrupt N-type inactivation) thus represent a new class of potential anticonvulsant drugs, and as such they may have unique properties and usefulness in multiple diseases of hyperexcitability. Lu et al. (2008) screened for compounds that prevent inactivation of Kv1.1/Kv β 1.1 channels by using a yeast two-hybrid screen. They found a variety of compounds that act as disinactivators and also inhibited pentylenetetrazole-induced seizures in mice. Hemin modulation of Kv1.1/Kv β 1.1 channels could be useful for reducing neuronal hyperexcitability in diseases such as epilepsy and neuropathic pain.

It has been reported that the neuroprotective substance riluzole prolongs the activation of Kv1.4 by slowing its N-type inactivation dramatically. This leads to a cAMP-independent inhibition of glutamate release in nerve terminals by a reduced depolarization-dependent Ca²⁺ influx (Xu et al., 2001). Riluzole has been used for the therapy of the degenerative motor neuron disease amyotrophic lateral sclerosis ALS. This substance may also exert beneficial effects in the treatment of pain.

A recent study reported that over 90% of the Kv1.4-positive neurons expresses cannabinoid receptor (CB1) and transient receptor potential channel of the vanilloid receptor type, subtype 1 (TRPV1) (Binzen et al., 2006). The metabotropic CB1 is known to play an important role in anti-nociception (Pertwee, 2001) and TRPV1 is essential for selective modulation of pain sensation and for tissue injury-induced thermal hyperalgesia (Caterina et al., 2000). Since CB1 and TRPV1 are highly co-localized with Kv1.4 and are expressed in nociceptive neurons, an anatomical basis for regulation of nociceptive transmission by cannabinoids and involvement of Kv1.4 as downstream of the CB1 and a possible implication in pain signaling can be suggested (Binzen et al., 2006). Kv1.4 channels of rat brain are concentrated in axons and presynaptic terminals of neurons in the cerebral cortex, hippocampus, thalamus, and basal ganglia (Sheng et al., 1992). Their presence in nerve terminals places Kv1.4 channels in a strategic position where they may regulate presynaptic spike duration, Ca²⁺ entry, and neurotransmitter release. Glutamate is a neurotransmitter at several of the synaptic sites where Kv1.4 channels are also expressed (Lipton and Rosenberg, 1994). The marked slowing of Kv1.4 channel inactivation by hemin could contribute to inhibition of transmitter release by any of several different mechanisms. At the nerve terminal, enhanced current flowing through the more slowly inactivating Kv1.4 channels would shorten the action potential, thereby reducing depolarization-dependent Ca²⁺ entry and transmitter release. At the cell body,

enhanced K^+ efflux would contribute to membrane hyperpolarization and a decrease in excitability (Fig. 43).

In summary, the pronounced slowing of Kv1.4 inactivation by hemin identifies a specific mechanism by which hemin may inhibit the release of glutamate, reducing excitotoxicity and producing neuroprotection in various neuropathological conditions.

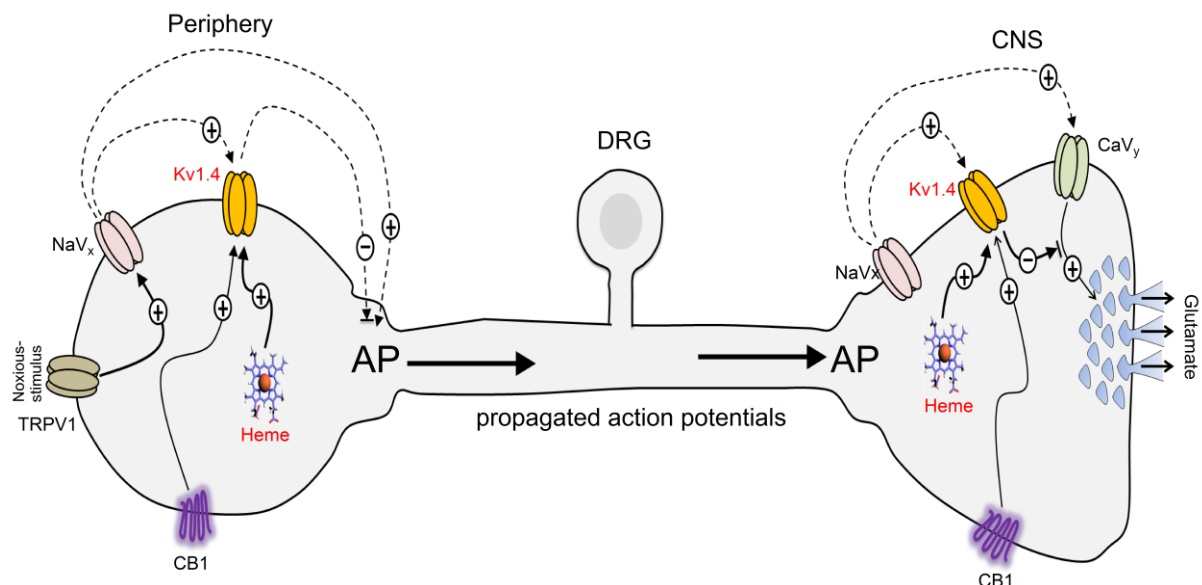


Fig. 43: Probable functional role of hemin modulation of Kv1.4 channels. Functional coupling of TRPV1, Kv1.4 and CB1 in nociceptive DRG neurons. Proposed interaction of the ion channels and receptors in the transduction process for noxious stimuli and heme in the periphery of primary nociceptive neurons (left). Mechanisms contributing to neurotransmitter release at the central synapse of nociceptors are shown on the right. Heme is probably controlling the glutamate release at the synapse (see text for further details). AP, action potential; CaV_y , diverse voltage-gated calcium channels; CB1, cannabinoid receptor 1; DRG, dorsal root ganglion; Glu, glutamate; Kv1.4, voltage-gated potassium channel subtype 1.4; NaV_x , diverse voltage-gated sodium channels; TRPV1, transient receptor potential channel of the vanilloid receptor type, subtype 1. (Source: adopted and modified from Binzen et al., 2006)

4.6 Mechanism of heme modulation of EAG1 potassium channels

We found that ether-à-go-go voltage-dependent potassium channels (EAG1, KCNH1, Kv10.1) expressed in *Xenopus* oocytes are sensitive to nanomolar concentrations of hemin. The half-maximal inhibitory concentration is about ~2 nM, indicating that the hemin effect on hEAG1 channel is 10-40 fold stronger than hemin effect on Kv1.4, Slo1, and ENaC channels. Kinetic analysis of the inhibitory interaction between the hEAG1 channel and hemin at multiple voltages and multiple hemin concentrations revealed that the “on” kinetics is concentration dependent, becoming faster with greater concentrations of hemin and the “off” kinetics is very slow and independent of the hemin concentration. Analysis of the kinetic data

at the lower concentration limit of 1 nM hemin were hampered by the slow current rundown that was found in all measurements. Apparent K_d values determined in the lower concentration range or, excluding the lowest concentration differed and that the existence of more than one hemin binding site appeared very likely.

For BK channels, it was described that hemin acts as a modulator, not a simple inhibitor, of the BK channel function, such that it increases the open probability (P_o) at negative voltages and decreases P_o at more positive voltages. Interaction of hemin with the RCK1-RCK2 linker segment was proposed to expand the gating ring and to impede the gating ring-voltage sensing domain (VSD) interaction that normally accompanies activation of the channel (Horrigan et al., 2005). In case of ENaC channels, hemin also consistently and significantly reduced the P_o (Wang et al., 2008). Our result also suggests that hemin alters the gating properties of hEAG1 channels. Hemin caused a positive shift of ~15 mV in the voltage of half-maximal activation. The inhibitory effect of hemin becomes stronger at negative voltages and the effect becomes weaker at depolarizing voltages. Furthermore, hemin slowed the activation kinetics at positive voltages and accelerated the deactivation kinetics. The kinetics at extreme positive and negative voltages is particularly important as one-step opening and closing transitions may largely determine the current relaxation kinetics.

4.6.1 Identification of hemin target sites that regulate hEAG1 channel function

From the observation of high sensitivity of the hemin effect, we predicted that hEAG1 channels harbor at least one hemin binding site. In fact, we could confirm a direct interaction between hemin and hEAG1 channels, as revealed by a hemin-agarose pull-down assay. To find the hemin target site on hEAG1 channels we used several approaches such as deletion mutagenesis, systematic cysteine mutagenesis, histidine mutagenesis, and chimeric approaches. The hEAG1 channel harbors a PAS domain in the N-terminus and it has been also reported that PAS domains can bind to heme and regulates protein function (Gilles-Gonzalez and Gonzalez, 2004). However, our study showed that deletion of the PAS domain of hEAG1 channels still retains hemin sensitivity, indicating that the PAS domain is not responsible for the hemin-mediated hEAG1 current inhibition.

4.6.1.1 Evaluation of critical cysteine residues responsible for hEAG1 channel function

Our studies on hemin modulation of Kv1.4 channels suggest that a cysteine residue inside the ball domain plays a critical role for hemin binding. The same cysteine residue is known to be

responsible for redox regulation of fast N-type inactivation (Ruppersberg et al., 1991; Stephens et al., 1996; Rettig et al., 1994). Another study reported that reversible binding of heme to the heme-regulated initiation factor eIF-2 alpha kinase (HRI) involved in genomic actions of heme, is dependent on its cysteine residues, potentially causing their oxidation (Yang et al., 1992). Following this observation, we analyzed cysteine residues in hEAG1 for their redox modulation by sulfhydryl-modifying reagents.

Our study indicates that the hEAG1 channel activity is indeed altered by treatment with select cysteine modifiers such as DTNB. Intracellular application of DTNB inhibited hEAG1 channels in a biphasic manner. Our study provides evidence that DTNB is a gating modifier. It shifts the voltage of half-activation towards right. Our systematic cysteine mutagenesis result suggested that four critical cysteines are responsible for DTNB-mediated hEAG1 current inhibition. The fast component was contributed by two cysteine residues (C145 and C214) in the N-terminus, close to the transmembrane segment S1 and also responsible for positive shift of half-maximal activation, while the slow component was contributed by two cysteine residues (C532 and C562) in the C-linker region of the C-terminus of hEAG1 channels. A recent study by Kolbe et al. (2010) showed that C723 and C740 in the C-linker region of hERG1 channels are responsible for oxidative modification, and mutation of these cysteine residues rendered the hERG1 channel less sensitive to reactive oxygen species. The corresponding position in hEAG1 channels are C532 and C562. This observation provided an insight about the importance of the C-linker region for hEAG1 channel function. However, it was not clear how cysteine residues in the N-terminus and C-terminus of hEAG1 channels contribute oxidation sensitivity.

A recent study by Stevens et al. (2009) has shown that on the surface of both the PAS and cNBD domains of EAG1 channels, there are bands of residues that contribute to determining the activation kinetics of the channel. These surface bands of residues correspond to bands of conserved residues within the EAG family, as well as including many hydrophobic residues, suggestive of regions of domain–domain interaction via these surfaces. DTNB might induce its inhibitory effect by interfering with the cross talk between PAS and cNBD domain. An interaction between the N-terminal and the C-linker regions of CNGA1 channels has been previously demonstrated using electrophysiological and biochemical methods (Gordon et al., 1997). It was shown that a disulfide bond between a cysteine residue at position 35 of the N-terminal region and a cysteine residue at position 481 of the C-linker region can be induced by mild oxidizing conditions. Formation of this disulfide bond alters channel function, giving

a left shift of the dose-response curve for activation by cGMP and an increase in the fractional current activated by the partial agonist cAMP (Gordon et al., 1997). These data suggest that the N-terminal and the C linker regions lie in close proximity in the tertiary structure. Such a mechanism may also explain cysteine-mediated regulation of hEAG1 channels.

Based on our initial hypothesis whether redox-sensitive cysteines take part in hemin sensitivity in hEAG1 channels, we analyzed the impact of hemin on oxidation insensitive cysteine-less NC channels. We found that intracellular hemin efficiently inhibited the cysteine-less NC channels. This observation suggests that hemin-mediated hEAG1 current inhibition is not mediated by redox-sensitive cysteine residues. Analysis of transmembrane segment critical cysteines for their impact on hemin sensitivity revealed that the mutant C303A showed hemin sensitivity but the time course of development of the inhibition was slower. This finding suggests that C303 may take part in hemin binding.

4.6.1.2 Hemin interacts with the histidine residues of hEAG1 channels

From the analysis of scanning histidine mutagenesis, we found that none of the functional histidine mutants abolished hemin sensitivity, as observed from patch-clamp experiments. However, histidine mutations in the S5 region (H364) and histidines in the C-linker region (H543 and H552) produced non-functional channels. Our observations from spectroscopic experiments indicate that hemin interacts with peptides corresponding to the C-linker regions and mutation of these histidine residues abolishes the interaction.

hEAG1 is a member of the cyclic nucleotide binding domain (cNBD) family of channels, which includes hyperpolarization activated channels, cyclic nucleotide gated channels, and numerous plant and bacterial channels (Yu et al., 2005). Alignment of cNBD channels from bacteria, plants, and animals revealed a conserved sequence HwX(A/G)C in the S5 transmembrane domain (Fig. 37A). The evolutionary conservation of this region suggests that it could play an important, but as yet unknown role in the functional activity of cNBD family of channels. hERG1 channels, important members of the EAG family and responsible for repolarization of the heart action potential also contain histidine (H562) in the S5 region. H562 is known to form hydrogen bonds with threonine (T618) and serine (S621) in the pore helix and plays a critical role in stabilizing the structure and function of the S5-pore helix. This interaction is functionally important for deactivation, V_m of activation, and, to a lesser extent, ion selectivity (Lees-Miller et al., 2009). Unfortunately, hERG current rundown from excised inside-out patches is too rapid to test the impact of hemin from the intracellular side

of the channels. Alignment of the S5-region also revealed that the plant potassium channels KAT1 and AKT1 harbor a classical cytochrome *c* heme binding motif but in opposite order HCxxC (Fig. 37A). S5 peptide comprising of 5 amino acids (HCAAC) of AKT1 channels binds hemin and mutation of histidine residue abolishes the interaction, as revealed by UV-Vis spectroscopic method. From this observation we can speculate that H364 of hEAG1 channel may play a role in hemin-mediated sensitivity.



Fig. 44: Proposed heme binding sites in the cNBD family of channels. Multiple sequence alignment of the C-linker region of the cNBD family of channels. Red box indicates the relevant histidine residues presumably responsible for hemin binding to hEAG1 channels. Alignments were performed using Clustal W (Thompson et al., 1994), protein-domain homologies and motifs predicted using the Prosite database (Bairoch et al., 1996).

Alignment of the C-linker region of the cNBD family of channels also revealed conserved histidines in hERG1 channels corresponding to position H543 and H552 of hEAG1 channels. KAT1, AKT1, and CNGA1 channels harbor only one histidine and HCN1 does not contain histidine in the C-linker region (Fig. 44). The histidine residue in the C-linker region of CNGA1 channels is known to bind Ni^{2+} to potentiate channel activation. Ni^{2+} has no potentiating effect on CNGA2 channels because the histidine residue is substituted to a glutamine residue in CNGA2 (Gordon and Zagotta, 1995). It would be interesting to see whether these channels functionally interact with hemin, further work is needed to resolve this issue.

4.6.1.3 A chimeric approach narrowed down the hemin binding site on hEAG1 channels

We used a chimeric approach to map the regions that are critical for hemin binding on hEAG1 channels. Chimeras were engineered between hEAG1 where hemin inhibits the channel, Kv1.5 where hemin is without effect, and Kv2.1 where hemin opens the channel. Only one chimera “E-E-21” (i.e., hEAG1 N-terminus, hEAG1 transmembrane area and Kv2.1 C-terminus), was functional and produced macroscopic current. It has been reported that a small tetramerizing coiled coil (TCC) domain at the C-terminus is required for correct tetrameric

assembly of EAG family of channels. Disruption of the TCC domain leads to non-functional channels, and introduction of a heterologous domain (EAG1 TCC) rescues the function, indicating that the presence of a TCC is enough to drive the formation of functional channels (Jenke et al., 2003). In case of Kv2.1 channels, the tetramerization assembly (T1) domain is present in the N-terminus (Bocksteins et al., 2009). However, our result suggests that this TCC domain is not necessary for functional expression of hEAG1 channels. The C-terminus of hEAG1 channels harbor two calmodulin binding motifs which are responsible for binding of calmodulin (Schönherr et al., 2000; Ziechner et al., 2006) and S100B (Sahoo et al., 2010). The E-E-21 chimera lacks these sites and consistently we found that this chimera was insensitive to calmodulin (data not shown). In respect to heme binding, the E-E-21 chimera lacks the C-linker histidines (H543 and H552) but still retains the S5 histidine (H364). We found that E-E-21 chimera remained sensitive to hemin like wild-type, suggesting that the S5 region histidine is probably the major target of hemin-mediated hEAG1 current inhibition.

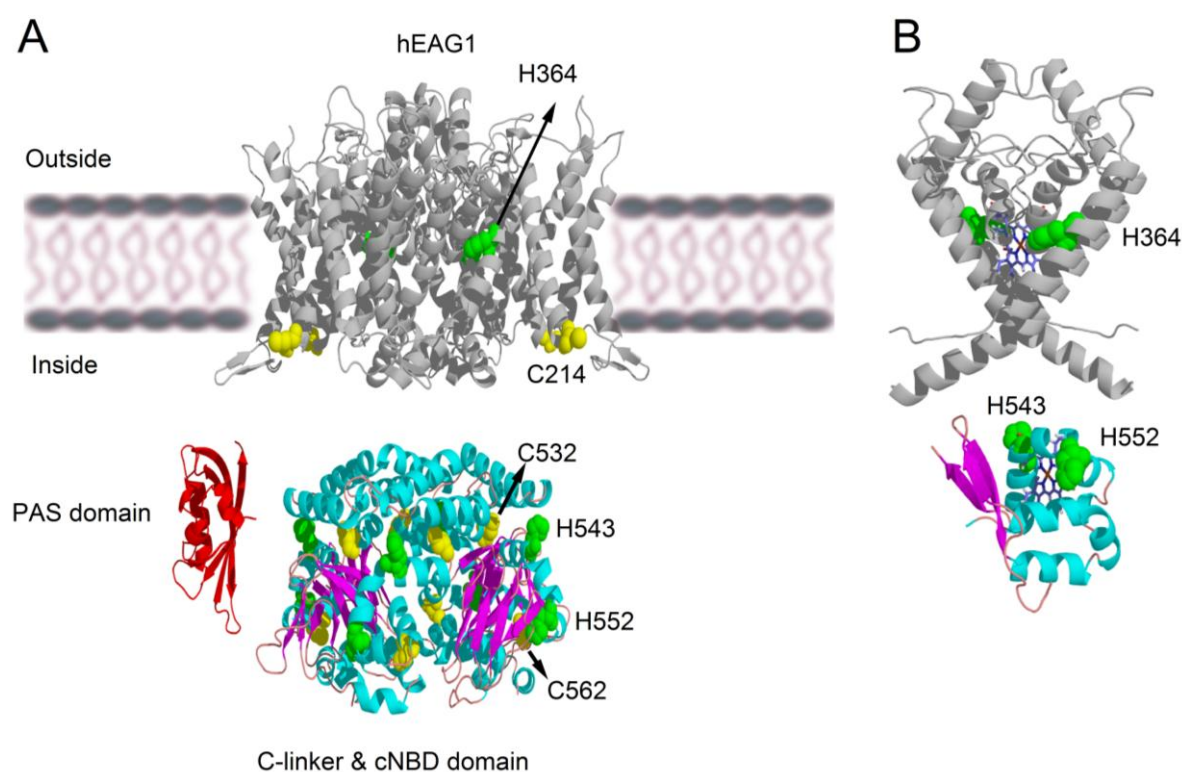


Fig. 45: Representation of heme binding sites on hEAG1 potassium channels. (A) Swiss model homology structures of hEAG1 channels, aligned to Kv1.2/Kv2.1 (2R9R, transmembrane domain, 4-subunit), HCN1 (1Q3E, C-terminal domain, 4-subunit) and hERG1 (1BYW, N-terminal PAS domain, 1-subunit). Cysteine residues relevant for oxidation sensitivity and histidine residues presumably responsible for heme regulation are indicated. (B) Hypothetical structural representation of heme binding to histidine residues (H364) at S5 segment (2R9R, S5-S6 segment, 2-subunits) and histidine residues (H543 and H552) in the C-linker region (1Q3E, C-linker region, 1-subunit).

Based on this finding, we propose that hEAG1 channels harbor a high affinity and a low affinity heme binding site (Fig. 45B). High affinity heme binding histidine (H364) in the S5 region is probably responsible for alteration of channel function. As described earlier (4.7.1.2), histidine H562 in the S5 region of hERG channel is known to form hydrogen bonding with threonine (T618) and serine (S621) in the pore helix. If we consider a similar mechanism existing in hEAG1 channels, heme may interfere with the hydrogen bonding and alter the channel function. The low affinity binding site may include histidine H543 and H552 in the C-linker region where heme probably binds but due to the presence of high affinity site we could not see functional role of these two histidines in patch-clamp method.

It has been shown that the cNBD domain of CoxA, a transcription factor from *Rhodospirillum rubrum* binds heme. This binding is mediated by cysteine (C75) and histidine (H77) residues and induces dimerization of 2 subunits. Carbon monoxide can bind to the heme site and known to activate the transcription factor (Lanzilotta et al., 2000). The mechanism of CO sensing is quite interesting. CoxA is an equilibrium mix between the off- and on-states. In the off-state the N-terminus of one monomer coordinates the heme iron of another monomer. In the on-state the N-terminus dissociates thus enabling CO to bind. The freed N-terminus undergoes a large repositioning that facilitates the N-terminal segment to provide a bridge between the heme- and cNBD domains effectively holding the DNA-binding domain in the orientation required for DNA binding. These changes allow the movement of the C-helical interface and heme which triggers the tight CO binding (Poulos, 2007). A similar mechanism would be possible in case of hEAG1 channels. Our preliminary results on the effect of carbon monoxide on hEAG1 channels suggest that CO gas inhibits hEAG1 channels in excised cell free patches (data not shown).

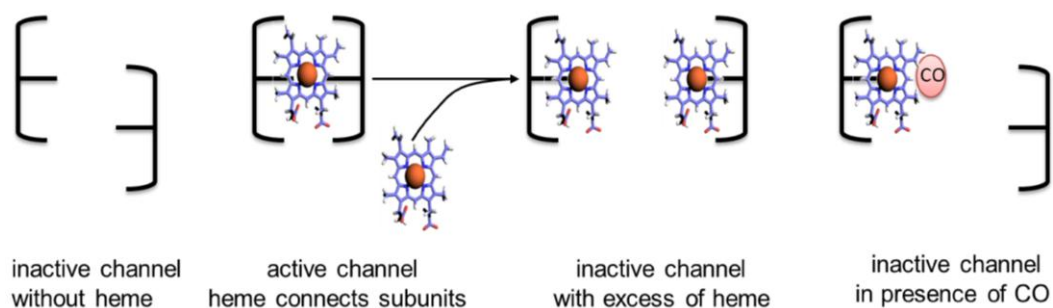


Fig. 46: Proposed model of action heme on hEAG1 channels. (See text for details).

Based on this observation we propose a model that channels are probably inactive in the absence of heme and an active channel is produced when heme is bound to C-linker histidines (H543 and H552) which connects subunits. When excess heme is present, it probably targets S5 histidine (H364) which in turn alters the function probably by separation of the subunits. CO could bind to the heme which in turn makes channel inactive (Fig. 46).

4.7 Possible physiological role of heme modulation of hEAG1 potassium channels

As described in Section 1.2.3.1, EAG channels are predominantly expressed in neuronal tissues and probably play an essential role in neuronal signaling (Frings et al., 1998; Lecain et al., 1999; Ludwig et al., 1994; Occhiodoro et al., 1998). However, there are no reports about EAG-mediated currents in normal mammalian neuronal tissue and the physiological role of EAG in the central nervous system of mammals has still to be elucidated. The importance of EAG1 channel has been studied in other species. A role for EAG1 in neuronal function was first suggested by an ether-induced leg shaking phenotype associated with EAG, as well as Sh and Hk, mutants (Kaplan and Trout, 1969; Warmke et al., 1991). This observation showing physiological and behavioral defects in EAG mutants, demonstrates that the EAG channel is essential for neuronal function. A series of observations strongly implicate EAG channel involvement in learning and memory and mutation in EAG causes learning defects in *Drosophila melanogaster* (Griffith et al., 1993, 1994; Siegel and Hall, 1979).



Fig. 47: Proposed heme binding sites in EAG channels of different species. Multiple sequence alignment of S5 segment (A) and C-linker region (B) of EAG channels of different species: hEAG1-human EAG1; dEAG1-*drosophila melanogaster* EAG1; egl-2-*caenorhabditis elegans* EAG1 and zEAG1-zebrafish EAG1. Conserved histidines presumably responsible for heme binding are marked green and cysteines are marked yellow. Alignments were performed using Clustal W (Thompson et al., 1994), protein-domain homologies and motifs predicted using the Prosite database (Bairoch et al., 1996).

A study from our group provided evidence for the first time the role of EAG channels in zebra fish (*Danio rerio*) development. The functional properties of zebra fish EAG1 (zEAG1) in respect to Cole-Moore shift and Ca^{2+} /CaM sensitivity are essentially the same as human EAG1. We also found that zEAG1 is sensitive to hemin (not shown). Morpholino knock-down of the EAG genes caused abnormal development, suggesting that EAG channels are essential for the development (Stengel et al. Unpublished).

A study has identified behavioral phenotypes associated with EAG in other species. The *C. elegans* homolog of EAG, called egl-2, is necessary for proper egg-laying and muscle contraction as well as chemotactic behavior to volatile odorants (Weinshenker et al., 1999). *C. elegans* is a heme auxotroph and known to be used as an excellent genetic model to identify the regulatory molecules and dissect the cellular pathways that modulate heme homeostasis (Rao et al., 2005; Rajagopal et al., 2008). There are ~370 genes in *C. elegans* transcriptionally responsive to environmental heme (Rajagopal et al., 2008). Analysis of alignment of EAG channels from different species revealed that the S5 histidine and C-linker histidines are conserved (Fig. 47). It would be interesting in exploring the role of EAG channels in response to heme in these animal models.

It has been described that under pathophysiological conditions, such as subarachnoid haemorrhage (SAH) and brain trauma, results in death or severe disability of 50-70% of victims. Delayed cerebral vasospasm, is the most critical clinical complication that occurs after SAH, known to be associated with both impaired dilator and increased constrictor mechanisms in cerebral arteries (Sobey and Faraci, 1998). Mechanisms contributing to development of vasospasm and abnormal reactivity of cerebral arteries after SAH have been intensively investigated in recent years. One of the major mechanisms that may contribute to vasospasm after SAH involves changes in activity of potassium channels in cerebral vessels. Cerebral vascular muscle is depolarized after SAH and this depolarization is probably contributes to vasoconstriction and, perhaps, vasospasm (Zuccarello et al., 1996; Harder et al., 1987). Consistent with this, haemolysate extracted from isolated erythrocytes induces both depolarizations and contraction of the basilar artery (Fujiwara and Kuriyama, 1984). Depolarization of vascular muscle after SAH is most likely due to inhibition of potassium channels (Harder et al., 1987). From this observation we can speculate that heme mediated inhibition of EAG channels would contribute the severity associated with SAH.

The electrophysiological properties of EAG1 can control cell-cycle processes. Conversely, cell-cycle progression also affects EAG current. When EAG is heterologously expressed in *Xenopus* oocytes, which are physiologically arrested in the G2 phase during the first meiotic division, subsequent activation of mitosis-promoting factor (MPF) both relieves this arrest and reverses the rectification properties of EAG currents (Bruggemann et al., 1997). The cell cycle-related changes of EAG channels are presumably due to a reorganization of the cytoskeleton during the G2/M transition (Camacho et al., 2000). It has been described that heme controls the expression of cell cycle regulators and cell growth of human epithelial cervix carcinoma HeLa cells. Inhibition of heme synthesis by succinyl acetone caused cell cycle arrest and induced the expression of molecular markers associated with senescence and apoptosis, such as increased formation of PML nuclear bodies. More than 60% of the succinyl acetone-treated HeLa cells accumulated in the S phase of the cell cycle (Ye and Zhang, 2004). From this observation we can speculate that there may be a link between the heme deficiency and hEAG1 channel function and a possible involvement in cell cycle progression.

5. Outlook

Acute modulation of the A-type and hEAG1 potassium channels by heme greatly expands their functional repertoires, allowing the channels to contribute to multitudes of physiological and pathophysiological phenomena. The knowledge obtained from studies of the modulator action of heme could contribute to rational design of therapeutically useful low-molecular-weight compounds targeting pathophysiological states such as epilepsy and pain. Future studies should investigate the physiological significance of heme regulation of these channels *in vivo*.

6 References

- Abbott GW, Mercer EA, Miller RT, Ramesh B, Srail SK** (1998) Conformational changes in a mammalian voltage-dependent potassium channel inactivation peptide. *Biochemistry* 37: 1640–1645.
- Allen ER** (1977) Properties and reactions of carbon monoxide, in *Carbon Monoxide* (National Research Council—Subcommittee on Carbon Monoxide). National Academy of Sciences pp. 4–27.
- Amersi F, Shen XD, Anselmo D, Melinek J, Iyer S, Southard DJ, Katori M, Volk HD, Busuttil RW, Buelow R, Kupiec-weglinski JW** (2002) Ex-vivo exposure to carbon monoxide prevents hepatic ischemia/reperfusion injury through p38 mitogen-activated protein kinase pathway. *Hepatology* 35: 815–823.
- Antz C, Geyer M, Fakler B, Schott MK, Guy HR, Frank R, Ruppersberg JP, Kalbitzer HR** (1997) NMR structure of inactivation gates from mammalian voltage-dependent potassium channels. *Nature* 385: 272–175.
- Antz C, Fakler B** (1998) Fast inactivation of voltage-gated K⁺ channels: from cartoon to structure. *News Physiol Sci* 13: 177–182.
- Antz C, Bauer T, Kalbacher H, Frank R, Covarrubias M, Kalbitzer HR, Ruppersberg JP, Baukrowitz T, Fakler B** (1999) Control of K⁺ channel gating by protein phosphorylation structural switches of the inactivation gate. *Nat Struct Biol* 6: 146–150.
- Ascenzi P, Bocedi A, Leoni L, Visca P, Zennaro E, Milani M, Bolognesi M** (2004) CO sniffing through heme-based sensor proteins. *IUBMB Life* 56: 309–315.
- Atamna H, Killilea DW, Killilea AN, Ames BN** (2002) Heme deficiency may be a factor in the mitochondrial and neuronal decay of aging *Proc Natl Acad Sci* 99: 14807–14812.
- Badawy AA** (1978) Tryptophan pyrrolase, the regulatory free haem and hepatic porphyrias. Early depletion of haem by clinical and experimental exacerbators of porphyria. *Biochem J* 172: 487–494.
- Bähring R, Milligan CJ, Vardanyan V, Engeland B, Young BA, Dannenberg J, Waldschutz R, Edwards JP, Wray D, Pongs O** (2001) Coupling of voltage-dependent potassium channel inactivation and oxidoreductase active site of Kvβ subunits. *J Biol Chem* 276: 22923–22929.
- Bairoch A, Bucher P, Hofmann K** (1996) The PROSITE database, its status in 1995. *Nucleic Acids Res* 24: 189–196.
- Balla G, Vercellotti GM, Muller-Eberhard U, Eaton J, Jacob HS** (1991) Exposure of endothelial cells to free heme potentiates damage mediated by granulocytes and toxic oxygen species. *Lab Invest* 64: 648–655.
- Barhanin J, Lesage F, Guillemare E, Fink M, Lazdunski M, Romey G** (1996) K(V)LQT1 and IsK (minK) proteins associate to form the I(Ks) cardiac potassium current. *Nature* 360: 78–80.
- Bauer CK** (1998) The erg inwardly rectifying K⁺ current and its modulation by thyrotrophin-releasing hormone in giant clonal rat anterior pituitary cells. *J Physiol* 510: 63–70.
- Beech DJ, Barnes S** (1989) Characterization of a voltage-gated K⁺ channel that accelerates the rod response to dim light. *Neuron* 3: 573–581.

- Berk PD, Blaschke TF, Scharschmidt BF, Waggoner JG, Berlin NI** (1976) A new approach to quantitation of the various sources of bilirubin in man. *J Lab Clin Med* 87: 767–780.
- Berk PD, Howe RB, Bloomer JR** (1979) Studies on bilirubin kinetics in normal adults. *J Clin Invest* 48: 2176–2190.
- Binzen U, Greffrath W, Hennessy S, Bausen M, Saaler-Reinhardt S, Treede RD** (2006) Co-expression of the voltage-gated potassium channel Kv1.4 with transient receptor potential channels (TRPV1 and TRPV2) and the cannabinoid receptor CB1 in rat dorsal root ganglion neurons. *Neuroscience* 142: 527–539.
- Bocksteins E, Labro AJ, Mayeur E, Bruyns T, Timmermans JP, Adriaensen D, Snyders DJ** (2009) Conserved negative charges in the N-terminal tetramerization domain mediate efficient assembly of Kv2.1 and Kv2.1/Kv6.4 channels. *J Biol Chem* 284: 31625–31634.
- Boczkowski J, Poderoso JJ, Motterlini R** (2006) CO-metal interaction: Vital signaling from a lethal gas. *Trends Biochem Sci* 31: 614–621.
- Boon EM, Marletta MA** (2005) Ligand discrimination in soluble guanylate cyclases and the H-NOX family of heme sensor proteins. *Curr Opin Chem Biol* 9:441–446.
- Brautigan DL, Feinberg BA, Hoffman BM, Margoliash E, Preisach J, Blumberg WE** (1977) Multiple low spin forms of the cytochrome c ferrihemochrome. EPR spectra of various eukaryotic and prokaryotic cytochromes c. *J Biol Chem* 252: 574–582.
- Brazier SP, Telezhkin V, Mears R, Müller CT, Riccardi D, Kemp PJ** (2009) Cysteine residues in the C-terminal tail of the human BK(Ca) α subunit are important for channel sensitivity to carbon monoxide. *Adv Exp Med Biol* 648: 49–56.
- Brown SB, Dean TC, Jones P** (1970) Aggregation of ferrihaems. Dimerization and protolytic equilibria of protoferrihaem and deuterioferrihaem in aqueous solution. *Biochem J* 117: 733–739.
- Bruggemann A, Stuhmer W, Pardo LA** (1997) Mitosis-promoting factor-mediated suppression of a cloned delayed rectifier potassium channel expressed in *Xenopus* oocytes. *Proc Natl Acad Sci* 94: 537–542.
- Camacho J, Sanchez A, Stuhmer W, Pardo LA** (2000) Cytoskeletal interactions determine the electrophysiological properties of human EAG potassium channels. *Pflugers Arch* 441: 167–174.
- Castellani RJ, Harris PL, Lecroisey A, Izadi-Pruneyre N, Wandersman C, Perry G, Smith MA** (2000) Evidence for a novel heme-binding protein, HasAh, in Alzheimer disease. *Antioxid. Redox Signal* 2: 137–142.
- Caterina MJ, Leffler A, Malmberg AB, Martin WJ, Trafton J, Petersen-Zeit K, Koltzenburg M, Basbaum AI, Julius D** (2000) Impaired nociception and pain sensation in mice lacking the capsaicin receptor. *Science* 288: 306–313.
- Chapman JT, Otterbein LE, Elias JA, Choi AM** (2001) Carbon monoxide attenuates aeroallergen-induced inflammation in mice. *Am J Physiol Lung Cell Mol Physiol* 281: 209–216.
- Chen ML, Hoshi T, Wu CF** (1996) Heteromultimeric interactions among K⁺ channel subunits from Shaker and eag families in *Xenopus* oocytes. *Neuron* 17: 535–542.
- Chen ML, Hoshi T, Wu CF** (2000) Sh and eag K⁺ channel subunit interaction in frog oocytes depends on level and time of expression. *Biophys J* 3: 1358–1368.

- Chernova T, Nicotera P, Smith AG** (2006) Heme deficiency is associated with senescence and causes suppression of N-methyl-D-aspartate receptor subunits expression in primary cortical neurons. *Mol Pharmacol* 69: 697–705.
- Chernova T, Steinert JR, Guerin CJ, Nicotera P, Forsythe ID, Smith AG** (2007) Neurite degeneration induced by heme deficiency mediated via inhibition of NMDA receptor-dependent extracellular signal-regulated kinase 1/2 activation. *J Neurosci* 27: 8475–8485.
- Choi CY, Cerda JF, Chu HA, Babcock GT, Marletta MA** (1999) Spectroscopic characterization of the heme-binding sites in *Plasmodium falciparum* histidine-rich protein 2. *Biochemistry* 38: 16916–16924.
- Clark JF, Sharp FR** (2006) Bilirubin oxidation products (BOXes) and their role in cerebral vasospasm after subarachnoid hemorrhage. *J Cereb Blood Flow Metab* 26: 1223–1233.
- Clark JF, Loftspring M, Wurster WL, Beiler S, Beiler C, Wagner KR** (2008) Bilirubin oxidation products, oxidative stress, and intracerebral hemorrhage. *Acta Neurochir Suppl* 105: 7–12.
- Coburn RF, Williams WJ, Forster RE** (1965) Effect of erythrocyte destruction on carbon monoxide production in man. *J Clin Invest* 43: 1098–1103.
- Coburn RF** (1970b) The carbon monoxide body stores. *Ann NY Acad Sci* 174: 11–22.
- Connor JA, Stevens CF** (1971) Voltage clamp studies of a transient outward membrane current in gastropod neural somata. *J Physiol* 213: 21–30.
- Cooper EC, Milroy A, Jan YN, Jan LY, Lowenstein DH** (1998) Presynaptic localization of Kv1.4-containing A-type potassium channels near excitatory synapses in the hippocampus. *J Neurosci* 18: 965–974.
- Covarrubias M, Wei A, Salkoff L, Vyas TB** (1994) Elimination of rapid potassium channel inactivation by phosphorylation of the inactivation gate. *Neuron* 13:1403–1412.
- Dawson JH** (1988) Probing structure–function relations in heme containing oxygenases and peroxidases. *Science* 240: 433–439.
- Decher N, Gonzalez T, Streit AK, Sachse FB, Renigunta V, Soom M, Heinemann SH, Daut J, Sanguinetti MC** (2008) Structural determinants of Kv β 1.3-induced channel inactivation: a hairpin modulated by PIP₂. *EMBO J* 27: 3164–3174.
- Díaz L, Ceja-Ochoa I, Restrepo-Angulo I, Larrea F, Avila-Chávez E, García-Becerra R, Borja-Cacho E, Barrera D, Ahumada E, Gariglio P, Alvarez-Rios E, Ocadiz-Delgado R, Garcia-Villa E, Hernández-Gallegos E, Camacho-Arroyo I, Morales A, Ordaz-Rosado D, García-Latorre E, Escamilla J, Sánchez-Peña LC, Saqui-Salces M, Gamboa-Dominguez A, Vera E, Uribe-Ramírez M, Murbartíán J, Ortiz CS, Rivera-Guevara C, De Vizcaya-Ruiz A, Camacho J** (2009) Estrogens and human papilloma virus oncogenes regulate human ether-à-go-go-1 potassium channel expression. *Cancer Res* 69: 3300–3007.
- Ding XW, Luo HS, Jin X, Yan JJ, Ai YW** (2007) Aberrant expression of Eag1 potassium channels in gastric cancer patients and cell lines. *Med Oncol* 24: 345–350.
- Ding XW, Luo HS, Yan JJ, An P, Lü P** (2007) Aberrant expression of EAG1 potassium channels in colorectal cancer. *Zhonghua Bing Li Xue Za Zhi* 36: 410–411.
- Ding XW, Wang XG, Luo HS, Tan SY, Gao S, Luo B, Jiang H** (2008) Expression and prognostic roles of Eag1 in resected esophageal squamous cell carcinomas. *Dig Dis Sci* 53: 2039–2044.
- Dodson PD, Forsythe ID** (2004) Presynaptic K⁺ channels: electrifying regulators of synaptic terminal excitability. *Trends Neurosci* 27: 210–217.

- Doyle DA, Morais Cabral J, Pfuetschner RA, Kuo A, Gulbis JM, Cohen SL, Chait BT, MacKinnon R** (1998) The structure of the potassium channel: molecular basis of K^+ conduction and selectivity. *Science* 280: 69–77.
- Engelard B, Neu A, Ludwig J, Roeper J, Pongs O** (1998) Cloning and functional expression of rat ether-à-go-go like K^+ channel genes. *J Physiol* 513: 647–654.
- England SK, Uebele VN, Kodali J, Bennett PB, Tamkun MM** (1995a) A novel K^+ channel beta-subunit (hKv β 1.3) is produced via alternative mRNA splicing. *J Biol Chem* 270: 28531–28534.
- England SK, Uebele VN, Shear H, Kodali J, Bennett PB, Tamkun MM** (1995b) Characterization of a voltage-gated K^+ channel beta subunit expressed in human heart. *Proc Natl Acad Sci* 92: 6309–6313.
- Farias LMB, Ocaña DB, Díaz L** (2004) Ether-à-go-go potassium channels as human cervical cancer markers. *Cancer Res* 64: 6996–7001.
- Feng Y, Sligar SG, Wand AJ** (1994) Solution structure of apocytochrome b562. *Nat Struct Biol* 1: 30–35.
- Frings S, Brull N, Dzeja C, Angele A, Hagen V, Kaupp UB, Baumann A** (1998) Characterization of ether-à-go-go channels present in photoreceptors reveals similarity to IK_x, a K^+ current in rod inner segments. *J Gen Physiol* 111: 583–599.
- Fujiwara S, Kuriyama H** (1984) Hemolysate-induced contraction in smooth muscle cells of the guinea pig basilar artery. *Stroke* 15: 503–510.
- Gage FH, Buzsaki G, Armstrong DM** (1990) NGF-dependent sprouting and regeneration in the hippocampus. *Prog Brain Res* 83: 357–370.
- Ganetzky B, Wu CF** (1983) Neurogenetic analysis of potassium currents in *Drosophila*: synergistic effects on neuromuscular transmission in double mutants. *J Neurogenet* 1: 17–28.
- Garcia-Ferreiro RE, Kerschensteiner D, Major F, Monje F, Stühmer W, Pardo LA** (2004) Mechanism of block of hEag1 K^+ channels by imipramine and astemizole. *J Gen Physiol* 124: 301–317.
- Garrick MD, Scott D, Kulju D, Romano MA, Dolan KG, Garrick LM** (1999) Evidence for and consequences of chronic heme deficiency in Belgrade rat reticulocytes. *Biochim Biophys Acta* 1449: 125–136.
- Geiger JRP, Jonas P** (2000) Dynamic control of presynaptic Ca^{2+} inflow by fast-inactivating K^+ channels in hippocampal mossy fiber boutons. *Neuron* 28: 927–939.
- Giese KP, Storm JF, Reuter D, Fedorov NB, Shao LR, Leicher T, Pongs O, Silva AJ** (1998) Reduced K^+ channel inactivation, spike broadening, and after-hyperpolarization in Kv β 1.1-deficient mice with impaired learning. *Learn Mem* 5: 257–273.
- Gilles-Gonzalez MA, Gonzalez G** (2004) Signal transduction by heme-containing PAS-domain proteins. *J Appl Physiol* 96: 774–783.
- Gilles-Gonzalez MA, Gonzalez G** (2005) Heme-based sensors: defining characteristics, recent developments, and regulatory hypotheses. *J Inorg Biochem* 99: 1–22.
- Goldstein SA, Bockenhauer D, O'Kelly I, Zilberberg N** (2001) Potassium leak channels and the KCNK family of two-P-domain subunits. *Nat Rev Neurosci* 2: 175–184.
- Gómez-Varela D, Zwick-Wallasch E, Knötgen H, Sánchez A, Hettmann T, Ossipov D, Weseloh R, Contreras-Jurado C, Rothe M, Stühmer W, Pardo LA** (2007) Monoclonal antibody blockade of the human Eag1 potassium channel function exerts antitumor activity. *Cancer Res* 15: 7343–7349.

- Gordon SE, Zagotta WN** (1995) A histidine residue associated with the gate of the cyclic nucleotide-activated channels in rod photoreceptors. *Neuron* 14: 177–183.
- Gordon SE, Varnum MD, Zagotta WN** (1997) Direct interaction between amino and carboxyl-terminal domains of cyclic nucleotide-gated channels. *Neuron* 19: 431–441.
- Guarente L, Mason T** (1983) Heme regulates transcription of the CYC1 gene of *S. cerevisiae* via an upstream activation site. *Cell* 32: 1279–1286.
- Gunther L, Berberat PO, Haga M, Brouard S, Smith RN, Soares MP, Bach FH, Tobiasch E** (2002) Carbon monoxide protects pancreatic cells from apoptosis and improves islet function/survival after transplantation. *Diabetes* 51: 994–999.
- Gupta Roy B, Griffith LC** (1996) Functional heterogeneity of alternatively spliced isoforms of *Drosophila* Ca^{2+} /calmodulin-dependent protein kinase II. *J Neurochem* 66: 1282–1288.
- Gutman GA** (2005) International Union of Pharmacology. LIII. Nomenclature and molecular relationships of voltage-gated potassium channels. *Pharmacol Rev* 57: 473–508.
- Guy HR, Durell SR, Warmke J, Drysdale R, Ganetzky B** (1991) Similarities in amino acid sequences of *Drosophila* eag and cyclic nucleotide-gated channels. *Science* 254: 730.
- Hagiwara S, Kusano K, Saito N** (1961) Membrane changes of *Onchidium* nerve cell in potassium-rich media. *J Physiol* 155: 470–489.
- Harder DR, Dernbach P, Waters A** (1987) Possible cellular mechanism for cerebral vasospasm after experimental subarachnoid hemorrhage in the dog. *J Clin Invest* 80: 875–880.
- Heinemann S, Rettig J, Scott V, Parcej DN, Lorra C, Dolly J, Pongs O** (1994) The inactivation behaviour of voltage-gated K^+ channels may be determined by association of α - and β -subunits. *J Physiol* 88: 173–180.
- Heinemann SH, Rettig J, Graack HR, Pongs O** (1996) Functional characterization of Kv channel beta-subunits from rat brain. *J Physiol* 493: 625–633.
- Heirwegh KPM, Brown SB**. Eds., Bilrubin (CRC Press, Boca Raton, FL, 1982), vols. 1 and 2; R Sch}nid and AF McDonagh, in *The Metabolic Basis of Inherited Disease*, **Stanbury JB, Wyngaarden JB, Fredrickson DS**, Eds. (McGraw- Hill, New York, 1978), pp. 1221–1257.
- Hemmerlein B, Weseloh RM, DeQueiroz FM** (2006) Overexpression of Eag1 potassium channels in clinical tumours. *Mol Cancer* 5: 41.
- Ho SN, Hunt HD, Horton RM, Pullen JK, Pease LR** (1989) Site-directed mutagenesis by overlap extension using the polymerase chain reaction. *Gene* 77: 51–59.
- Horrigan FT, Heinemann SH, Hoshi T** (2005) Heme regulates allosteric activation of the Slo1 BK channel. *J Gen Physiol* 126: 7–21.
- Hoshi T, Zagotta WN, Aldrich RW** (1990) Biophysical and molecular mechanisms of Shaker potassium channel inactivation. *Science* 250: 533–538.
- Hoshi T, Zagotta WN, Aldrich RW** (1991) Two types of inactivation in Shaker K^+ channels: effects of alterations in the carboxy-terminal region. *Neuron* 7: 547–556.
- Hoshi T, Lahiri S** (2004) Cell biology. Oxygen sensing: it's a gas! *Science* 306: 2050–2051.
- Hou S, Xu R, Heinemann SH, Hoshi T** (2008) The RCK1 high-affinity Ca^{2+} sensor confers carbon monoxide sensitivity to Slo1 BK channels. *Proc Natl Acad Sci* 105: 4039–4043.
- Hou S, Heinemann SH, Hoshi T** (2009) Modulation of BKCa channel gating by endogenous signaling molecules. *Physiology* 24: 26–35.
- Hou S, Xu R, Clark JF, Wurster WL, Heinemann SH, Hoshi T** (2010) Bilirubin oxidation end products directly alter $\text{K}(+)$ channels important in the regulation of vascular tone. *J Cereb Blood Flow Metab.* [Epub ahead of print]

- Hsieh CP** (2008) Redox modulation of A-type K⁺ currents in pain-sensing dorsal root ganglion neurons. *Biochem Biophys Res Commun* 370: 445–449.
- Hunt NH, Stocker R** (2007) Heme moves to center stage in cerebral malaria. *Nat Med* 13: 667–669.
- Ingi T, Chiang G, Ronnett GV** (1996) The regulation of heme turnover and carbon monoxide biosynthesis in cultured primary rat olfactory receptor neurons. *J Neurosci* 16: 5621–5628.
- Ishikawa S, Tamaki S, Ohata M, Arihara K, Itoh M** (2010) Heme induces DNA damage and hyperproliferation of colonic epithelial cells via hydrogen peroxide produced by heme oxygenase: a possible mechanism of heme-induced colon cancer. *Mol Nutr Food Res* 54: 1182–1191.
- Jaggard JH, Li A, Parfenova H, Liu J, Umstot ES, Dopico AM, Leffler CW** (2005) Heme is a carbon monoxide receptor for large-conductance Ca²⁺-activated K⁺ channels. *Circ Res* 97: 805–812.
- Jenke M, Sánchez A, Monje F, Stühmer W, Weseloh RM, Pardo LA** (2003) C-terminal domains implicated in the functional surface expression of potassium channels. *EMBO J* 22: 395–403.
- Jow F, Zhang ZH, Kopsco DC, Carroll KC, Wang K** (2004) Functional coupling of intracellular calcium and inactivation of voltage-gated Kv1.1/Kvβ1.1 A-type K⁺ channels. *Proc Natl Acad Sci* 101: 15535–15540.
- Kaplan WD, Trout WE** (1969) The behavior of four neurological mutants of *Drosophila*. *Genetics* 61: 399–409.
- Kaplan BH** (1977) Synthesis of heme. In **Williams WJ, Beutler E, Erslev AJ, Wayne R** (Eds.), *Hematology* (2nd ed.) (pp. 287–294). New York: McGraw-Hill.
- Kaya AH, Plewinska M., Wong DM** (1994) Human δ-aminolevulinate dehydratase (ALAD) gene: structure and alternative splicing of the erythroid and housekeeping mRNAs. *Genomics* 19: 242–248.
- Kranc KR, Pyne GJ, Tao L, Claridge TD, Harris DA, Cadoux-Hudson TA** (2000) Oxidative degradation of bilirubin produces vasoactive compounds. *Eur J Biochem.* 267: 7094–7101.
- Kumar S, Bandyopadhyay U** (2005) Free heme toxicity and its detoxification systems in human. *Toxicol Lett* 157: 175–188.
- Kwak YG, Hu N, Wei J, George AL Jr, Grobaski TD, Tamkun MM, Murray KT** (1999) Protein kinase A phosphorylation alters Kvβ1.3 subunit-mediated inactivation of the Kv1.5 potassium channel. *J Biol Chem* 274: 13928–13932.
- Lanzilotta WN, Schuller DJ, Thorsteinsson MV, Kerby RL, Roberts GP, Poulos TL** (2000) Structure of the CO sensing transcription activator CooA. *Nat Struct Biol* 7: 876–780.
- Lecain E, Sauvaget E, Crisanti P, Van Den Abbeele T, Huy PT** (1999) Potassium channel ether-à-go-go mRNA expression in the spiral ligament of the rat. *Hear Res* 133: 133–138.
- Lee BC** (1992) Isolation of an outer membrane hemin-binding protein of *Haemophilus influenzae* type B. *Infect. Immun* 60: 810–816.
- Lee TE, Philipson LH, Nelson DJ** (1996) N-type inactivation in the mammalian Shaker K⁺ channel Kv1.4. *J. Membrane Biol* 151: 225–235.
- Lees-Miller JP, Subbotina JO, Guo J, Yarov-Yarovoy V, Noskov SY, Duff HJ** (2009) Interactions of H562 in the S5 helix with T618 and S621 in the pore helix are important determinants of hERG1 potassium channel structure and function. *Biophys J* 96: 3600–3610.

- Lipton S, Rosenberg PA** (1994) Excitatory amino acids as a final common pathway for neurologic disorders. *N Engl J Med* 330: 613–622.
- Lu Q, Peevey J, Jow F, Monaghan MM, Mendoza G, Zhang H, Wu J, Kim CY, Bicksler J, Greenblatt L, Lin SS, Childers W, Bowlby MR** (2008) Disruption of Kv1.1 N-type inactivation by novel small molecule inhibitors (disinactivators). *Bioorg Med Chem* 16: 3067–3075.
- Lu Y, Berry SM, Pfister TD** (2001) Engineering novel metalloproteins: design of metal-binding sites into native protein scaffolds. *Chem Rev* 101: 3047–3080.
- Ludwig J, Terlau H, Wunder F, Brüggemann A, Pardo LA, Marquardt A, Stühmer W, Pongs O** (1994) Functional expression of a rat homologue of the voltage gated ether-à-go-go potassium channel reveals differences in selectivity and activation kinetics between the *Drosophila* channel and its mammalian counterpart. *EMBO J* 13: 4451–4458.
- Ludwig J, Owen D, Pongs O** (1997) Carboxy-terminal domain mediates assembly of the voltage-gated rat ether-à-go-go potassium channel. *EMBO Journal* 16 : 6337–6345.
- Ludwig J, Weseloh R, Karschin C, Liu Q, Netzer R, Engeland B, Stansfeld C, Pongs O** (2000) Cloning and functional expression of rat eag2, a new member of the ether-à-go-go family of potassium channels and comparison of its distribution with that of eag1. *Mol Cell Neurosci* 16: 59–70.
- MacKinnon R, Aldrich RW, Lee AW** (1993) Functional stoichiometry of Shaker potassium channel inactivation. *Science* 262: 757–759.
- Maines MD** (1988) Heme oxygenase: function, multiplicity, regulatory mechanisms, and clinical applications. *FASEB J* 2: 2557–2568.
- Maines MD** (2000) The heme oxygenase system and its functions in the brain. *Cell Mol Biol* 46: 573–585.
- Maines MD** (2005) The heme oxygenase system: updat 2005 *Antioxid Redox Signal* 7: 1761–1716.
- Marble DD, Hegle AP, Snyder ED, Dimitratos S, Bryant PJ, Wilson GF** (2005) Camguk/CASK enhances ether-à-go-go potassium current by a phosphorylation-dependent mechanism. *J Neurosci* 20: 4898–4907.
- Mastrogiacomo A, Parsons SM, Zampighi GA, Jenden DJ, Umbach JA, Gundersen CB** (1994) Cysteine string proteins: a potential link between synaptic vesicles and presynaptic Ca^{2+} channels. *Science* 264: 981–982.
- May BK, Dogra SC, Sadlon TJ** (1995) Molecular regulation of heme biosynthesis in higher vertebrates. *Prog Nucleic Acid Res Mol Biol* 51: 1–51.
- McCoubrey WK Jr, Huang TJ, Maines MD** (1997) Isolation and characterization of a cDNA from the rat brain that encodes hemoprotein heme oxygenase-3. *European Journal of Biochemistry* 247: 725–732.
- McNamara JO** (1999) Emerging insights into the genesis of epilepsy: cellular and molecular basis of epilepsy. *Nature* 399: 15–22.
- Mello de Queiroz F, Suarez-Kurtz G, Stühmer W, Pardo LA** (2006) Ether-à-go-go potassium channel expression in soft tissue sarcoma patients. *Mol Cancer* 5: 42.
- Mense SM, Zhang L** (2006) Heme: a versatile signaling molecule controlling the activities of diverse regulators ranging from transcription factors to MAP kinases. *Cell Res* 16: 681–692.
- Meyer R, Heinemann SH** (1998) Characterization of an eag-like potassium channel in human neuroblastoma cells. *J Physiol* 508: 49–56.

- Meyer R, Schonherr R, Gavrilova-Ruch O, Wohlrab W, Heinemann SH** (1999) Identification of ether-à-go-go and calcium-activated potassium channels in human melanoma cells. *J Membr Biol* 171: 107–115.
- Mogi T, Saiki K, Anraku Y** (1994) Biosynthesis and functional role of haem O and haem A. *Mol Microbiol*. 14: 391–398.
- Morais Cabral JH, Lee A, Cohen SL, Chait BT, Li M, Mackinnon R** (1998) Crystal structure and functional analysis of the HERG potassium channel N terminus: a eukaryotic PAS domain. *Cell* 95: 649–655.
- Motterlini R, Gonzales A, Foresti R, Clark JE, Green CJ, Winslow RM** (1998) Heme oxygenase-1-derived carbon monoxide contributes to the suppression of acute hypertensive responses *in vivo*. *Circ Res* 83: 568–577.
- Motterlini R, Clark JE, Foresti R, Sarathchandra P, Mann BE, Green CJ** (2002) Carbon monoxide-releasing molecules: characterization of biochemical and vascular activities. *Circ Res* 90: E17–E24.
- Motterlini R, Mann BE, Johnson TR, Clark JE, Foresti R, Green CJ** (2003) Bioactivity and pharmacological actions of carbon monoxide-releasing molecules. *Curr Pharm Des* 9: 2525–2539.
- Muller-Eberhard U, Fraig M** (1993) Bioactivity of heme and its containment. *Am J Hematol* 42: 59–62.
- Nagababu E, Rifkind JM** (2004) Heme degradation by reactive oxygen species. *Antioxid Redox Signal* 6: 967–978.
- Napp J, Monje F, Stühmer W, Pardo LA** (2005) Glycosylation of Eag1 (Kv10.1) potassium channels: intracellular trafficking and functional consequences. *J Biol Chem* 280: 29506–29512.
- Neher E** (1971) Two fast transient current components during voltage clamp on snail neurons. *J Gen Physiol* 58: 36–53.
- Norat T, Lukanova A, Ferrari P, Riboli E** (2002) Meat consumption and colorectal cancer risk: dose-response meta-analysis of epidemiological studies. *Int J Cancer* 98: 241–256.
- Occhiodoro T, Bernheim L, Liu JH, Bijlenga P, Sinnreich M, Bader CR, Fischer-Lougheed J** (1998) Cloning of a human ether-à-go-go potassium channel expressed in myoblasts at the onset of fusion. *FEBS Lett* 434: 177–182.
- Ogawa K, Sun J, Taketani S, Nakajima O, Nishitani C, Sassa S, Hayashi N, Yamamoto M, Shibahara S, Fujita H, Igarashi K** (2001) Heme mediates derepression of Maf recognition element through direct binding to transcription repressor Bach1. *EMBO J* 20: 2835–2843.
- Oliver D, Lien CC, Soom M, Baukrowitz T, Jonas P, Fakler B** (2004) Functional conversion between A-type and delayed rectifier K⁺ channels by membrane lipids. *Science* 304: 265–270.
- Otterbein L** (2002) Carbon monoxide: innovative anti-inflammatory properties of an age-old gas molecule. *Antioxid Redox Signal* 4: 309–319.
- Ozawa N, Goda N, Makino N, Yamaguchi T, Yoshimura Y, Suematsu M** (2002) Leydig cell-derived heme oxygenase-1 regulates apoptosis of premeiotic germ cells in response to stress. *J Clin Invest* 109: 457–467.
- Padanilam BJ, Lu T, Hoshi T, Padanilam BA, Shibata EF, Lee HC** (2002) Molecular determinants of intracellular pH modulation of human Kv1.4 N-type inactivation. *Mol Pharmacol* 62: 127–134.

- Pamplona A, Ferreira A, Balla J, Jeney V, Balla G, Epiphany S, Chora A, Rodrigues CD, Gregoire IP, Cunha-Rodrigues M, Portugal S, Soares MP, Mota MM** (2007) Heme oxygenase-1 and carbon monoxide suppress the pathogenesis of experimental cerebral malaria. *Nat Med* 13: 703–710.
- Pan Y, Weng J, Kabaleeswaran V, Li H, Cao Y, Bhosle RC, Zhou M** (2008) Cortisone dissociates the Shaker family K⁺ channels from their beta subunits. *Nat Chem Biol* 4: 708–714.
- Panyi G** (2005) Biophysical and pharmacological aspects of K⁺ channels in T lymphocytes. *Eur Biophys J* 34: 515–529.
- Paoli M, Marles-Wright J, Smith A** (2002) Structure-function relationships in heme-proteins. *DNA Cell Biol* 21: 271–280.
- Pardo LA, Heinemann SH, Terlau H, Ludwig U, Lorra C, Pongs O, Stuhmer W** (1992) Extracellular K⁺ specifically modulates a rat brain K⁺ channel. *Proc Natl Acad Sci* 89: 2466–2470.
- Pardo LA, Bruggemann A, Camacho J, Stuhmer W** (1998) Cell cycle-related changes in the conducting properties of r-eag K⁺ channels. *J Cell Biol* 143: 767–775.
- Pardo LA, del Camino D, Sanchez A, Alves F, Bruggemann A, Beckh S, Stuhmer W** (1999) Oncogenic potential of EAG K⁺ channels. *Embo J* 18: 5540–5547.
- Pardo LA, Contreras-Jurado C, Zientkowska M, Alves F, Stuhmer W** (2005) Role of voltage-gated potassium channels in cancer. *J Membr Biol* 205: 115–124.
- Patt S, Preussat K, Beetz C, Kraft R, Schrey M, Kalff R, Schonherr K, Heinemann SH** (2004) Expression of ether-à-go-go potassium channels in human gliomas. *Neurosci Lett* 368: 249–253.
- Pertwee RG** (2001) Cannabinoid receptors and pain. *Prog Neurobiol* 63: 569–611.
- Piros ET, Shen L, Huang XY** (1999) Purification of an EH domain-binding protein from rat brain that modulates the gating of the rat ether-à-go-go channel. *J Biol Chem* 274: 33677–33683.
- Pongs O, Leicher T, Berger M, Roeper J, Bähring R, Wray D, Giese KP, Silva AJ, Storm JF** (1999) Functional and molecular aspects of voltage-gated K⁺ channel beta subunits. *Ann N Y Acad Sci* 868: 344–355.
- Ponka P** (1999) Cell biology of heme. *Am J Med Sci* 318: 241–256.
- Poulos TL** (2007) The Janus nature of heme. *Nat Prod Rep* 24: 504–510.
- Prüss H, Grosse G, Brunk I, Veh RW, Ahnert-Hilger G** (2010) Age-dependent axonal expression of potassium channel proteins during development in mouse hippocampus. *Histochem Cell Biol* 133: 301–312.
- Pyne Geithman GJ, Morgan CJ, Wagner K, Dulaney EM, Carrozzella J, Kanter DS** (2005) Bilirubin production and oxidation in CSF of patients with cerebral vasospasm after subarachnoid hemorrhage. *J Cereb Blood Flow Metab* 25: 1070–1077.
- Rajagopal A, Rao AU, Amigo J, Tian M, Upadhyay SK, Hall C, Uhm S, Mathew MK, Fleming MD, Paw BH, Krause M, Hamza I** (2008) Haem homeostasis is regulated by the conserved and concerted functions of HRG-1 proteins *Nature* 453: 1127–1131.
- Rao AU, Carta LK, Lesuisse E, Hamza I** (2005). Lack of heme synthesis in a free-living eukaryote. *Proc Natl Acad Sci* 102: 4270–4275.
- Rasband MN, Park EW, Vanderah QW, Lai J, Porreca F, Trimmer JS** (2001) Distinct potassium channels on pain-sensing neurons. *Proc Natl Acad Sci* 98: 13373–13378.

- Rasmusson RL, Morales MJ, Wang S, Liu S, Campbell DL, Brahmajothi MV & Strauss HC** (1998). Inactivation of voltage gated cardiac K⁺ channels. *Circ Res* 82: 739–750.
- Reddy SV, Alcantara O, Roodman GD, Boldt DH** (1996) Inhibition of tartrate-resistant acid phosphatase gene expression by hemin and protoporphyrin IX. Identification of a hemin-responsive inhibitor of transcription. *Blood* 88: 2288–2297.
- Reedy CJ, Gibney BR** (2004) Heme protein assemblies. *Chem Rev* 104: 617–649.
- Rettig J, Heinemann SH, Wunder F, Lorra C, Parcej DN, Dolly JO, Pongs O** (1994) Inactivation properties of voltage-gated K⁺ channels altered by presence of beta-subunit. *Nature* 369: 289–294.
- Rhodes KJ, Monaghan MM, Barrezueta NX, Nawoschik S, Bekele-Arcuri Z, Matos MF, Nakahira K, Schechter LE, Trimmer JS** (1996) Voltage-gated K⁺ channel beta subunits: expression and distribution of Kv beta 1 and Kv beta 2 in adult rat brain. *J Neurosci* 16: 4846–4860.
- Robertson GA, Warmke JM, Ganetzky B** (1996) Potassium currents expressed from *Drosophila* and mouse EAG cDNAs in *Xenopus* oocytes. *Neuropharmacology* 35: 841–850.
- Roeper J, Lorra C, Pongs O** (1997) Frequency-dependent inactivation of mammalian A-type K⁺ channel KV1.4 regulated by Ca²⁺/calmodulin-dependent protein kinase. *J Neurosci* 17: 3379–3391.
- Ryter SW, Tyrrel RM** (2000) The heme synthesis and degradation pathways: role in oxidant sensitivity. Heme oxygenase has both pro- and antioxidant properties. *Free Radic Biol Med* 28: 289–309.
- Ruppersberg J, Stocker M, Pongs O, Heinemann SH, Frank R, Koenen M** (1991) Regulation of fast inactivation of cloned mammalian IK(A) channels by cysteine oxidation. *Nature* 352: 711–714.
- Saganich MJ, Vega-Saenz de Miera E, Nadal MS, Baker H, Coetzee WA, Rudy B** (1999) Cloning of components of a novel subthreshold activating K⁺ channel with a unique pattern of expression in the cerebral cortex. *J Neurosci* 19: 10789–10802.
- Saganich MJ, Machado E, Rudy B** (2001) Differential expression of genes encoding subthreshold-operating voltage-gated K⁺ channels in brain. *J Neurosci* 21: 4609–4624.
- Salkoff L, Baker K, Butler A, Covarrubias M, Pak MD, Wei A** (1992) An essential “set” of K⁺ channels conserved in flies, mice and humans. *Trends Neurosci* 15: 161–166.
- Sanguinetti MC, Jiang C, Curran ME, Keating MT** (1995) A mechanistic link between an inherited and an acquired cardiac arrhythmia: HERG encodes the IKr potassium channel. *Cell* 81: 299–307.
- Sassa S** (1976) Sequential induction of heme pathway enzymes during erythroid differentiation of mouse Friend leukemia virus-infected cells. *J Exp Med* 143: 305–315.
- Sassa S** (1990) Regulation of the genes for heme pathway enzymes in erythroid and in non-erythroid cells. *Int J Cell Cloning* 8: 10–26.
- Sassa S** (2004) Why heme needs to be degraded to iron, biliverdin IXalpha, and carbon monoxide? *Antioxid Redox Signal* 6: 819–824.
- Schäfer G, Purschke WG, Gleissner M, Schmidt CL** (1996) Respiratory chains of archaea and extremophiles. *Biochim Biophys Acta* 1275: 16–20.
- Schmidt CL, Shaw L** (2001) A comprehensive phylogenetic analysis of Rieske and Rieske-type iron-sulfur proteins. *J Bioenerg Biomembr* 33: 9–26.
- Schneider S, Marles-Wright J, Sharp KH, Paoli M** (2007) Diversity and conservation of interactions for binding heme in b-type heme proteins. *Nat Prod Rep* 24: 621–630.

- Schönherr R, Löber K, Heinemann SH** (2000) Inhibition of human ether-à-go-go potassium channels by Ca^{2+} /calmodulin. *The EMBO Journal* 19: 3263–3271.
- Schopperle WM, Holmqvist MH, Zhou Y, Wang J, Wang Z, Griffith LC, Keselman I, Kusnitz F, Dagan D, Levitan IB** (1998) Slob, a novel protein that interacts with the Slowpoke calcium-dependent potassium channel. *Neuron* 20: 565–573.
- Schott MK, Antz C, Frank R, Ruppersberg JP, Kalbitzer HR** (1998) Structure of the inactivating gate from the Shaker voltage gated K^+ channel analyzed by NMR spectroscopy. *Eur Biophys J* 27: 99–104.
- Schulte U, Thumfart JO, Klöcker N, Sailer CA, Bildl W, Biniossek M, Dehn D, Deller T, Eble S, Abbass K, Wangler T, Knaus HG, Fakler B** (2006) The epilepsy-linked Lg1 protein assembles into presynaptic Kv1 channels and inhibits inactivation by Kvbeta1. *Neuron* 49: 697–706.
- Schwartz S, Ellefson M** (1985) Quantitative fecal recovery of ingested hemoglobin-heme in blood: comparisons by HemoQuant assay with ingested meat and fish. *Gastroenterology*. 89: 19–26.
- Scragg JL, Dallas ML, Wilkinson JA, Varadi G, Peers C** (2008) Carbon monoxide inhibits L-type Ca^{2+} channels via redox modulation of key cysteine residues by mitochondrial reactive oxygen species. *J Biol Chem* 283: 24412–24419.
- Sengupta A, Hon T, Zhang L** (2005) Heme deficiency suppresses the expression of key neuronal genes and causes neuronal cell death *Brain Res Mol Brain Res* 137: 23–30
- Sheng M., Tsaur ML, Jan YN, Jan LY** (1992) Subcellular segregation of two A-type K^+ channel proteins in rat central neurons. *Neuron* 9: 271–284.
- Shi W, Wymore RS, Wang HS, Pan Z, Cohen IS, McKinnon D, Dixon JE** (1997) Identification of two nervous system-specific members of the erg potassium channel gene family. *J Neurosci* 17: 9423–9432.
- Shi G, Nakahira K, Hammond S, Rhodes KJ, Schechter LE, Trimmer JS** (1996) Beta subunits promote K^+ channel surface expression through effects early in biosynthesis. *Neuron*. 4: 843–852.
- Shi W, Wang HS, Pan Z, Wymore RS, Cohen IS, McKinnon D, Dixon JE** (1998) Cloning of a mammalian elk potassium channel gene and EAG mRNA distribution in rat sympathetic ganglia. *J Physiol* 511: 675–682.
- Shriver DT** (1981) Activation of carbon monoxide by carbon and oxygen coordination, in *Catalytic Activation of Carbon Monoxide* (Ford PC ed) pp 1–18, American Chemistry Society, Washington, DC.
- Silva AJ, Paylor R, Wehner J M, Tonegawa S** (1992a) Impaired spatial learning in alpha-calcium-calmodulin kinase II mutant mice. *Science* 257: 206–211.
- Silva AJ, Stevens CF, Tonegawa S, Wang Y** (1992b) Deficient hippocampal long-term potentiation in alpha-calcium-calmodulin kinase II mutant mice. *Science* 257: 201–206.
- Silverman WR, Roux B, Papazian DM** (2003) Structural basis of two-stage voltage-dependent activation in K^+ channels. *Proc Natl Acad Sci* 100: 2935–2940.
- Sobey CG, Faraci FM** (1998) Subarachnoid haemorrhage: what happens to the cerebral arteries? *Clin Exp Pharmacol Physiol* 25: 867–876.
- Spitzner M, Martins JR, Soria RB, Ousingsawat J, Scheidt K, Schreiber R, Kunzelmann K** (2008) Eag1 and Bestrophin 1 are up-regulated in fast-growing colonic cancer cells. *J Biol Chem* 283: 7421–7428.

- Stephens GJ, Owen DG, Robertson B** (1996) Cysteine-modifying reagents alter the gating of the rat cloned potassium channel Kv1.4. *Pflügers Arch* 431: 435–442.
- Stevens L, Ju M, Wray D** (2009) Roles of surface residues of intracellular domains of heag potassium channels. *Eur Biophys J* 38: 523–532.
- Stewart RD** (1975) The effect of carbon monoxide on humans. *Annu Rev Pharmacol* 17: 409–423.
- Stuhmer W, Ruppersberg JP, Schroter KH, Sakmann B, Stocker M, Giese KP, Perschke A, Baumann A, Pongs O** (1989) Molecular basis of functional diversity of voltage-gated potassium channels in mammalian brain. *EMBO J* 8: 3235–3244.
- Stupfel M, Bouley G** (1970) Physiological and biochemical effects on rats and mice exposed to small concentrations of carbon monoxide for long periods. *Ann NY Acad Sci* 174: 342–368.
- Stocker R, Yamamoto Y, McDonagh A, Glazer A, Ames BN** (1987) Bilirubin is an antioxidant of possible physiological importance. *Science* 235: 1043–1045.
- Sun XX, Hodge JJ, Zhou Y, Nguyen M, Griffith LC** (2004) The eag potassium channel binds and locally activates calcium/calmodulin-dependent protein kinase II. *J Biol Chem* 279: 10206–10214.
- Tahara T, Sun J, Nakanishi K, Yamamoto M, Mori H, Saito T, Fujita H, Igarashi K, Taketani S** (2004) Heme positively regulates the expression of beta-globin at the locus control region via the transcriptional factor Bach1 in erythroid cells. *J Biol Chem* 279: 5480–5487.
- Taketani S** (2005) Acquisition, mobilization and utilization of cellular iron and heme: endless findings and growing evidence of tight regulation. *Tohoku J Exp Med*. 205: 297–318.
- Tang XD, Xu R, Reynolds MF, Garcia ML, Heinemann SH, Hoshi T** (2003) Haem can bind to and inhibit mammalian calciumdependent Slo1 BK channels. *Nature* 425: 531–535.
- Tempel BL, Papazian DM, Schwarz TL, Jan YN, Jan LY** (1987) Sequence of a probable potassium channel component encoded at Shaker locus of *Drosophila*. *Science* 237: 770–775.
- Tenhunen R, Ross ME, Maver H, Schmid R** (1970) Reduced nicotinamide adenine dinucleotide phosphate dependent biliverdin reductase: partial purification and characterization. *Biochem* 9: 298–303.
- Terlau H, Ludwig J, Steffan R, Pongs O, Stühmer W, Heinemann SH** (1996) Extracellular Mg^{2+} regulates activation of rat eag potassium channel. *Pflügers Archiv* 432: 301–312.
- Thompson SH** (1977) Three pharmacologically distinct potassium channels in molluscan neurones. *J Physiol* 265: 465–488.
- Thompson JD, Higgins DG, Gibson TJ** (1994) CLUSTAL W: improving the sensitivity of progressive multiple sequence alignment through sequence weighting, positionspecific gap penalties and weight matrix choice. *Nucleic Acids Res* 22: 4673–4680.
- Trakshel GM, Kutty RK, and Maines MD** (1986) Purification and characterization of the major constitutive form of testicular heme oxygenase. *J Biol Chem* 261: 11131–11137.
- Trumpower BL, Gennis RB** (1994) Energy transduction by cytochrome complexes in mitochondrial and bacterial respiration: the enzymology of coupling electron transfer reactions to transmembrane proton translocation. *Annu Rev Biochem* 63: 675–716.
- Tseng-Crank JCL, Tseng GN, Schwartz A, Tanouye MA** (1990) Molecular cloning and functional expression of a potassium channel cDNA isolated from a rat cardiac library. *FEBS Lett* 268: 63–68.

- Tsiftoglou AS, Tsamadou AI, Papadopoulou LC** (2006) Heme as key regulator of major mammalian cellular functions: molecular, cellular, and pharmacological aspects. *Pharmacol Ther* 111: 327–345.
- Tyler DD** (1992) *The Mitochondrion in Health and Disease*, VCH Publishers, Inc., New York.
- Vercellotti GM, Balla G, Balla JM, Nath K, Eaton JW, JacobMem Inst Oswaldo Cruz, Rio de Janeiro HS** (1994) Heme and the vasculature: an oxidative harzard that induces antioxidant defense of the endothelium. *Artif Cells Blood Substit Immobil Biotechnol* 22: 207–213.
- Verma A, Hirsch DJ, Glatt CE, Ronnett GV, Snyder SH** (1993) Carbon monoxide: a putative neural messenger. *Science* 259: 381–384.
- Ye W, Zhang L** (2004) Heme controls the expression of cell cycle regulators and cell growth in HeLa cells. *Biochem Biophys Res Commun* 315: 546–554.
- Yu FH, Yarov-Yarovoy V, Gutman GA, Catterall WA** (2005) Overview of molecular relationships in the voltage-gated ion channel superfamily. *Pharmacol Rev* 57: 387–395.
- Wang R, Wu L** (1997) The chemical modification of KCa channels by carbon monoxide in vascular smooth muscle cells. *J Biol Chem* 272: 8222–8226.
- Wang MH** (2004) A technical consideration concerning the removal of oocyte vitelline membranes for patch clamp recording. *Biochem Biophys Res Comm* 324, 971–972.
- Wang S, Publicover S, Gu Y** (2009) An oxygen-sensitive mechanism in regulation of epithelial sodium channel. *Proc Natl Acad Sci* 106: 2957–2962.
- Wang X., Chowdhury JR, Chowdhury NR** (2006) Bilirubin metabolism: Applied physiology. *Current Paediatrics* 16: 70–74.
- Wang Z, Wilson GF, Griffith LC** (2002b) Calcium/calmodulin-dependent protein kinase II phosphorylates and regulates the *Drosophila* eag potassium channel. *J Biol Chem* 277: 24022–24029.
- Warmke J, Drysdale R, Ganetzky B** (1991) A distinct potassium channel polypeptide encoded by the *Drosophila* eag locus. *Science*. 252: 1560–1562.
- Warmke JW, Ganetzky B** (1994) A family of potassium channel genes related to eag in *Drosophila* and mammals. *Proc Natl Acad Sci* 91: 3438–3442.
- Weinstein JD, Branchaud R, Beale SI, Bement WJ, Sinclair PR** (1986) Biosynthesis of the farnesyl moiety of heme a from exogenous mevalonic acid by cultured chick liver cells. *Arch Biochem Biophys* 245: 44–50.
- Wells JA and McClendon CL** (2007) Reaching for high-hanging fruit in drug discovery at protein-protein interfaces. *Nature* 450: 1001–1009.
- Williams S E, Wootton P, Mason HS, Bould J, Iles DE, Riccardi D** (2004) Hemoxygenase-2 is an oxygen sensor for a calcium sensitive potassium channel. *Science* 306: 2093–2097.
- Wilson GF, Wang Z, Chouinard SW, Griffith LC, Ganetzky B** (1998) Interaction of the K channel beta subunit, Hyperkinetic, with eag family members. *J Biol Chem* 273: 6389–6394.
- Wissmann R, Baukrowitz T, Kalbacher H, Kalbitzer HR, Ruppersberg JP, Pongs O, Antz C, Fakler B** (1999) NMR structure and functional characteristics of the hydrophilic N terminus of the potassium channel beta-subunit Kvbeta1.1. *J Biol Chem* 274: 35521–35525.
- Wissmann R, Bildl W, Oliver D, Beyermann M, Kalbitzer HR, Bentrop D, Fakler B** (2003) Solution structure and function of the "tandem inactivation domain" of the neuronal A-type potassium channel Kv1.4. *J Biol Chem* 278: 16142–16150.

- Wong WT, Schumacher C, Salcini AE, Romano A, Castagnino P, Pelicci PG, Di Fiore PP** (1995) A protein-binding domain, EH, identified in the receptor tyrosine kinase substrate Eps15 and conserved in evolution. *Proc Natl Acad Sci* 92: 9530–9534.
- Woodard SI, Dailey HA** (2000) Multiple regulatory steps in erythroid heme biosynthesis. *Arch Biochem Biophys* 384: 375–378.
- Wu L, Wang R** (2005) Carbon monoxide: endogenous production, physiological functions, and pharmacological applications. *Pharmacol Rev* 57: 585–630.
- Xu L, Enyeart JA, Enyeart JJ** (2001) Neuroprotective agent riluzole dramatically slows inactivation of Kv1.4 potassium channels by a voltage-dependent oxidative mechanism. *J Pharmacol Exp Ther* 299: 227–237.
- Yang JM, London IM, Chen JJ** (1992) Effects of heme and porphyrin compounds on intersubunit disulfide formation of heme-regulated eIF-2 alpha kinase and the regulation of protein synthesis in reticulocyte lysates. *J Biol Chem* 267: 20519–20524.
- Yu FH, Catterall WA** (2004) The VGL-chanome: a protein superfamily specialized for electrical signaling and ionic homeostasis. *Sci STKE* re15.
- Zagotta WN, Hoshi T, Aldrich RW** (1990) Restoration of inactivation in mutants of Shaker potassium channel peptide derived from ShB. *Science* 250: 568–571.
- Zhang L, Hach A** (1999) Molecular mechanism of heme signaling in yeast: the transcriptional activator Hap1 serves as the key mediator. *Cell Mol Life Sci* 56: 415–426.
- Zhong Y, Wu CF** (1991) Alteration of four identified K⁺ currents in *Drosophila* muscle by mutations in eag. *Science* 252: 1562–1564.
- Zhong Y, Wu CF** (1993) Modulation of different K⁺ currents in *Drosophila*: a hypothetical role for the eag subunit in multimeric K1 channels. *J. Neurosci* 13: 4669–4679.
- Zhu Y, Hon T, Ye W, Zhang L** (2002) Heme deficiency interferes with the Ras-mitogen-activated protein kinase signaling pathway and expression of a subset of neuronal genes. *Cell Growth Differ* 13: 431–439.
- Ziechner U, Schönherr R, Born AK, Gavrilova-Ruch O, Glaser R, Malesevic M, Küllertz G, Heinemann SH** (2006) Inhibition of human ether-à-go-go potassium channels hEAG1 by Ca²⁺/calmodulin binding to the cytosolic N- and C-termini. *FEBS Journal* 273: 1074–1086.
- Zuccarello M, Bonasso CL, Lewis AI, Sperelakis N, Rapoport RM** (1996) Relaxation of subarachnoid hemorrhage-induced spasm of rabbit basilar artery by the K⁺ channel activator cromakalim. *Stroke* 27: 311–316.

7. Appendix

Abbreviation

| | |
|------------------|--|
| wt | Wild type |
| mt | Mutant |
| pp-IX | Protoporphyrin IX |
| GSH | Reduced Glutathione |
| SEM | Standard Error of the Mean |
| EGTA | Glycol-bis (2-aminoethylether)-N, N, N', N'-tetraacetic acid |
| Kv channel | Voltage-gated potassium channel |
| EC ₅₀ | Half-maximal Effective Concentration |
| IC ₅₀ | Half-maximal Inhibitory Concentration |
| MP-11 | Microperoxidase-11 |
| ROS | Reactive Oxygen Species |
| HEPES | 4-(2-hydroxyethyl)-1-piperazineethanesulfonic acid |
| HEK293 | Human Embryonic Kidney 293 cells |
| DTT | Dithiothreitol |
| DTNB | 5, 5'- dithiobis[2-nitrobenzoic acid] |
| DTNP | 2, 2'-dithio-bis [5-nitropyridine] |
| Kv1.4-IP | Kv1.4 Inactivation Peptide |
| PAS domain | Per-Arnt-Sim domain |
| cNBD | Cyclic Nucleotide-Binding Domain |
| MTSET | [2-(trimethylammonium)ethyl] methane thiosulfonate bromide |
| MTSES | 2-sulfonatoethyl methanethiosulfonate sodium salt |
| CaM | Calmodulin |
| ID | Inactivation domain |
| EPR | Electron Paramagnetic Resonance |

Acknowledgement

There are number of people who I can thank for contributing to my love of science and helping me throughout my graduate study. First, I would like to thank my supervisor Prof. Stefan H. Heinemann for giving me an opportunity to continue my doctoral thesis under his supervision. I consider him as my guru. He always inspired and motivated me throughout my doctoral thesis. He has always been unconditionally supportive of me and his kindness and encouragement truly kept me going. I am so thankful for all that he has done for me.

I am very much thankful to Dr. Roland Schönherr for his humble suggestions, inspiration and support and providing me with unlimited help and also for critical reading of the early versions of this manuscript, and translating the necessary parts of it into German. I am always encouraged by his scientific ability and new innovative ideas.

I take this opportunity also to thank Prof. Toshinori Hoshi, University of Pennsylvania, for his valuable suggestions and motivation.

I would like to thank Dr. Guido Gessner for his fun loving and kindly advice, Dr. Enrico Leipold for his energetic and valuable suggestions.

I am also grateful to Gurdun Albrecht and Dorith Schmidt for their helping hands, Angela Roßner and Steffi Arend for their help.

Special thanks to our early lunch group Rayk, Mario, René and Katrin for their nice valuable and lively discussions (both scientific and non-scientific).

I would like to extend my thanks to Martin for his helping hand and Oxana, Nadine, Tina, Jana, Ehsan and Holger for the provision of technical help in a number of methods.

I also thank our collaborators Dr. Diana Imhof and Dr. Manfred Friedrich for their useful discussions, constant help and assistance.

I am very grateful to my friends Rama, Bibhu and Farhan for their invaluable support in my everyday life.

Finally, I would like to thank my father and mother for their support, love and affection, brother and sister (Mitu, Litu and Biyani) for their love and last but never the least, Sasmita my wife for her love, help and understanding throughout my PhD thesis and giving me a beautiful angel "Sunakhi" (my daughter) .

Lebenslauf

Name: Sahoo
Vorname: Nirakar
Geburtsdatum: 01.07.1978
Geburtsort: Kendrapara, Orissa, Indien
Staatsbürgerschaft: Indisch
Familienstand: Verheiratet
Anschrift: Hugo-Schrade-Str 30, Jena-07745

Pädagogische Qualifikation:

| Degree | Major | Year | Institution | Marks/CGPA |
|-----------------------------|--|-----------|---|----------------------------------|
| Diploma in Pharmacy | Pharmacology, Anatomy & Physiology, Biochemistry | 1995-1999 | Orissa State Board of Pharmacy, Orissa, India | First class with 72.5% |
| Bachelor of Science (B.Sc.) | Zoology, Botany and Chemistry | 2000-2003 | Utkal University, Bhubaneswar, Orissa, India | 57.50% with distinction |
| Master of Science (M.Sc.) | Biotechnology | 2003-2005 | Department of Biotechnology, Pondicherry University, Pondicherry, India | First class with CGPA of 8.45/10 |

Research experience

2005-2006 Arbeit als Wissenschaftlicher Mitarbeiter am Jawaharlal Nehru Centre for Advanced Scientific Research (JNCASR), Bangalore, Indien

Seit 2006 (Juli) Doktorand am Center for Molecular Biomedicine (CMB), Friedrich-Schiller-Universität Jena bei Prof. Dr. Stefan H. Heinemann.

Finanziert durch: Collaborative Research Centre 604 - Multifunctional Signaling Proteins (SFB 604), TP A4.

Häm und Häm-Abbauprodukte: Alternative Funktionen und Signalmechanismen (ProExzellenz Thüringen)

List of Publications and Posters:

Publications:

Sahoo N, Tröger J, Heinemann SH, Schönherr R (2010) Current inhibition of human EAG1 potassium channels by the Ca²⁺ binding protein S100B. FEBS Lett 584: 3896-3900.

Kolbe K, Schönherr R, Gessner G, **Sahoo N**, Hoshi T, Heinemann SH (2010) Cysteine 723 in the C-linker segment confers oxidative inhibition of hERG1 potassium channels. J Physiol 588: 2999-3009.

Naik PR, **Sahoo N**, Goswami D, Ayyadurai N, Sakthivel N (2008) Genetic and functional diversity among fluorescent pseudomonads isolated from the rhizosphere of banana. Microbial Ecology 56: 492-504.

Karmodiya K, Modak R, **Sahoo N**, Sajad S, Surolia N (2008) Deciphering the key residues in Plasmodium falciparum beta-ketoacyl acyl carrier protein reductase responsible for interactions with Plasmodium falciparum acyl carrier protein. FEBS Journal 275: 4756-4766.

Poster:

Sahoo N, Schönherr R, Kolbe K, Hoshi T, Heinemann SH (2009) Thiol-dependent modulation of human EAG1 potassium channels. Acta Physiologica 195: 54 (Gießen, Germany) (**Awarded with a poster prize**).

Kolbe K, **Sahoo N**, Schönherr R, Hoshi T, Heinemann SH (2008) Site-specific regulation of hERG potassium channels by intracellular cysteine modification. Biophysics Journal 94:1340 (Long beach, California, US).

Sahoo N, Litzenberg J, Born AK, Heinemann SH, Schönherr R (2007) Inhibition of human ether a` go-go potassium channels by Ca²⁺/S100B. Jena, Germany (SFB 604, September 20th-22nd, 2007).

Talk:

Sahoo N, Romas T, Hoshi T, Heinemann SH (2010) Intracellular hemin removes inactivation of A-type voltage-gated potassium channels. Copenhagen, Denmark, Acta Physiologica 2010; Volume 198, Supplement 677: O-SUN-2-6 (March 27-30, 2010).

Sahoo N, Schönherr R, Hoshi T, Heinemann SH (2009) Hemin, potassium channels, and erythroid differentiation. Lecture Hall FLI/HKI, Beutenbergstraße 11, Jena, Germany, CMB seminar (June 16, 2009).

Selbstständigkeitserklärung

Hiermit erkläre ich, dass ich die vorliegende Arbeit selbstständig und nur unter Verwendung der angegebenen Hilfsmittel, Literatur und persönlichen Mitteilungen angefertigt habe.

Jena,

Nirakar Sahoo

Erklärung zur Bewerbung

Hiermit erkläre ich, dass ich mich mit der vorliegenden Arbeit an keiner anderen Hochschule um den akademischen Grad Doctor rerum naturalium beworben habe und dass ich weder früher noch gegenwärtig die Eröffnung eines Verfahrens zum Erwerb des oben genannten akademischen Grades an einer anderen Hochschule beantragt habe. Die Promotions-Ordnung der Biologisch-Pharmazeutischen-Fakultät der FSU Jena ist mir bekannt.

Jena,

Nirakar Sahoo